CHARLES UNIVERSITY PRAGUE

Faculty of Mathematics and Physics

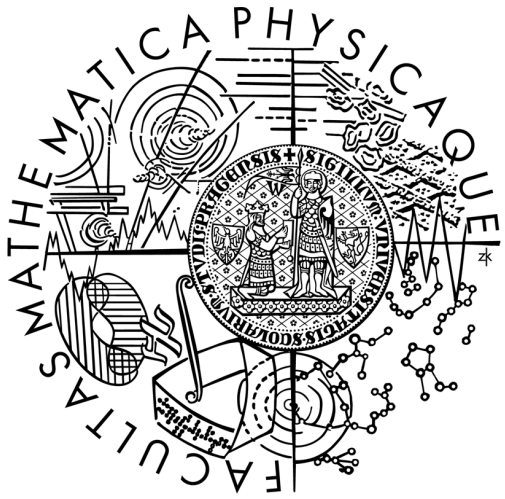

Spectroscopic Study of Singlet Oxygen in Biological Systems

Doctoral thesis

Alexander Molnár

Department of Chemical Physics and Optics

Prague, 2008

Acknowledgement

I would like to express my deepest thanks to my supervisor RNDr. Roman Dědic, Ph.D. for his very valuable help during my Ph.D. studies. I am also very grateful to Prof. RNDr. Jan Hala, DrSc. for his kind assistance and advices, to Mgr. Milan Bašta for his willingness and language corrections, to Prof. Čestmír Koňák for his kind help with elastic light scattering measurements, and to Assoc. Prof. Peter Mojzeš for his worthy assistance with the factor analysis. My thanks belong also to the team of the Low temperature laser laboratory at the Department of Chemical Physics and Optics for useful consultations. Finally, I would like to thank to all my family and friends for their support during my Ph.D. study, namely to Vlk Šikoun, Mišutka, Puf, Malá, Zuzka, my father, my grandmother, Milo, King, and many others.

This work was supported by the Czech Grant Agency under the Grant No. GD202/05/H003, GP202/01/D100, by projects MSM113200001 and MSM0021620835 from the Ministry of Education, and by GA UK 184/2002.

Contents

List of abbreviations

[A]	-	concentration of a compound A
EET	-	excitation energy transfer
HpD	-	hematoporphyrin derivatives
HSA	-	human serum albumin
ISC	-	intersystem crossing
k_{IC}	-	rate constant of internal conversion
k_{ISC}	-	rate constant of intersystem crossing
k_{NR}	-	rate constant of non-radiative deactivation of singlet oxygen or PS
k_f	-	rate constant of fluorescence
k_{pO2}	-	rate constant of phosphorescence of singlet oxygen
k_{pPS}	-	rate constant of phosphorescence of photosensitizer
k_{EET}	-	rate constant of excitation energy transfer
k_R	-	rate constant of vibrational relaxations
M	-	Mol per litre
$^1O_2$	-	first singlet excited state of oxygen
$^3O_2$	-	ground state of oxygen
PDT	-	photodynamic therapy
PpIX	-	protoporphyrin IX
PS	-	photosensitizer
$^1PS^*$	-	first singlet excited state of photosensitizer
^3PS	-	first triplet state of photosensitizer
t_{SO}	-	lifetime of singlet oxygen
TPP	-	meso-tetraphenylporphyrin
$TPPS_4$	-	meso-tetra(4-sulfonatophenyl)porphyrin
$\phi_{^1O_2}$	-	quantum yield of singlet oxygen production

1. Motivation and the Aim of the Work

Singlet oxygen plays a key role in the so called photodynamic therapy (PDT). Photodynamic therapy is a progressive method of treatment of cancer and other chronic diseases (age-related macular degeneration, psoriasis). The main advantage of this method is in the high selectivity towards diseased tissues. That means that PDT destroys tumour only, with no effect to the healthy tissue. In PDT, a light, a light-sensitive drug (so called photosensitizer, PS), and oxygen are combined to produce highly reactive substances lethal to the tumour cells. First, the PS is administered into patient's body. After a delay, when PS is accumulated predominantly in the tumour tissue, the tumour is irradiated at an appropriate wavelength. Under the irradiation, PS undergoes the transition into excited singlet state, which easily converts to the triplet state. The ground state of molecular oxygen is a triplet ($^3O_2$). On the other hand, the first excited state of oxygen is a singlet ($^1O_2$). As the triplet state of PS exhibits higher energy than the singlet state of oxygen and the process is spin-allowed, energy transfer from PS to singlet oxygen occurs easily. In this way, highly reactive singlet oxygen is produced, which destroys biologically significant molecules in tumour tissue, such as proteins or lipids. In addition, a PS in triplet state can interact directly with substrate molecules, causing the generation of free radicals, which can also destroy the cancer cells.

Research in this area is not finished yet, of course. Scientists are still looking for PS with better and better properties and ways, how they can get PS into the tumour as efficiently as possible. Optical spectroscopy showed to be a powerful tool to investigate photogeneration of $^1O_2$. The main advantage of the direct detection of singlet oxygen phosphorescence over other methods is its ability to determine not only singlet oxygen quantum yield but also detailed kinetic characteristics of excitation energy transfer between PS and oxygen.

The aim of this work is to investigate the interactions of different PS with singlet oxygen in different environments by means of time- and spectral-resolved phosphorescence. The understanding of this action is essential for successful application of PDT. As the human body represents too much complicated system, it is necessary to begin with investigation of the interactions in simplified systems. Various PS in environments of increasing complexity and similarity to the conditions in the human body were studied in this work.

The initiatory experiments were done in simple solvents, such as phosphate buffers or acetone. The first step on the way towards the biological systems was done by the use of the buffers with pH of skin, tumour tissue, and blood.

Finally, those simple environments were replaced by environments of higher complexity, such as lipids, liposomes, or buffers with the most abundant blood plasma protein, Human Serum Albumine (HSA).

2. Introduction

2.1. Energetic states of dye molecules and transitions between them

As a molecule undergoes transition from an energetically higher to an energetically lower state, photon emission may occur. This process is called luminescence. The majority of complex polyatomic molecules exhibit no luminescence. On the other hand, intensive luminescence was observed in the case of many aromatic molecules. In this work we have studied porphyrine derivates, which exhibit strong luminescent properties.

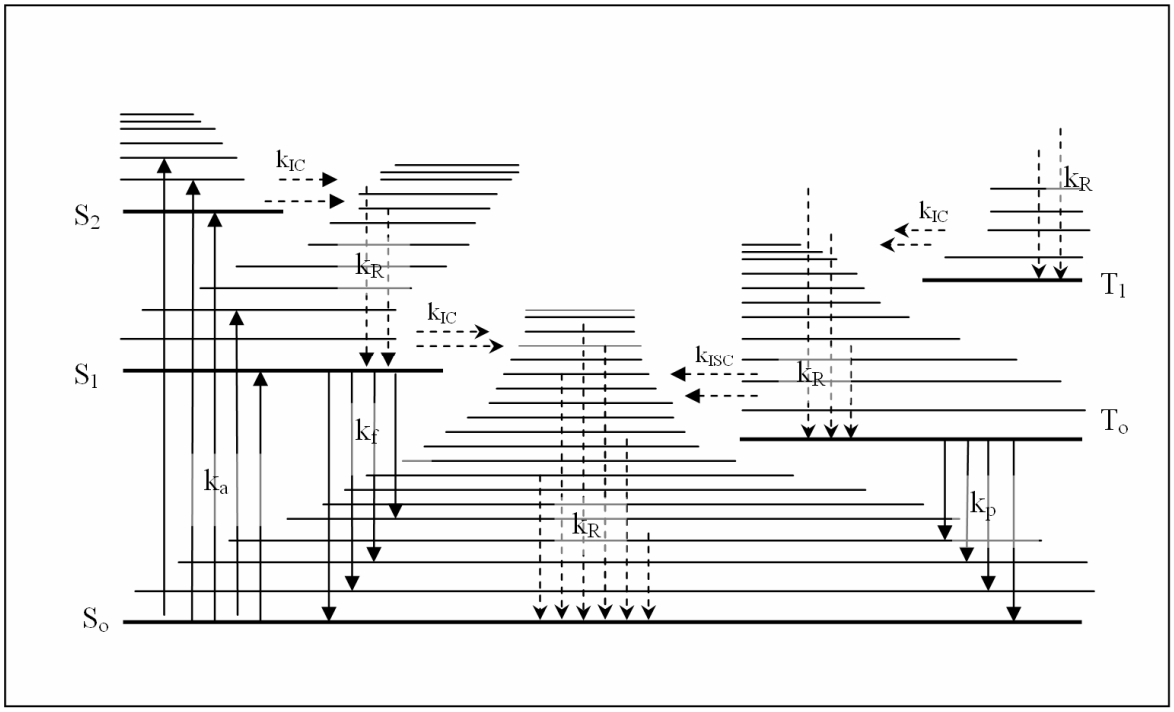

Figure 1 A schematic description of energy states of dye-molecule together with the transitions between them

Horizontal lines in Figure 1 correspond to electronic-vibronic levels of the molecule. For the sake of clarity, lines situated higher correspond to electronic-vibronic levels with a higher energy state of the molecule. Each electronic-vibronic level can be found in one of different spin states: a singlet or a triplet state. The molecule in the triplet state has an overall spin equal to one in contrast to the molecule in a singlet state with an overall spin equal to zero.

The lowest energetic state of the molecule (i.e. the ground state) is usually singlet, denoted by S_0. Singlet states with higher energies are denoted by S_1, …, S_n in Figure 1,

while triplet states with higher energies are denoted by T_1, …, T_n. Bold horizontal lines correspond to pure electronic levels, the energy of which is equal to the sum of electronic energies and energies of zero normal vibrations. Mixed electron-vibration levels are presented by the thin horizontal lines.

The molecule can get from one electron-vibration level to another one. Let us assume that the molecule is in the ground state S_0. After the excitation by the electromagnetic radiation at an appropriate wavelength, the molecule undergoes the transition to one of the excited states S_1, …, S_n.

There are two pathways, either radiative transitions (luminescence) or non-radiative transitions, through which the molecule can get back from the excited state to the ground state:

Non-radiative transitions (k_{NR}) are processes, when no photons are emitted. These include the internal conversion (see k_{IC} arrows in Figure 1), the intersystem crossing (k_{ISC} arrows) and vibration relaxations (k_R arrows).

1. The internal conversion is the isoenergetic transition between electron levels of the same spin multiplicity.

2. The intersystem crossing is an isoenergetic transition between electron levels of a different spin multiplicity.

3. Vibrational relaxation processes involve the dissipation of the vibrational energy to the surrounding environment. This kind of relaxations plays a very important role in the condensed media where it is much faster than other kinds of deactivation processes. This is the reason, why the radiative transitions to the ground state mostly occur from the lowest vibrational levels of the excited states, *i. e.* pure electronic levels only.

Radiative transitions, luminescence, can be divided into fluorescence (k_f), phosphorescence (k_p) and delayed fluorescence.

1. Fluorescence is defined as a spin-allowed transition from the equilibrium vibrational level of an excited state to one of the vibrational levels of the ground state, accompanied by the emission of photon [1]. Fluorescence is usually observed from the

lowest vibrational level of the excited state S_1. According to the Kasha's rule, a molecule in the excited state S_2 or a higher one undergoes a transition to a pure electron level of the first excited state S_1 by non-radiative processes at first. Subsequently, fluorescence may occur.

2. Phosphorescence is a radiative transition between levels of different spin multiplicity, which is a spin-forbidden process. This is the reason, why the lifetime of the lowest excited state T_1 is longer than the lifetime of S_1 level by many orders of magnitude.

3. Delayed fluorescence is very similar to normal fluorescence. It is also a radiative transition from one of the singlet excited states to the ground state. In the case of delayed fluorescence, the molecule undergoes the transition from the excited singlet state S_1 to the triplet state T_1 and then back from T_1 to S_1 again, and afterwards fluorescence occurs. It implies that the lifetime of delayed fluorescence is similar to the lifetime of phosphorescence.

2.2. Singlet oxygen

Molecular oxygen in air is found in its energetically lowest, triplet ground state. Triplet multiplicity of its ground state is a unique property, because most of natural compounds have a ground state singlet.

Atmospheric oxygen is not highly reactive towards biological molecules under normal conditions due to the Wigner's spin selection rule, as the chemical reactions of one reactant in singlet state with reactant in triplet state generating products in singlet state are strictly spin-forbidden. This situation changes after a chemical or physical transformation of the oxygen molecule to the singlet state and thus oxygen becomes extremely reactive.

The energy of transition between the lowest singlet excited state and the triplet ground state is 95 kJ mol^{-1} [2-4]. It corresponds to the absorption wavelength of 1269 nm in the gas phase [5].

2.2.1 Energetic levels of a molecular oxygen

The MO-LCAO model (Molecular Orbital-Linear Combination of Atomic Orbitals) predicts two low-lying excited singlet states of O_2, in spectroscopic terms abbreviated by $^1\Delta_g$ and $^1\Sigma_g^+$. They differ only in the structure of the π-antibonding orbitals. Two paired electrons are situated in the same π-antibonding orbital in the excited state labelled $^1\Delta_g$, while in the case of singlet state $^1\Sigma_g^+$ two paired electrons occupy two different π-antibonding orbitals. The electronic structure of the triplet ground state $^3\Sigma_g^-$ together with the electronic structure of the energetically lowest excited state $^1\Delta_g$ is depicted in Figure 2.

Molecular oxygen remains only very shortly in the singlet state $^1\Sigma_g^+$. It undergoes a rapid transition to the lower-lying singlet state $^1\Delta_g$, usually by vibrational relaxations. This transition is very fast as the spin multiplicity remains unchanged and is therefore spin-allowed.

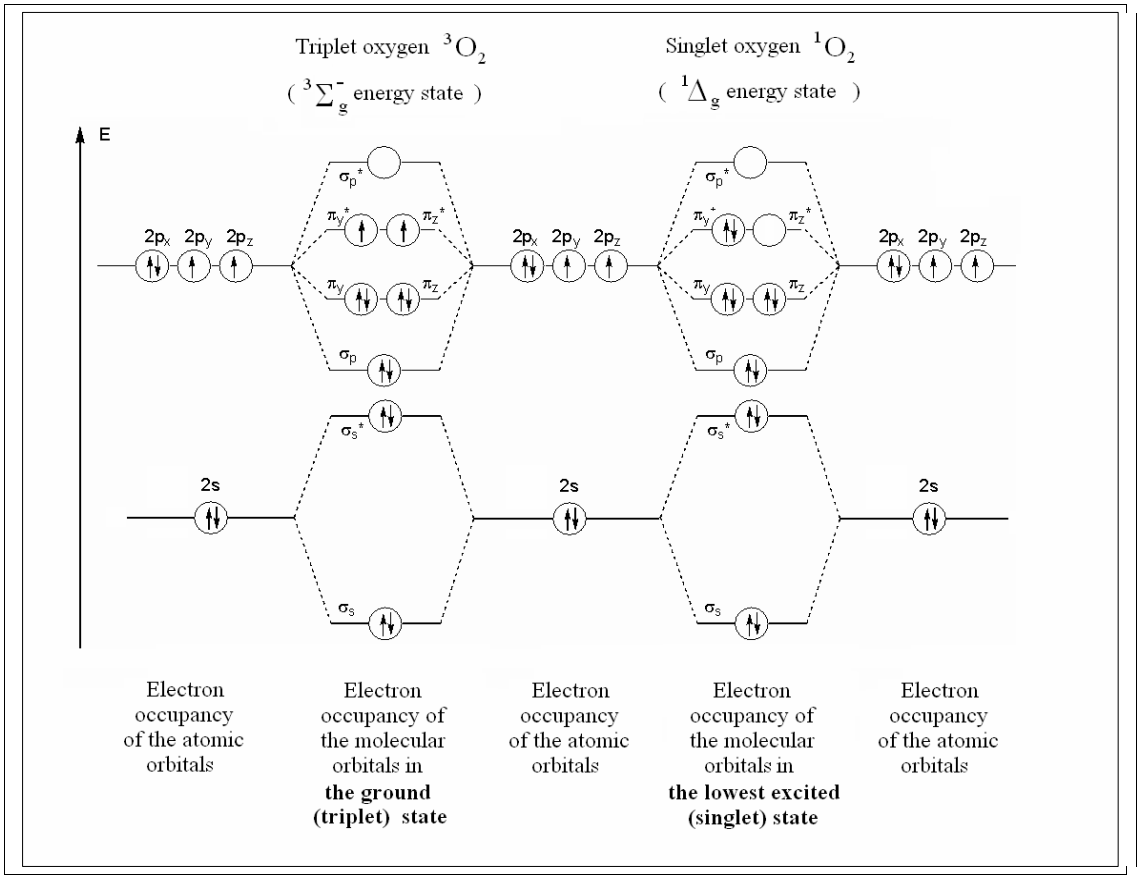

Figure 2 Electron occupancy of the atomic and molecular orbitals of oxygen

On the other hand, the transition from $^1\Delta_g$ to the ground state $^3\Sigma_g^-$ is spin-forbidden, making $^1\Delta_g$ relatively long-lived. Quantitatively, the lifetime of the singlet state $^1\Delta_g$ in the gas phase is about 45 minutes, while the lifetimes of $^1\Sigma_g^+$ only a few seconds (approximately 7–12 s) [6]. The lifetime of these states is much shorter in condensed media: 10^{-6} – 10^{-3} s for $^1\Delta_g$ state and 10^{-11}–10^{-9} s for $^1\Sigma_g^+$ state [7].

Only the chemically active state $^1\Delta_g$ is commonly referred to as singlet oxygen, due to the very short lifetime of $^1\Sigma_g^+$ state in comparison with $^1\Delta_g$ state. Terms “singlet oxygen” and “$^1\Delta_g$” are used as synonyms in further text.

2.2.2 Generation of singlet oxygen

Singlet oxygen can be generated by many different ways. The basic classification of these methods is to the chemical and physical ones.

Chemical methods

There are several different chemical methods of the $^1O_2$ production *in vitro*. $^1O_2$ is often generated in exothermic chemical reactions. These processes are usually accompanied by luminescence due to the radiative decay of the $^1O_2$. The best known reactions to generate $^1O_2$ as a product are reaction of hypochlorite with hydrogen peroxide or the thermal decomposition of endoperoxides [8].

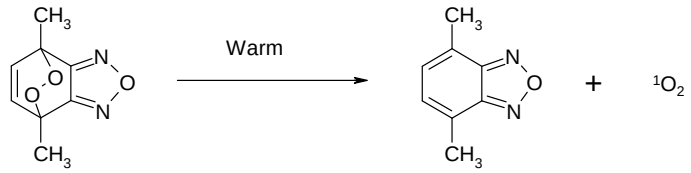

Figure 3 Thermal decomposition of 4,7-dimethyl benzofurazan-4,7-endoperoxide

In vivo, leukocytes can produce $^1O_2$ in the response to different particles [9-11]. Singlet oxygen generated in this way predominantly serves as a weapon against a wide range of pathogens, such as viruses or cancer cells. It was also verified that singlet oxygen has antiviral effects [12].

Physical methods

According to Wilkinson *et al.* [4], there are more physical methods to generate singlet oxygen, such as: direct absorption, pulsed radiolysis, microwaves, organic molecule charge-transfer and photosensitized production. The photosensitized production of singlet oxygen plays a key role in our study, so it is briefly described in the next paragraph.

Photosensitized production of singlet oxygen refers to a light-activated process that requires the presence of a light-absorbing molecule, PS, which initiates excitation energy transfer to oxygen after an absorption of photon. The schematic description of this action is depicted in the Jablonsky diagram (Figure 4).

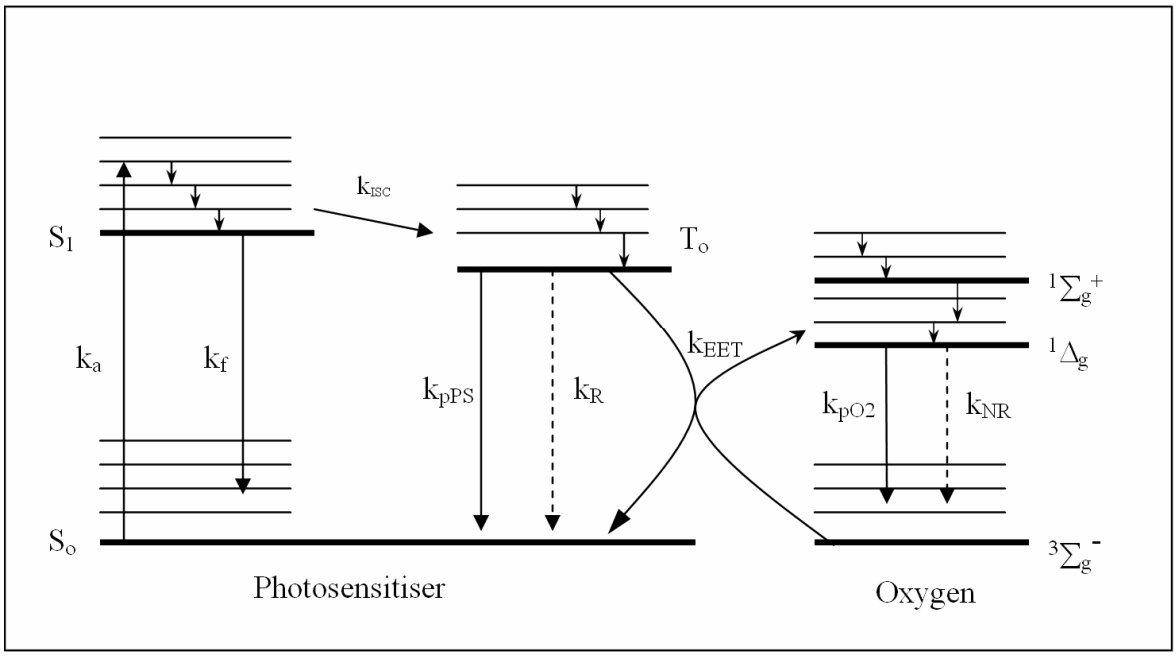

Figure 4 Schematic description of the photodynamic action

The initial act of light absorption elevates one electron in the ground singlet state (S_0) to a vibrationally-excited level of the S_1 state, without a change of the spin orientation. Subsequently, vibrational relaxations occur, in which the excessive vibrational energy is dissipated as heat. This process leaves the excited molecule in the thermally-equilibrated S_1 state.

$$PS(S_0) \longrightarrow PS(S_1) + h\nu_1 \quad (1)$$

After a certain time, the PS molecule undergoes a transition to the ground state S_0 by fluorescence (2) or by vibrational relaxations (3), or to the energetically lower triplet state T_1 (4) by intersystem crossing (and subsequently by vibrational relaxations).

$$PS(S_1) \xrightarrow{k_f} PS(S_0) + h\nu_2 \quad (2)$$

$$PS(S_1) \xrightarrow{k_R} PS(S_0) \quad (3)$$

$$PS(S_1) \xrightarrow{k_{ISC}} PS(T_1) \quad (4)$$

where k_R, k_{ISC} and k are rate constants of vibrational relaxations, intersystem crossing and fluorescence.

PS in the triplet state may also transfer the excitation energy to triplet oxygen (5). This results in the production of singlet oxygen:

$$PS(T_1) + {}^3O_2 \xrightarrow{k_{EET}} PS(S_0) + {}^1O_2 \quad (5)$$

k_{EET} is a rate constant of the excitation energy transfer. This process is allowed by Wigner's rule [13]. That is a reason why it is relatively fast in comparison to other ways of ^{3}PS deactivation.

The overall efficiency of the $^1O_2$ photogeneration by PS can be quantified by the quantum yield of the singlet oxygen production ϕ_{1O2}

$$\phi_{1O2} \equiv \frac{J_{O2}}{J_a} \quad (6)$$

J_0 is a number of photogenerated $^1O_2$ molecules and J_a is a number of absorbed photons by PS molecule.

The overall amount of photogenerated $^1O_2$ molecules (and thus a quantum yield of singlet oxygen) depends on the rates of particular processes in PS molecule (fluorescence, ISC, phosphorescence, IC, EET, vibrational relaxations, etc.). It depends also on the concentration of triplet oxygen dissolved in samples [14].

On the other hand, the ^{3}PS–$^3O_2$ interactions need not necessarily lead to the formation of singlet oxygen. Other physical deactivations of ^{3}PS (7) or the chemical reactions (oxidations) of ^{3}PS with $^3O_2$ (8) may occur:

$$PS(T_1) + {}^3O_2 \xrightarrow{k_{dO2}} PS(S_0) + {}^3O_2 \quad (7)$$

$$PS(T_1) + {}^3O_2 \longrightarrow \text{product} \quad (8)$$

k_{dO2} is a quenching constant of the physical deactivation of ^{3}PS by oxygen.

2.2.3 Deactivation of singlet oxygen

After O_2 has undergone the transition to the excited singlet state, there are two ways of its deactivation: physical and chemical ones.

Physical deactivation

$^1O_2$ can get back to the ground triplet state either by radiative or non-radiative processes. Radiative transition — phosphorescence (9) — can be observed at 1270 nm [15-20].

$$^1O_2 \xrightarrow{k_{pO2}} {}^3O_2 + h\nu \quad (9)$$

Intersystem crossing and following vibrational relaxations (10) are the representatives of non-radiative transitions to the ground state:

$$^1O_2 \xrightarrow{k_R} {}^3O_2 \quad (10)$$

Quenching (11) of singlet oxygen by another molecule is very important process through which $^1O_2$ can undergo the transition back to the ground triplet state. This deactivation of $^1O_2$ by the interaction with the molecule of quencher Q_P leads to no chemical changes of Q_P:

$$^1O_2 + Q_P \xrightarrow{k_{QP}.[Q_P]} {}^3O_2 + Q_P \quad (11)$$

k_{QP} is a quenching constant of the physical deactivation of $^1O_2$ by molecule Q_P and $[Q_P]$ is concentration of Q_P in solvent.

Many molecules can physically deactivate $^1O_2$. Sodium azide, for instance, is a strong, well-known physical quencher of $^1O_2$ [21-23] which is often used for the verification of the singlet oxygen involvement in oxidation processes [18,24,25].

PS may often play the role of the quencher — it can not only photogenerate singlet oxygen, but can also efficiently deactivate it in many cases.

Finally, as it will be shown further as one of the results of this work, singlet oxygen can be quenched by oxygen, even predominantly by singlet oxygen itself.

Chemical deactivation

The chemical reaction of $^1O_2$ with an interacting molecule Q_{CH} is called the chemical quenching of oxygen (12) or photosensitized oxidation. The product of this reaction is abbreviated to Q''_{CH} which is not the same chemical entity as Q_{CH}.

$$^1O_2 + Q_{CH} \xrightarrow{k_{QCH}.[Q_{CH}]} Q''_{CH} \qquad (12)$$

k_{QCH} is a rate constant of the chemical reaction of $^1O_2$ with molecule Q_{CH} and $[Q_{CH}]$ is concentration of Q_{CH} in solvent.

"Ene" reaction, [4+2] cycloaddition, [2+2] cycloaddition and heteroatom oxidation reactions are the well-know archetypical reactions of singlet oxygen in organic chemistry [26-28]. Figure 5 shows examples of these actions.

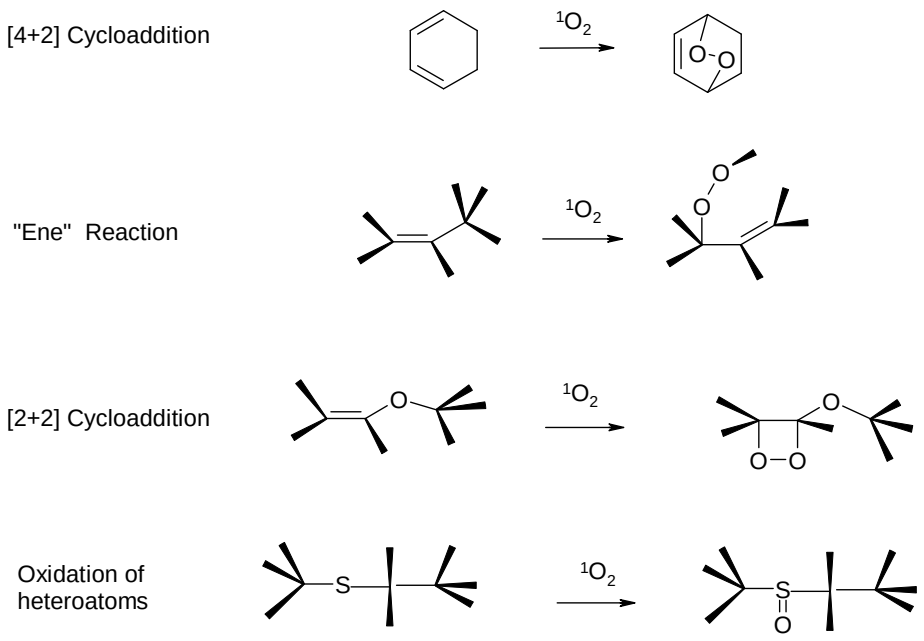

Figure 5 Typical reactions of singlet oxygen

All of these reactions describe the interactions of singlet oxygen with unsaturated carbon-carbon bonds (or with heteroatom). They also have great importance in biological systems

due to a particularly high concentration of unsaturated carbon-carbon bonds in a wide range of biomolecules, such as proteins or lipids. The description of $^1O_2$ interactions with these biomolecules is briefly presented in the paragraph on photodynamic therapy.

PS could be also a chemical quencher. So called photobleaching refers to the degradation of PS by singlet oxygen. This phenomenon was observed in many different PS [29-34].

One molecule of PS can typically photogenerate 10^2–10^5 molecules of singlet oxygen, until it undergoes an irreversible chemical reaction with singlet oxygen it has produced, and thus becomes useless [3].

2.2.4 Applications of $^1O_2$

Singlet oxygen can be very useful in a wide range of applications. It can play a key role in the photodegradation of pollutants in waste water treatment, such as fenols [35,36] mercaptans [37], sulfides [38], and thiosulfates [39,40] which are often unwanted by-products of industrial processes.

The high reactivity of $^1O_2$ together with its excellent stereoselectivity makes singlet oxygen also a very effective reagent in fine chemical synthesis and organic chemistry. In this way, optically active alpha-methyl beta-hydroperoxy esters [41] or 5-aminolevulinic acid [42] may be synthesised.

A deep understanding of the $^1O_2$ deactivation can by very important in the food industry, where an undesirable oxidation of nourishment by singlet oxygen occurs [43,44]. Adding $^1O_2$ quenchers such as carotenoids and tocopherols into food can prevent nutritional losses and toxic compounds production.

The application of singlet oxygen can also be found in medicine [45]. $^1O_2$ is photogenerated as a cytotoxic agent during the photodynamic therapy (PDT) by PS in a cancer tissue, causing its necrosis [46-49]. The focus of this doctoral thesis is the energy transfer from the well-known PS used in PDT to singlet oxygen. As PDT is related to our investigations, attention will be paid to it in the next paragraph.

2.3. Photodynamic therapy

Photodynamic therapy is an effective modality of treatment of cancer and many other chronic diseases. In the first step, PS is administered into the tumour tissue. Afterwards, PS located in tumour is illuminated by the light of appropriate wavelength. Subsequently, PS undergoes a transition to its excited state. The triplet excited states of PS have many orders of magnitude longer lifetimes in comparison to the excited singlet states, which enable ^{3}PS to interact much longer with the surrounding environment. ^{3}PS can initiate biophysical and biochemical mechanisms of tumour necrosis via type I. or type II. reaction mechanisms [48,50].

Type I. reaction mechanism involves a direct interaction between ^{3}PS and substrate molecules, causing the generation of free radicals. Free radicals are highly reactive chemical entities due to the presence of their unpaired valence shell electrons. The substrate molecule can be an oxidizing (A_O, B_O) or a reducing agent (A_RH, B_R). Proton (13) or electron (14) is transferred from reducing agents to the ^{3}PS molecule:

$$PS(T_1) + A_RH \longrightarrow PS(S_1)H^{\bullet+} + A_R^{\bullet-} \quad (13)$$

$$PS(T_1) + B_R \longrightarrow PS(S_1)^{\bullet-} + B_R^{\bullet+} \quad (14)$$

In case of oxidizing agents, a proton (15) or electron (16) transfer can occur from ^{3}PS to the oxidants:

$$PS(T_1) + A_O \longrightarrow PS(S_1)^{\bullet-} + A_OH^{\bullet+} \quad (15)$$

$$PS(T_1) + B_O \longrightarrow PS(S_1)^{\bullet+} + B_O^{\bullet-} \quad (16)$$

Free radicals may chemically react with surrounding biomolecules, such as lipids or proteins. This causes a serious disruption of biological processes, which are crucially needed for the tumour cell survival. Type I. reaction mechanism can also initiate a cascade of reactions, where further cytotoxic species may arise. Products of $^3O_2$-free radical reactions can be reactive oxygen species, such as superoxide radical anion $O_2^{\bullet-}$. On the

other hand, $O_2^{\bullet -}$ can be generated directly in reaction (34) where $^3O_2$ was used as an oxidizing agent.

In case of the **type II. reaction mechanism**, the excitation energy transfer from ^{3}PS to oxygen results in singlet oxygen as a product. A photosensitized process of $^1O_2$ generation was described above, by equation (5):

Since singlet oxygen is extremely reactive, chemical or physical quenching of $^1O_2$ by proteins, DNA, RNA, lipids, and sterols can occur very easily. This interaction proceeds in agreement with the above mentioned reactions of singlet oxygen: [4+2] cycloaddition, [2+2] cycloaddition, heteroatom oxidation reaction, or “ene” reaction.

Interactions of $^1O_2$ with proteins

According to the Davie’s simple model [51], approximately 70 % of the overall amount of singlet oxygen in a typical cell (leukocyte) is consumed by the reaction with proteins.

Amino-acids histidine, tyrosine, methionine, cysteine, cystine, and tryptophan are among the main oxidative targets of $^1O_2$ within the protein polypeptide chain. The most interactions of $^1O_2$ with amino acids occur via chemical quenching. Among aminoacids, significant physical quenching was observed only in the case of tryptophan. The rate constants describing the chemical and physical quenching differ strongly and depend on the surrounding environment. For example, they are highly pH dependent. An excellent description of the $^1O_2$ interaction with all the mentioned amino acids can be found in Davies’ review [2].

Interaction of $^1O_2$ with cholesterol

The addition of $^1O_2$ to a carbon–carbon double bond can be observed in case of singlet oxygen interaction with cholesterol. The fact, that the double C-C bond is a site with a high electron density confirms the electrophilic character of processes in PDT. Hydroxyperoxide as a product is generated in reactions of $^1O_2$ with cholesterol (or with other sterols):

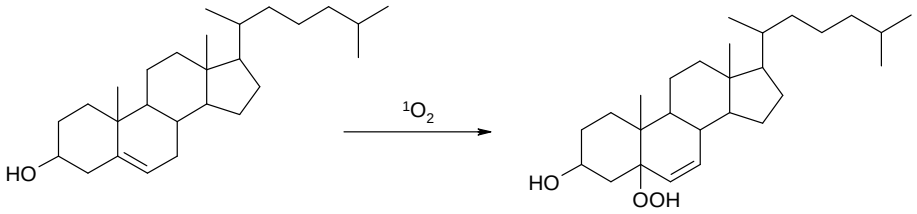

Figure 6 Reaction of $^1O_2$ with cholesterol

Interaction of $^1O_2$ with lipids

A transfer of the carbon-carbon double bond with a subsequent generation of hydroperoxides occurs in case of the lipids–$^1O_2$ interaction, which represents the above mentioned singlet oxygen "ene" reaction.

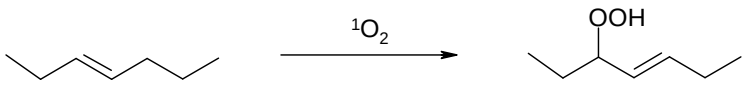

Figure 7 Reaction of $^1O_2$ with part of a typical lipid chain

Lipids are the main component of cell membranes. Therefore, the photosensitized oxidation of lipids by $^1O_2$ can seriously affect their functions.

Interactions of $^1O_2$ with DNA and RNA

It is known, that singlet oxygen ($^1O_2$) is involved in oxidative damage to DNA and RNA [25,52-54].

Cytosine, guanine, adenine, thymine (DNA), and uracil (RNA) are parts of RNA and DNA, the so-called nucleobases. $^1O_2$ has a tendency of a selective modification of the guanine base. The involvement of $^1O_2$ in this modification has been proved by the usage of D_2O as a solvent and azide as a quencher [55,56]. The high selectivity of $^1O_2$ for guanine base was also confirmed by observations of Devasagayam *et al.* [57] and Piette *et al.* [58].

It is widely believed that singlet oxygen is the main cytotoxic agent in PDT. That means that a type II. reaction mechanism prevails in the tumour destruction, although the ratio of the relative importance of type I. and type II. mechanisms in PDT depends strongly on circumstances [48].

The main advantage of photodynamic therapy is the selective accumulation of administered PS in the tumour. That means that the concentration of PS in tumour is substantially higher in comparison with the PS concentration in the surrounding healthy tissue. Therefore, local illumination generates cytotoxic species predominantly in the tumour, and has negligible effects to normal tissue. The selective accumulation of PS in tumour is due to an enhanced capillary permeability and a poor lymphatic drainage of many tumours [59] or due to different metabolism of cancer cells.

On the other hand, PDT has also some disadvantages. PS used in PDT often tends to accumulate not only in tumour, but also in kidneys, liver, or skin. Moreover, PDT can not be used in case of a big tumour, due to a low penetration depth of the light in the tissue.

2.4. Photosensitizers

PS, by definition, is a drug with the ability to absorb light and transfer this excitation energy to molecular oxygen. Various PS are used in PDT, which may differ in many for PDT important properties, such as:

- absorption wavelength; The most desirable absorption interval is between 600 nm and 800 nm, the “therapeutic window”, due to the deepest penetration of light of this wavelengths into the human tissues.
- level of dark toxicity (the toxicity of administered PS in the absence of illumination)
- efficiency of the generation of singlet oxygen as well as of other reactive species
- degree of selectivity, that can be defined as the ratio of PS concentration in tumour and in healthy tissue
- level of disintegration of PS in human body, or the rate of clearance of PS from liver, kidney, and skin, where PS also tend to accumulate.

No single PS can be the best in all the above mentioned fields. For example, protoporphyrin IX posses 5 times shorter duration of skin photosensitivity in comparison to phthalocyanines. On the other hand, phthalocyanines absorb between 670 and 680 nm very well, where the light exhibits higher penetration depth than at 635 nm used for protoporphyrin IX excitation [49].

2.4.1 Haematoporphyrin derivatives

Derivatives of haematoporphyrin (HpD) were one of the first photosensitizers used in PDT [29]. HpD is a strong PS, but suffers from a low selective accumulation in tumor. Moreover, a prolonged photosensitivity of skin (2 or 3 months) was observed after application of HpD.

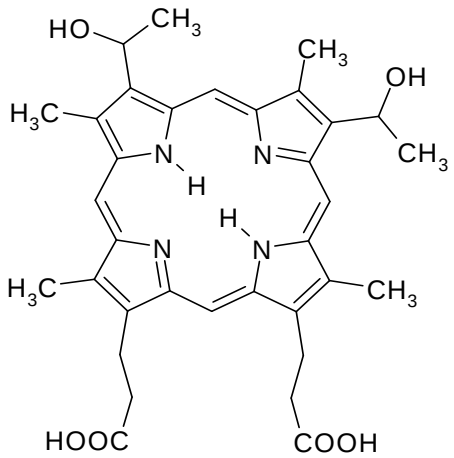

Figure 8 Structural formula of Haematoporphyrin

Acetylation and reduction of haematoporphyrin produces a complex mixture of HpD with a better selectivity and a better efficiency of the generation of singlet oxygen. Photofrin® (from QLT PhotoTherapeutics), which is a partially purified form of HpD, has received the approval for clinical use in Europe, Japan, USA, and Canada [49,60,61].

2.4.2 Protoporphyrin IX

Protoporphyrin IX (PpIX) is a metabolic product of δ-aminolevulinic acid (ALA) in human body [62]. ALA and PpIX are therefore molecules that occur naturally in almost all cells. PpIX is also a powerful PS.

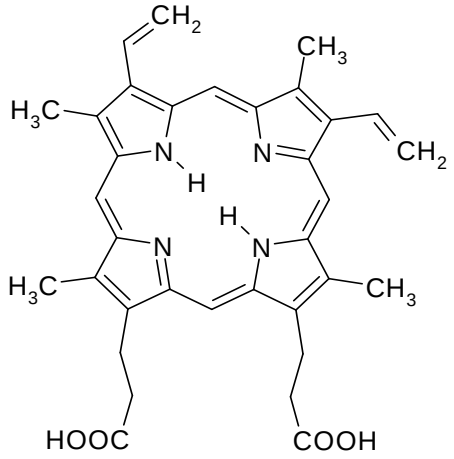

Figure 9 Structural formula of Protoporphyrin IX

In contrast to a normal concentration of PpIX within a cell, a much higher concentration of PpIX is necessary for successful PDT applications. This is achieved by

exogenous administration of ALA to patients. ALA enters the porphyrin biosynthetic pathway, which results in an overloaded PpIX concentration. Tumours and other proliferating tissues usually have tendency to accumulate more ALA-induced PpIX than the surrounding healthy tissues. Despite PpIX has the strongest absorption around 400 nm (Soret band), the excitation wavelength 635 nm corresponding to one of its much weaker Q bands is used in PDT.

Fluorescent and photosensitizing properties of PpIX biosynthesized after the administration of ALA can serve to visualize and destroy malignant cells in PDT. Many clinical δ-aminolevulinic acid-PDT applications to malignant and non-malignant pathologies are currently in use [63].

2.4.3 Meso-tetraphenyl-porphyrin

TPP belongs to modified porphyrins, which are generated by addition of various chemical groups to the porphyrin core. In the case of TPP, four phenyl groups are added to the porphyrin cycle.

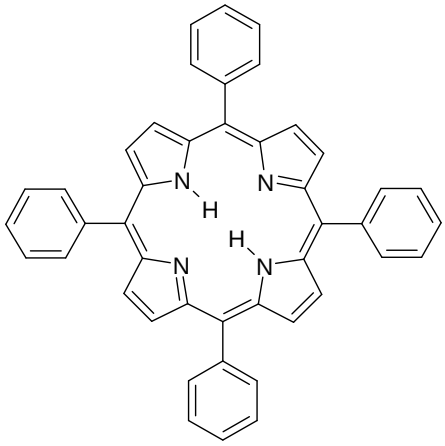

Figure 10 Structural formula of meso-tetraphenyl-porphyrin

TPP is a hydrophobic molecule with strong photosensitizing properties. The efficiency of TPP in PDT was tested in human amelanotic melanomas implanted in nude mice [64]. TPP was incorporated to liposomes, administered intravenously, and irradiated. The tumour reduction to zero volume confirms that TPP is a potentially suitable agent for PDT.

2.4.4 Meso-tetra(4-sulfonatophenyl)porphyrin ($TPPS_4$)

It is possible to generate a water soluble derivate of hydrophobic TPP from hydrophobic TPP by a simple chemical reaction, such as sulfonation. In this way $TPPS_4$ is produced. Similarly to TPP, $TPPS_4$ also has a high singlet oxygen quantum yield. On the other hand, $TPPS_4$ exhibits certain properties like many other water-soluble porphyrins. For example it aggregates in water [65-68]. Moreover, addition of central metal ions to $TPPS_4$ has strong effect on its properties. The influence of addition of various central metal ions to $TPPS_4$ on its photophysical properties was described by Kubát *et al*. [69].

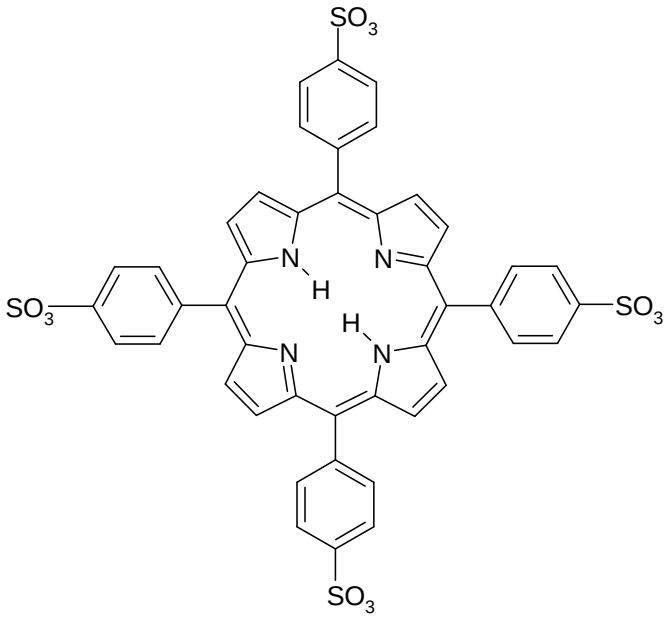

Figure 11 Structural formula of meso-tetra (4-sulfonatophenyl) porphyrin

$TPPS_4$ has been successfully applied in breast cancer treatment in the Czech Republic [70].

Apart from the above described PS, which were studied in the presented work, other photosensitizers also exist, such as texaphyrins, phthalocyanines, rhodamines, psoralens, porphycenes, and many others [49]. These differ in chemical structure and photophysical properties.

2.5. Kinetics of PS and $^1O_2$

Let's assume a simple system: PS together with oxygen dissolved in a simple solvent, such as acetone. No other molecules which could serve as physical or chemical quenchers are dissolved in the solvent.

At first, an excitation pulse elevates PS molecules from their ground states to an energetically higher singlet states ^{1}PS*. As was mentioned above, a part of these excited PS emits fluorescence rapidly, part relaxes nonradiatively, and the rest undergoes a transition to the closest lower triplet state by ISC (and subsequently by vibration relaxations). The lifetime of singlet excited state is usually negligible compared to lifetimes of triplet states, therefore the subsequent time evolution of concentration of the PS molecules is triplet state can be described by equation (17)

$$\frac{\mathrm{d}[^3\mathrm{PS}(t)]}{\mathrm{d}t} = -\left(k_{\mathrm{pPS}} + k_{\mathrm{NR}} + k_{\mathrm{EET}}.[^3\mathrm{O}_2]\right).[^3\mathrm{PS}(t)] \tag{17}$$

This equation contains all three channels, by which ^{3}PS can undergo transition to the ground state: by phosphorescence (k_{pPS}), by nonradiative transitions (k_{NR}), or by excitation energy transfer to oxygen (k_{EET}). In most cases, back transitions to the singlet excited state can be neglected. Usually, the $^3O_2$ concentration decrease due to its transformation to singlet oxygen is very low compared to the overall oxygen concentration. Finally, no quenching of ^{3}PS by $^1O_2$ and vice versa is taken into account. Under these assumptions, the equation (17) has simple monoexponential solution

$$[^3\mathrm{PS}(t)] = I_{\mathrm{PS}} \,.\, \mathrm{e}^{-\left(k_{\mathrm{pPS}} + k_{\mathrm{NR}} + k_{\mathrm{EET}}.[^3\mathrm{O}_2]\right).t} \tag{18}$$

where I_{PS} is a constant. The lifetime of ^{3}PS is thus given by relation (19):

$$t_{3\mathrm{PS}} = \frac{1}{\left(k_{\mathrm{pPS}} + k_{\mathrm{NR}} + k_{\mathrm{EET}}.[^3\mathrm{O}_2]\right)} \tag{19}$$

$[^3\mathrm{PS}(t)]$ is proportional to the observed intensity of the PS phosphorescence, thus the measured phosphorescence data enabled us to obtain the lifetime of ^{3}PS by fitting the data with eq. (18).

The kinetics of singlet oxygen is more complicated. The rise of the singlet oxygen concentration [$^1O_2$] is accompanied by the decrease of [^{3}PS] by EET. The singlet oxygen concentration decay is described by the $^1O_2$ phosphorescence rate constant k_{pO2} and by the non-radiative transitions rate constant k_{NR}.

$$\frac{d[^1O_2(t)]}{dt} = k_{EET}.[^3PS(t)].[^3O_2] - (k_{pO2} + k_{NR}).[^1O_2(t)] \quad (20)$$

Assuming equation (18) for time evolution of PS concentration, solution to this equation can be found:

$$[^1O_2(t)] = \frac{I_0}{1/t_1 - 1/t_{SO}}\left(e^{-t/t_{SO}} - e^{-t/t_1} \right) \quad (21)$$

Where I_0 is a constant, t_1 is the risetime of singlet oxygen, which is equal to lifetime of ^{3}PS:

$$t_1 = t_{3PS} \quad (22)$$

t_{SO} is the lifetime of singlet oxygen. In the absence of quenchers, t_{SO} is given by the equation (23):

$$t_{SO} = 1/(k_{pO2}+k_{NR}) \quad (23)$$

The lifetime of singlet oxygen is highly solvent dependent. In water or in a phosphate buffer of pH 7.4 the t_{SO} is around 3.5 µs [15,71] whereas in most organic solvents the lifetime is much longer. For example, the $^1O_2$ lifetime around 54 µs was observed in acetone [72]. The relatively long $^1O_2$ lifetime was also reported in D_2O (68 µs) [73]. This can be explained by different vibrational levels of OD bonds in deuterium oxide compared to OH groups in water, which are responsible for $^1O_2$ quenching [5].

In the presence of quenchers, the reciprocal value of the lifetime of singlet oxygen is given by the equation (24):

$$1/t_{SO} = k_{pO2} + k_{NR} + \Sigma[Q_{CH}]*k_{QCH} + \Sigma[Q_P]*k_{QP} \quad (24)$$

[Q_{CH}] ([Q_P]) is the concentration of the chemical (physical) quencher of singlet oxygen Q_{CH} (Q_P) and k_{NR} is the rate constant of non-radiative transitions excluding physical and chemical quenching.

In cellular systems, where many important biomolecules serve as quenchers, the lifetime of $^1O_2$ is considerably shorter. According to Niedre *et al.* [18] t_{SO} is only 30–180 ns in the tissue. The short intracellular lifetime of singlet oxygen suggests very efficient quenching of $^1O_2$ by its reaction with surrounding biomolecules. However, surprisingly long lifetimes of singlet oxygen in living cells were found by Skovsen *et al.*[74].

$^1O_2$ phosphorescence kinetics described by equation (21)was observed in many cases of different PS and in different environments. For example, this kinetics follows singlet oxygen phosphorescence in case of $^1O_2$ produced by riboflavin and flavin mononucleotide in water [14], by clinically used Photofrin® and 9-acetoxy-2,7,12,17-tetrakis-(beta-methoxyethyl)-porphycene in water, lipid suspensions, and in aqueous suspensions of living cells [15], by meso-tetraphenylporphine in acetone [72] or by meso-tetra(4-sulphonatophenyl)porphin in phosphate buffer of pH 7.5 [71].

The concentration of singlet oxygen is proportional to the intensity of the observed $^1O_2$ phosphorescence. That means the rise and decay times of the concentration of singlet oxygen in solution are given by the rise and decay times of $^1O_2$ phosphorescence.

3. Materials

The photophysical properties of four above mentioned PS together with their interactions with singlet oxygen were investigated: protoporphyrin IX (PpIX), hematoporphyrin derivatives (HpD), mesotetraphenyl-porphyrin (TPP) and meso-tetra(4-sulfonatophenyl)porphyrin ($TPPS_4$).

All photosensitizers used in this work were obtained from Frontier Scientific Porphyrin products, Logan, USA. No further purification or chemical modification was applied.

While $TPPS_4$ is a hydrophilic molecule, TPP, PpIX and HpD are all lipophilic. Therefore, a different solvent had to be used to dissolve $TPPS_4$. In this study, acetone was used as a solvent for lipophilic PS (PpIX, TPP and HpD). For hydrophilic $TPPS_4$ phosphate buffers were used. Phosphate buffers of pH 7.4, 6.5, and 5.5 corresponding to pH of blood, cancer tissue and skin, respectively, were prepared to mimic different biological environments important for PDT.

The concentration of oxygen in the samples was changed in particular experiments on aqueous solutions of $TPPS_4$. Usually, three identical samples were prepared, which differed only in the concentration of oxygen:

- samples saturated by air,
- samples saturated by nitrogen,
- samples saturated by oxygen.

To achieve oxygen saturated conditions, the samples were purged by oxygen for at least one hour. The concentration of oxygen dissolved in the phosphate buffer then reaches the saturated value of 1400 $\mu mol.l^{-1}$ [75]. In the case of samples bubbled by nitrogen, almost all oxygen was removed after 1 hour of purging them. The concentration of oxygen was 280 $\mu mol.l^{-1}$ [75] in the air saturated samples.

It was impossible to change the oxygen concentration in acetonic solutions by purging them by gases due to the fact that acetone evaporates very easily. The concentration of oxygen in air saturated acetone is 2400 $\mu mol.l^{-1}$

Human serum albumin was bought from Sigma Aldrich. The structure of human serum albumin is shown in Figure 12.

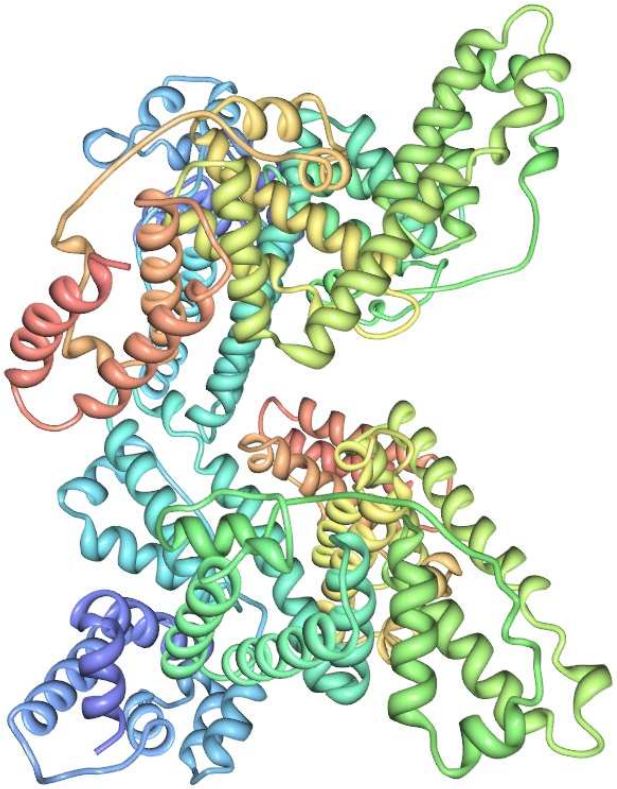

Figure 12 The structure of human serum albumin [76]

HSA was dissolved in phosphate buffer of pH 7.4. Concentration of HSA in the samples was in the range from 1 to 50 μmol l^{-1}, while the concentration of $TPPS_4$ was 10 μmol l^{-1} in all the samples.

Liposomes were prepared from completely saturated L-α-phosphatidylcholine by Avanti Mini-Extruder®. Fig.13 shows structural formula of the used lipid.

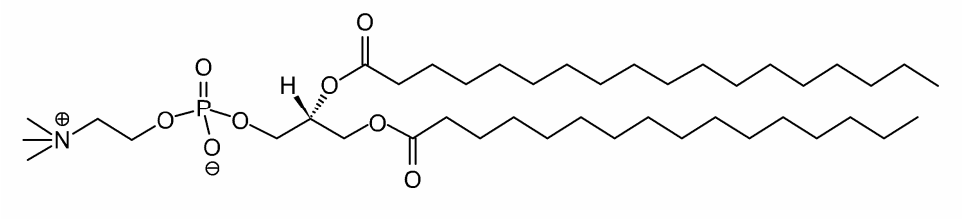

Figure 13 The structure of saturated L-α-Phosphatidylcholine

Completely saturated lipid L-α-Phosphatidylcholine was used to eliminate possible chemical reactions of singlet oxygen with double bonds of the liposome.

3.1. Preparation of liposomal samples

Both L-α-phosphatidylcholine and Mini-Extruder were bought from Avanti Polar Lipids. Lipids together with PS were dissolved and mixed in chloroform to assure a homogeneous mixture of lipids. Next, chloroform was removed by evaporating with dry nitrogen to yield a lipid film.

Hydration of the dry lipid film was accomplished by adding H_2O to the container and agitating. The products of hydration were large multilamellar vesicles, with each lipid bilayer separated by a layer of water. After the stable, hydrated multilamellar vesicle suspension was produced, the particles were downsized by extrusion to get unilamellar vesicles of well defined size.

This method improves the homogeneity of the size distribution of the final suspension in comparison to sonication. Filters with 100 nm pores were used to produce liposomes. The extrusion was done at temperature of 75 ˚C, well above the transition temperature of the used lipids (~50 ˚C).

Distribution of liposome sizes was checked using elastic light scattering, on Zetasizer Nano ZS device (Malvern Instruments) in the Institute of Macromolecular Chemistry of the Academy of Sciences with kind assistance of Prof. Koňák. Fig. 14 shows the obtained size distribution of liposomes loaded with PpIX.

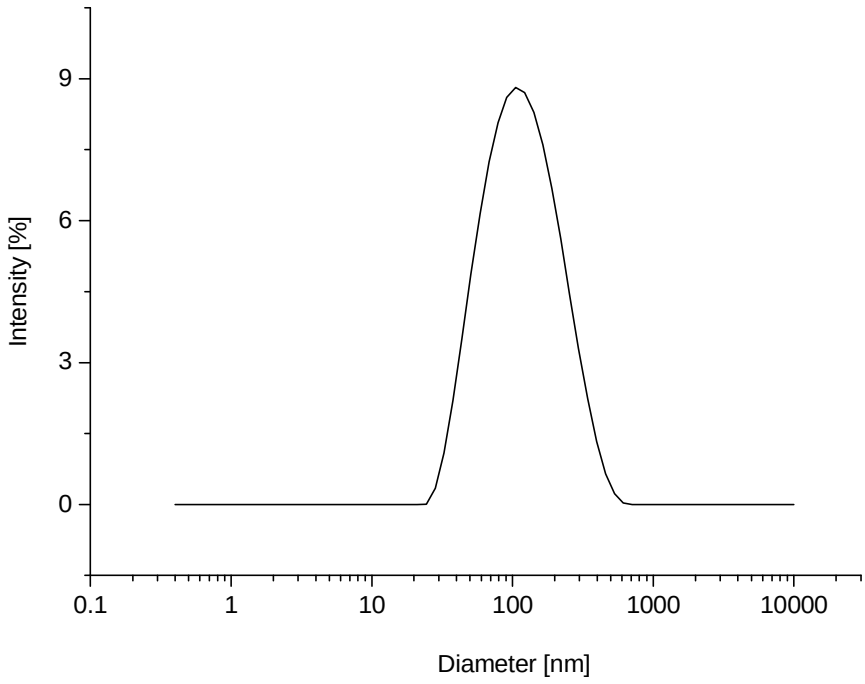

Figure 14 Size distribution of liposomes (loaded by PpIX) produced by extrusion through 100 nm membrane.

All spectroscopic measurements were performed at room temperature (20 ˚C), that means, under the transition temperature of the used lipids.

4. Methods

Standard spectroscopic techniques (absorption and fluorescence spectroscopy) were used to detect aggregation and verify photostability of studied PS. They were also used to check purity of the samples and to characterize them spectrally. Absorption measurements were done on Perkin Elmer Lambda 12 UV/VIS and Avantes Avaspec-1024 absorption spectrometers, while fluorescence measurements were carried out using Avantes S2000 spectrometer.

All luminescence experiments were carried out at room temperature (20 °C).

4.1. Experimental setup

The research was focused on time and spectral phosphorescence measurements of photosensitizers and singlet oxygen. Those measurements were made on a very sensitive home-built setup [71]. The schematic of the setup is displayed in Fig. 15.

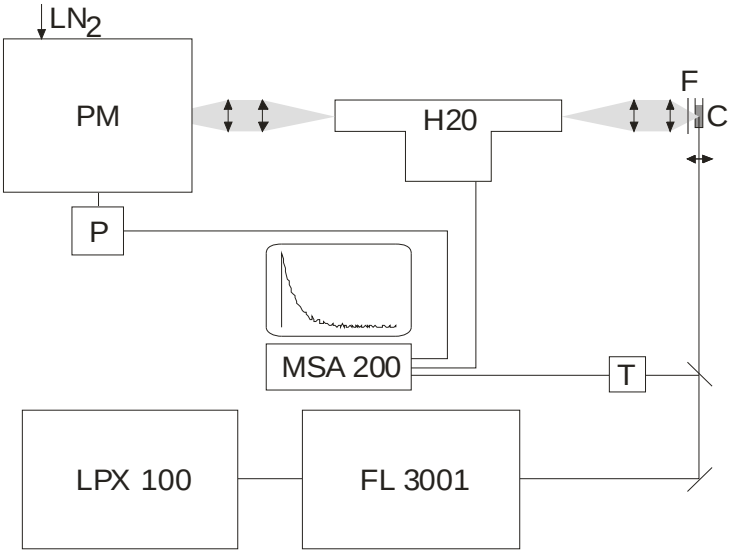

Figure 15 Scheme of a setup for time and spectral resolved IR luminescence: FL 3001—dye laser; LPX 100—excimer laser; T—triggering photodiode; C—cuvette with the sample; F—long pass filter; H20—monochromator; PM—liquid nitrogen cooled photomultiplier; P—preamplifier; and MSA 200—photon-counter/multiscaler.

The samples were excited at 420 nm by laser pulses. The duration of laser pulses was around 15 ns with 40 Hz repetition frequency. The energy of the pulses was around 25 μJ. The excitation pulses were provided by a dye laser Lambda Physik FL 3001 (Stilbene 3

in methanol) pumped by excimer laser Lambda Physik LPX 100. The laser beam was focused to a fluorescence cell through its optically polished bottom. The phosphorescence was collected from excitation spot by lens assembly through a long-pass filter (Schott RG 7) and high luminosity monochromator Jobin-Yvon H20 IR to the infrared sensitive photomultiplier Hamamatsu R5509 (cooled to −80 ˚C by liquid nitrogen). The photomultiplier output was fed through Becker-Hickl HF AC-26 dB preamplifier to Becker-Hickl MSA 200 photon counter/multiscaler MSA 200 triggered by a fast PIN photodiode. The time and spectral resolved phosphorescence was typically measured between 750 and 1342 nm with 16nm step to monitor photosensitizer and singlet oxygen phosphorescence together. Detailed time-resolved measurements of singlet oxygen between 1242 and 1306 nm with step 4 nm were performed. In this way we obtained a set of time and spectral resolved phosphorescence data of both PS and singlet oxygen.

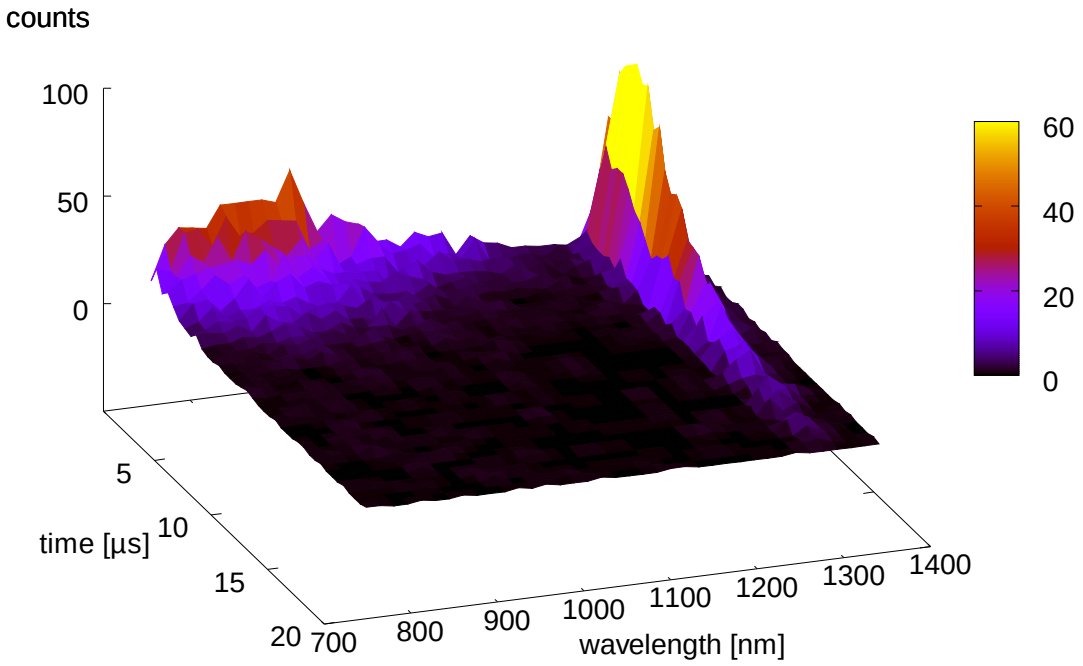

Figure 16 Typical 3D plot of time and spectral resolved phosphorescence of PS and singlet oxygen (30 µmol l^{-1} $TPPS_4$ in phosphate buffer)

5. Summary of Results and their Discussion

The study of PS-singlet oxygen interactions by means of time and spectral resolved phosphorescence was performed in this work. Spectrally resolved kinetics of different PS and singlet oxygen in various environments were determined: lifetimes of PS in triplet state, the rise and decay times of singlet oxygen, and the quenching constants of $^1O_2$ by PS. The obtained data enabled to determine kinetics parameters of processes of excitation energy transfer and quenching.

All photosensitizers studied in this work exhibit broad phosphorescence band with maximum between 800 and 1100 nm depending on the photosensitizer and the solvent. Quite narrow phosphorescence of $^1O_2$ appears at 1274 nm which is a little bit higher value than 1270 nm published in literature [15,17,19].

5.1. PpIX and HpD interactions with oxygen in acetone

It is crucial for successful application of PDT to know the photosensitizing properties of used PS. In this contribution photophysical properties of chemically similar porphyrin-like molecules of HpD and PpIX, were investigated.

PS phosphorescence

The PS phosphorescence kinetics together with the singlet oxygen production were measured in a wide range of PS concentrations (5–200 μM) in acetone. Both PpIX and HpD phosphorescence maxima (around 840 nm) were independent of the PS concentration. Phosphorescence of HpD follows mono-exponential decay with the lifetime of (0.35±0.01) μs. This lifetime does not dependent on HpD concentration.

On the other hand, the PpIX triplets lifetime increases with the increasing PpIX concentration from (0.15±0.02) μs to the saturated value (0.22±0.02) μs. This fact can be explained in the frame of aggregation. The increase of PpIX triplet lifetimes with the concentration corresponds to the increasing ratio of aggregates to monomeric forms.

The aggregation is also supported by bathochromic shifts observed in the fluorescence spectra, as well as by the absorption measurements. The absorbance of PpIX at 420 nm shows a nonlinear dependence for higher concentrations. A presence of at least

two spectral components was revealed by factor analysis. It was performed in the Institute of Physics of Charles University, Prague, with kind assistance of Assoc. Prof. Mojzeš.

$^1O_2$ phosporescence

After the excitation pulse at time t = 0 the singlet oxygen emission intensity I(t) follows the time evolution described by above mentioned equation (21).The fast rise-time of the singlet oxygen phosphorescence t_1 (0.28±0.01) μs for HpD and (0.24±0.02) μs for PpIX does not depend on the PS concentration. On the contrary, the lifetime of singlet oxygen t_{SO} depends on the PS concentration.

Quenching of $^1O_2$ by PS

The lifetime of singlet oxygen t_{SO} decreases with the increasing HpD concentration. This decrease corresponds to the bimolecular quenching of singlet oxygen by HpD described by Stern-Volmer equation:

$$k_2\left(c_{\mathrm{HpD}}\right) = k_0 + k_q \cdot c_{\mathrm{HpD}} \tag{25}$$

where k_2 is the rate constants of the depopulation of singlet oxygen:

$$k_2 = \frac{1}{t_{SO}} \tag{26}$$

The value of the quenching constant k_q was determined as (12.4 ± 1.2) $\times 10^6$ $M^{-1}s^{-1}$. The lifetime of singlet oxygen extrapolated to zero HpD concentration is (52.3 ± 1.1) μs.

In the case of PpIX the lifetime of singlet oxygen decreases with the increasing PpIX concentration again, but this time the decrease does not follow the bimolecular quenching. It can be due to the quenching of singlet oxygen predominantly by PpIX monomers. It is supported by the fact, that the quenching constant is higher in the low concentration region, where monomeric forms prevail. With the increasing concentration of PpIX, the relative portion of monomers decreases and so does the quenching constant.

PS-$^1O_2$ interaction

Our data show some discrepancy between life-times of HpD triplets of (0.35±0.01) μs and the singlet oxygen phosphorescence rise-times of (0.28±0.01) μs. To explain this fact, an existence of two distinct forms of HpD has to be assumed. One of these, a form, with lifetime equal to rise-times of singlet oxygen, transfers its excitation energy to oxygen. The other one, spectrally indistinguishable from the first one, cannot be quenched by oxygen which makes the effective life-times of HpD longer. Qualitatively same behaviour was reported earlier for meso-tetraphenylporphin in acetone [72].

However, the difference between the saturated value of PpIX life-times of (0.22±0.02) μs and the rise-times of $^1O_2$ of (0.24±0.02) μs cannot be explained in the frame of only two components: monomers and aggregates. Suggested explanation is based on dividing the aggregated molecules into two sets: envelope and core ones. Only those in the envelope can effectively transfer excited energy to oxygen and their phosphorescence life-times are equal to the singlet oxygen rise-times. The core molecules, inaccessible to oxygen quenching, cause shorter effective life-times of PpIX aggregates.

Anyway, it is very interesting, that chemically similar porphyrin-like molecules, HpD and Pp IX, exhibit significant difference in photosensitizer properties due to their different aggregation.

5.2. $TPPS_4$ interactions with oxygen in phosphate buffer

In contrast to HpD and PpIX, $TPPS_4$ is a hydrophilic PS. That means it is possible to study $TPPS_4$ excitation energy transfer to oxygen directly in water environment. To get closer to PDT applications, phosphate buffers of particular values of pH as a solvent were used. We have chosen pH values of buffers to be 7.4, 6.5 and 5.5 corresponding to pH of human blood [77], tumour tissue [78,79] and skin [80,81], respectively.

Photophysical properties of $TPPS_4$ in a wide range of its concentrations at each pH value were studied.

Moreover, the concentration of oxygen was varied:

1.samples without oxygen (purged by N_2 gas for 1 hour)
2.air saturated samples
3.oxygen saturated samples (purged by O_2 gas for 1 hour)

PS phosphorescence

The maximum of $TPPS_4$ phosphorescence (around 820 nm) does not dependent on the $TPPS_4$ concentration or the pH of the buffer.

The concentration of $TPPS_4$ has a very strong influence on the lifetime of the $TPPS_4$ phosphorescence. The lifetime slowly increases with increasing PS concentration to a saturated value at the highest concentrations of $TPPS_4$. Moreover, the $TPPS_4$ phosphorescence lifetime depends also on the concentration of oxygen.

On the other hand, the lifetimes were independent of pH value (within the experimental error). Oxygen proved to be a strong quencher of photosensitizer triplet states: In air saturated samples, the lifetime slowly increases with increasing $TPPS_4$ concentration from 1.8 ± 0.2 μs at $5\ \text{mmol}\ \text{l}^{-1}$ to a saturated value of 3.0 ± 0.2 μs at $200\ \text{mmol}\ \text{l}^{-1}$.

In the case of oxygen saturated samples, the situation is qualitatively the same, but the lifetimes are substantially shorter: Lifetimes of $TPPS_4$ triplets range from 0.37 ± 0.07 μs to 0.65 ± 0.08 μs.

$^1O_2$ phosporescence

The position and the shape of the singlet-oxygen phosphorescence depends neither on the $TPPS_4$ and oxygen concentration nor on the sample pH. Singlet oxygen kinetics follows equation (21) for all samples. This was also the case of kinetics of singlet oxygen photogenerated by PpIX or HpD in acetone.

The rise and decay times of the singlet oxygen phosphorescence were resolved in air- and O_2-saturated samples. (In N_2- saturated samples the very low phosphorescence signal made it impossible to obtain the rise and decay times of singlet oxygen). Both lifetimes were independent of the $TPPS_4$ concentration and the sample pH. The rise and decay times in air-saturated samples were 1.75±0.05 and 3.7±0.1 μs. After reaching the saturated value of O_2 in the samples, the rise and decay times of $^1O_2$ were shortened to 0.41±0.02 and 3.5±0.1 μs.

Quenching of $TPPS_4$ and $^1O_2$ by oxygen

We have determined a rate-constant of quenching $TPPS_4$ phosphorescence by oxygen (16.9±0.8) × 108 l mol^{-1} s^{-1}. Oxygen seems to be a strong quencher not only of photosensitizer triplet states, but also of singlet oxygen. (The $^1O_2$ lifetime decreases from 3.7±0.1 μs in air-saturated samples to 3.5±0.1 μs in O_2-saturated samples). This is caused probably by quenching singlet oxygen by interactions with other oxygen molecules.

PS-$^1O_2$ interaction

The lifetime of the $TPPS_4$ phosphorescence for the lowest concentration of the photosensitizer corresponds well to the rise-time of singlet oxygen. On the other hand, the $TPPS_4$ phosphorescence lifetime increases while $^1O_2$ rise time remains the same with higher PS concentrations. This behaviour is similar for all three pH values and both air- and O_2- saturated samples.

The explanation of this fact is based on different photophysical properties of monomers and aggregates. In $TPPS_4$ solutions, aggregates in triplet state do not transfer excitation energy to oxygen and thus their triplet state lifetime is longer. With increasing $TPPS_4$ concentration the aggregate to monomer ratio increases too, which makes the effective $^3TPPS_4$ lifetime longer. Singlet oxygen is probably generated only by monomers.

This is the reason, why the $^1O_2$ rise-time is independent of the total $TPPS_4$ concentration. The presence of aggregates at concentrations exceeding 30 μM was confirmed by absorption measurements of $TPPS_4$ in phosphate buffer at various concentrations.

5.3. Quenching of singlet oxygen by oxygen

As was mentioned above, singlet oxygen can be quenched by PS. Moreover, we have monitored very interesting phenomenon in our previous experiments. After increasing the concentration of oxygen from the air- to the oxygen-saturated value (from 280mmol l^{-1} to 1400mmol l^{-1}), the singlet oxygen lifetime in phosphate buffer solutions of $TPPS_4$ decreased from (3.7±0.1) μs to (3.5±0.1) μs. This observation implies that singlet oxygen is quenched not only by molecules of the solvent or PS but also by other oxygen molecules. In this chapter, we have investigated the effect of singlet oxygen quenching by oxygen in detail.

Kinetics of $TPPS_4$ phosphorescence together with singlet oxygen phosphorescence in phosphate buffer of pH 7.4 were measured at different concentrations of dissolved oxygen between zero and oxygen saturated value.

Quenching of PS by oxygen

The lifetimes of $TPPS_4$ triplets decrease with the increasing oxygen concentration. The corresponding rate-constants exhibit perfect linear dependence on the oxygen concentration. This confirms that the kinetics of excitation energy transfer from PS to oxygen follows a bimolecular mechanism in a wide range of oxygen concentrations. The value of this bimolecular quenching constant was determined as (1.5±0.1) $\times 10^9$ l/mol s.

$^1O_2$ phosphorescence

The behaviour of the rise-time of singlet oxygen was qualitatively the same. The rise-time increases with decreasing concentration of oxygen, providing the bimolecular quenching constant of (1.4±0.1) $\times 10^9$ l/mol s.

Quenching of $^1O_2$ by oxygen

The lifetime of singlet oxygen increases with the decreasing concentration of oxygen which is a proof of quenching of singlet oxygen by oxygen. In comparison with quenching of PS by oxygen, the obtained dependence of the rate-constants on oxygen concentration is more complex. A significant increase of singlet oxygen lifetimes with the decreasing dissolved oxygen concentration in the region below 280 mmol l^{-1} was observed.

Our measurements show that the lifetime of singlet oxygen in water extrapolated to the zero oxygen concentration is as long as (6.5 ± 0.4) μs.

In this point a question arises, whether $^1O_2$ is quenched predominantly by oxygen in the triplet or in the singlet state. This problem was solved by the following method: The intensity of excitation pulse at wavelength 420 nm was altered, which is reflected in the initial concentration of the photosensitizer triplet states and the subsequent increase of the singlet oxygen concentration accompanied by the decrease of triplet oxygen.

We have obtained the dependence of singlet oxygen depopulation rate-constants on absorbed energy in $TPPS_4$ in an air saturated buffer. The rate constants remain constant, within the experimental error, in the region of absorbed energies higher than ~3 μJ. In the region of lower absorbed energies, the rate constants decrease with decreasing absorbed energy.

A more detailed investigation of this dependence in the region of lower absorbed energies was impossible due to the very low signal of the singlet oxygen phosphorescence in water. That was the reason, why we studied the same dependence of mesotetraphenyl-porphyrin (TPP) in air-saturated acetone, where the concentration of dissolved oxygen was significantly higher (2400 μmol l^{-1}). TPP was used because it is a lipophilic analogue of $TPPS_4$. The wavelength of the excitation pulse remained the same, 420 nm.

The obtained dependence of singlet oxygen lifetimes on absorbed intensities less than 3 μJ was quasi-linear. The deviation from linearity was caused probably due to the existence of triplet–triplet transitions in TPP at wavelength ~ 440 nm. The concentration of PS triplets is not proportional to the measured absorbed energy because a part of the excitation energy is absorbed via the triplet–triplet transitions. This part increases with higher excitation intensity as more PS molecules is found in triplet state while number of PS molecules in ground state decreases. This effect makes the dependence of singlet oxygen depopulation rate-constants on absorbed energy non-linear.

There is no triplet–triplet absorption in the red spectral region. Therefore, the phosphorescence emission of singlet oxygen was measured at various energies of 645 nm excitation pulses. In this case the linear increase of the rate constants with the increasing absorbed energy was measured.

The overall concentration of the dissolved oxygen in the sample during the experiments remains the same. Then the increase of the concentration of photogenerated singlet oxygen with the increasing absorbed energy causes the decrease of the concentration of the triplet oxygen. When we take this fact into account, the linear increase of the rate constants with the increasing absorbed energy proves that singlet oxygen is quenched predominantly by singlet oxygen

5.4. Interactions between $TPPS_4$, $^1O_2$ and HSA

As the next step towards PDT aplications, the interaction between PS, singlet oxygen and the most abundant human protein, HSA, was studied. Proteins are present in most biological systems at particularly high concentrations and react rapidly with $^1O_2$. This suggests how the deep understanding of this interaction is important for the improvement of PDT applications.

The production of $^1O_2$ by $TPPS_4$ at various HSA concentrations under aerobic and anaerobic conditions together with effects of the $^1O_2$ interaction with HSA was investigated.

The concentration of HSA varied from 0 to 50 μM, in contrast to the concentration of $TPPS_4$, which remains constant 10 μM for all experiments. All samples were studied under aerobic and anaerobic conditions. Anaerobic conditions were reached by purging samples by N_2 gas for at least 1 hour. Solution of $TPPS_4$ in phosphate buffer was used for all measurements. The pH value of the buffer was the same as the pH value of human blood (7.4).

PS phosphorescence

Under anaerobic conditions, the $TPPS_4$ phosphorescence spectra and kinetics comprise of two different components, each of them exhibiting monoexponential kinetics. The lifetime of the shorter one (around 1.9 μs) does not change with the increasing HSA concentration. The maximum of this component lies at the wavelength of 820 nm. The lifetime of the long component rises with the increasing concentration of HSA from (405 ± 20) μs in the HSA-free sample to (990 ± 120) μs in the sample with the highest HSA concentration. This behaviour is probably caused by HSA shielding of the protein-bound $TPPS_4$ triplets from quenching by molecules of water.

The $TPPS_4$ phosphorescence in the presence of HSA under aerobic conditions consists again of two components. The faster one exhibits monoexponential decay with lifetime around 2 μs independent of the HSA concentration. The second phosphorescence component of much longer lifetime arises after the addition of HSA. Lifetimes of the slower component increase from (15.0 ± 1.4) to (100 ± 90) μs with the increasing HSA concentration. Integral intensity of the slower components also increases with the

increasing HSA concentration. It implies that the 2 μs component can be attributed to the phosphorescence of the free $TPPS_4$, while the other one corresponds to the phosphorescence of $TPPS_4$ bound to HSA. The ratio bound- / free- $TPPS_4$ rises with the increasing HSA concentration.The spectral behaviour of the long component is similar to the behaviour of the longer phosporescence component of $TPPS_4$ under anaerobic condition. The longer lifetime of bound $TPPS_4$ can be explained by the shielding of $TPPS_4$ by HSA against quenching by oxygen.

$^1O_2$ phosphorescence

The kinetics of the singlet oxygen phosphorescence can be described by an equation in the form of the linear combination of at least two expressions of Eq. (21) type with two different photosensitizer triplet lifetimes t_1 and t_2 corresponding to the free and bound $TPPS_4$. Taking into account the relatively high oxygen diffusion constant in water, it is rational to assume that each $^1O_2$ molecule is able to cross distances exceeding the size of HSA molecule as well as the space between them and interacts with both water and the HSA environment during its lifetime. This means, it is absolutely not important for the $^1O_2$ decay whether singlet oxygen was produced by free or bound $TPPS_4$. Therefore, the same effective value of t_{SO} for both components in Eq. (27) was used.

$$I(t) = \frac{I_2}{k_2 - k_3}\left[e^{-k_3 t} - e^{-k_2 t} \right] + \frac{I_1}{k_1 - k_3}\left[e^{-k_3 t} - e^{-k_1 t} \right] \qquad (27)$$

where $I(t)$ is the intensity of phosphorescence in the time t after excitation pulse, k_1 and k_2 are rate constants of population of singlet oxygen: $k_1 = \frac{1}{t_1}$, $k_2 = \frac{1}{t_2}$ and k_3 is the rate constants of depopulation of singlet oxygen: $k_3 = \frac{1}{t_{SO}}$.

The risetime t_1 = ~2 μs was obtained by fitting $^1O_2$ kinetics by Eq. (27). t_1 remains constant within the experimental error in the whole HSA concentration range. The risetime t_2 increases from (24.0 ± 4.0) to (47 ± 19) μs with increasing HSA concentration.

In the case of the t_{SO} lifetime, it also increases with the increasing HSA concentration. This prolonging (of the effective $^1O_2$ lifetime is due to the following fact: Molecules of water are more effective quenchers of singlet oxygen in comparision to

molecules of the majority of organic solvents. That means $^1O_2$ lives much longer in organic environments. After increasing the HSA concentration, the effective environment of singlet oxygen becomes more organic, what causes the above mentioned prolonging of the $^1O_2$ effective lifetime.

PS-$^1O_2$ interaction

Singlet oxygen lifetime t_1 corresponds to the lifetime of the free $TPPS_4$ phosphorescence very well. On the other hand, agreement between t_2 of bound ^{3}PS lifetime and t_2 $^1O_2$ rise time is not perfect. This suggests that singlet oxygen is photogenerated by free as well as by bound $TPPS_4$ and the shielding of bound $TPPS_4$ by HSA is not total.

HSA-$^1O_2$ interaction

The oxidation of HSA by singlet oxygen photogenerated by PS can appear during phosphorescence experiments. As the oxygen is consumed during this oxidation, the overall oxygen concentration in the sample decreases. The decrease of dissolved oxygen in the sample is reflected in the growth of $TPPS_4$ phosphorescence lifetimes t_2. To verify whether the oxidation occurs during our measurements, 38 kinetics measured in sequence were analysed. No detectable changes were observed for the lower HSA concentrations. On the other hand, a significant increase of t_2 appeared in the samples with the high HSA concentration (50 $\mu mol\ l^{-1}$).

5.5. PpIX and HpD incorporated in liposomes in H_2O and D_2O

There are various methods to transfer the water-insoluble PS via bloodstream to tumours. Among others, usage of liposomes as a drug delivery system seems to be very promising [59]: Liposomes are easily decomposable in the organism, are non-toxic (phospholipids are the part of cells membranes), can be used as a controlled transport system (composition of lipids, size, surface charge can be changed), and increase stability of various molecules by encapsulating them. In addition, liposomes can serve as a simple model of cell membrane.

In this chapter we have investigated the influence of the incorporation of PpIX and HpD into ≈100 nm unilamellar phosphatidylcholine liposomes on their photosensitizing properties and their interaction with singlet oxygen inside complex environments such as lipid membranes. H_2O and D_2O were used as solvents for liposomal solutions.

PS phosphorescence

Phosphorescence spectra of HpD and PpIX in liposomes in H_2O and D_2O exhibit their maxima around 830 nm. The phosphorescence decay of both PpIX and HpD in liposomes in H_2O follows a two-exponential decay with the lifetime t_1 of (0.28± 0.04) μs and t_2 of (3.3 ± 0.1) μs for PpIX and t_1 of (0.42± 0.05) μs and t_2 of (3.8 ± 0.1) μs for HpD.

In contrast with the phosphorescence of HpD and PpIX in acetone, two-exponential decays are necessary to successfully fit the phosphorescence of these pigments incorporated into liposomes. That suggests the presence of two different groups of the PS. As both studied PS are hydrophobic, their molecules are locked in the lipid bilayer. While the shorter component remained the same within our experimental accuracy after replacing H_2O by D_2O, the longer one increased to the value of (4.1±0.1) μs for PpIX and of (4.6±0.1) μs for HpD. It implies that the shorter phosphorescence lifetime corresponds to the group of pigments buried deep into the lipid bilayer, where they are effectively shielded from the outer environment influence. On the other hand, the longer component depends on the fact whether the liposomes are surrounded by normal or by heavy water. Therefore, the corresponding pigments are probably situated near the polar heads of the liposomes.

$^1O_2$ phosphorescence

Compared to the above mentioned measurements of the singlet oxygen luminescence in the acetonic solution of the PS, the signal of singlet oxygen in the case of the liposomes was very weak, causing a low signal-to-noise ratio.

The singlet oxygen phosphorescence maximum is found at 1278 nm. $^1O_2$ luminescence was superimposed on the tail of PS phosphorescence, thus it had to be corrected by subtracting the average of signals at 1242 and 1306 nm, where almost no $^1O_2$ luminescence is present. The corrected data were fitted by equation (27). This equation describes two mono-exponential rises and one effective mono-exponential decay of $^1O_2$. It was used also in the case of kinetics of singlet oxygen photogenerated by $TPPS_4$ in the presence of HSA.

The effective lifetime was used due to rather long diffusion length of singlet oxygen (≈0.4 μm). $^1O_2$ can easily escape the liposomes of 100 nm diameter and diffusion between different compartments is possible. Therefore, the decay of the singlet oxygen is mono-exponential and the effective lifetime is not related to the fact, whether photogeneration occured deep inside the bilayer or near the surface, making the two different singlet oxygen decay times irrelevant.

The decay times t_{SO}=(8.0±0.7) μs for HpD and t_{SO}=(7.3±0.6) μs for PpIX are the effective values between above mentioned decay time (3.7±0.1) μs of $^1O_2$ in water and 12.2 μs in pure phosphatidylcholine [82]. Moreover, it is in a good agreement with t_3=(9±2) μs for $^1O_2$ generated by Photofrin in lipid droplets in water [15].

The generally known fact, that the lifetime of singlet oxygen in D_2O is longer compared to H_2O was also confirmed in our results. The decay times t_3 were (41±2) μs for HpD and (37±1) μs for PpIX in D_2O.

PS-$^1O_2$ interaction

The transfer of the excitation energy from PS to singlet oxygen via two distinct pathways was observed. Both groups of PS with the different localizations (in the middle of the lipid bilayer and near to the liposome surface) are involved in this process. The ratio of phosphorescence intensity of the shorter component to that of the longer one is

approximately 1:4 for both PS for both solvents. It suggests, that the group of photosensitizer molecules situated near to the liposome surface plays a more important role in the PDT action in comparison with the group of PS molecules localised in the middle of lipid bilayer.

5.6. PpIX and HPD incorporated in liposomes samples saturated by air and by oxygen

The advantages of liposomes as a delivery system for lipophilic PS were described above. In this chapter, the penetration of oxygen into liposomes was studied. It was also examined how the PS are incorporated inside the lipid bilayer exposed to the environment of liposomes.

Phosphorescence measurements of PpIX, HpD and singlet oxygen in liposomal samples under different oxygen concentrations were performed in both H_2O and D_2O.

PS phosphorescence

Compared to air saturated liposomal solutions, HpD phosphorescence decreases about (40±5) %, while singlet oxygen luminescence increases approximately about (52±10) % after saturating samples by oxygen. Similar results were obtained for PpIX where we found PS decrease (24±5) % and $^1O_2$ increase (53±10) %. The decrease of PS phosphorescence is due to faster quenching of PS by oxygen. The accompanying increase of singlet oxygen phosphorescence corresponds to this faster quenching.

We have previously shown that kinetics of phosphorescence of both the investigated PS exhibits bi-exponential character with lifetimes t_1 = (0.42±0.05) μs, t_2 = (3.8±0.01) μs for HpD and t_1 = (0.28±0.04) μs, t_2 = (3.3±0.01) μs for PpIX. Increasing of oxygen concentration does not change the bi-exponential character of the decays. However, the lifetimes of both components change: For HpD lifetime t_1=(0.39±0.20) μs and t_2=(1.3±0.3) μs. PpIX in liposomes exhibits a little bit shorter lifetimes t_1=(0.25±0.04) μs and t_2=(1.2±0.03) μs.

As both HpD and PpIX are not soluble in water, it is reasonable to assume that all the PS is locked inside the lipid bilayer and singlet oxygen is generated in the liposomes solely. In the previous chapter, we have ascribed the two observed lifetimes to two distinct groups of PS: the group exhibiting the shorter lifetime is located deep inside the nonpolar lipid bilayer, whereas the group with longer lifetime is more exposed to the outer environment due to its localization near the bilayer surface. This identification of the PS

groups if further supported by our next results: the phosphorescence of the inner group is quenched less than that near the surface.

In HpD, this quenching is accompanied by corresponding change in contribution of the two components to the net PS phosphorescence signal — the shorter one contributes only 23 % of the total phosphorescence under air-saturated condition while 61 % after saturating by oxygen. In the case of PpIX, the observed change in contribution of the components is not that striking: from 23 % to 35 %. This is probably due to the lower polarity of PpIX compared to HpD (vinyl residues at carbon atoms C3 and C8 are in HpD substituted isopropanol residua), which makes it less exposed to the water environment. While the longer component exhibits dramatic decrease of the lifetime after purging by oxygen, the change of shorter one is only slight. This behaviour is based on the fact, that concentration of oxygen inside of the lipid bilayer is probably not proportional to the concentration of oxygen in the outer medium. The concentration of oxygen in lipid bilayer under transition temperature is known to be about 5 times lower than in surrounding water environment [83]. Further increase of oxygen concentration in the water leads only to minor increase of oxygen concentration inside lipid membrane. On the other hand, oxygen concentration in the water increases about 5 times and causes the significant change in slower decay component of the group of PS near the surface from 3.8 µs to 1.3 µs (HpD) and 3.3 µs to 1.2 µs (PpIX).

$^1O_2$ phosphorescence

Weak background signal of PS phosphorescence is present in case of both PpIX and HpD. The interpolated background signal between 1242 nm and 1306 nm (outside of singlet oxygen luminescence band) was subtracted to remove this phosphorescence.

The kinetics of singlet oxygen phosphorescence was fitted by model using two exponential increases and one mono-exponential decay (Equation 27). Two exponential increases were used to describe photogeneration of the singlet oxygen by the two different groups of PS. Again, taking into account relatively long diffusion length of singlet oxygen, only one effective singlet oxygen lifetime for the decay part of the kinetics was used.

Very low signal-to-noise ratio and strong scattered excitation light makes fitting of the data obtained for HpD by presented model with two rise-times unsuitable, as the shorter component provides unreasonable short value with enormous error. The obtained

value of t_2 = (0.5±0.3) µs therefore represents an effective value of both the PS groups. Anyway, this value lies between the lifetimes of HpD phosphorescence under oxygen saturated conditions.

On the other hand, it is possible to obtain two values of t_1 = (0.25±0.26) µs and t_2 = (1.1±0.6) µs in the case of singlet oxygen generated by PpIX in oxygen saturated H_2O. These values correspond well to the lifetimes of PpIX phosphorescence.

As was mentioned above, the obtained effective singlet oxygen lifetimes of 8.0 µs for HpD and 7.3 µs for PpIX in 100 nm liposomes in air saturated samples was observed. Under oxygen-saturated conditions the obtained decay time of singlet oxygen of (3.5±0.3) µs and (3.5±0.3) µs for HpD and PpIX respectively fit well with singlet oxygen lifetime of (3.5±0.1) µs in oxygen saturated sulphonato-tetraphenyl porphyrin aqueous solutions.

As oxygen saturation of the liposomal solution increases the concentration of oxygen inside the lipid bilayer only slightly, while the oxygen concentration in water rises 5 times, weight of the contribution of singlet oxygen lifetime in lipid to the effective lifetime of oxygen drops to almost insignificant portion, the observed lifetime of singlet oxygen is similar to that in pure oxygen saturated water.

It is generally known, that lifetime of singlet oxygen in D_2O (around 68 µs [73]) is order of magnitude longer compared to that in water. Therefore, similar experiments were performed also in D_2O. After saturating samples by oxygen, singlet oxygen lifetime decreases from 41±2 µs to 39±2 µs in PpIX samples and from 37±1 µs to 35±1 µs in HpD ones. This decrease is much weaker compared to that in H2O.

We have already shown above, that saturation of the sample by oxygen leads to substantial decrease of weight of the singlet oxygen lifetime in lipids in the effective lifetime of the singlet oxygen in both phases. This causes the effective lifetime to a change towards the singlet oxygen in water phase. While in H_2O this cause shortening of the effective lifetime, in case of D_2O, where singlet oxygen lifetime substantially exceeds that in pure lipids, leads to a longer one. Therefore, this prolongation of effective lifetime works in opposite direction than shortening of the lifetime due to singlet oxygen quenching by oxygen. This causes the observed effective lifetime shortening to appear relatively small compared to the situation in H_2O.

6. Conclusions

Our research begun with basic experiments where acetone was used as a solvent. It was shown, that PpIX and HpD exhibit striking difference in photosensitizer properties due to their different aggregation. Research has continued further towards biological systems.

In case of hydrophilic $TPPS_4$, phosphate buffers of particular values of pH were used as a solvent, instead of distilled water. pH values were carefully chosen with respect to the pH condition in biological systems. No concentration dependence was observed in the rise and decay times of the singlet-oxygen emission. On the other hand, the lifetimes of $TPPS_4$ phosphorescence exhibit an increase with the increasing concentration. These lifetimes are in a good agreement with the rise times of the singlet-oxygen luminescence for the lowest concentrations. An important piece of information was obtained: changing the pH value from 5.5 to 7.4 did not induce any changes of lifetimes, rate constants, or aggregation in $TPPS_4$ solutions.

Moreover, protein (HSA) was added into the samples of $TPPS_4$ in phosphate buffer in the next experiments to study very important interactions of singlet oxygen with proteins. It has proved the presence of two distinct groups of PS molecules: free ones and those bound to albumin. Although bound PS is partially shielded by HSA against quenching by water and by oxygen, both these groups generate singlet oxygen.

Attention was also paid to hydrophobic PS. HpD and PpIX were incorporated into the liposomal bilayer, which can simulate cell membrane very well. Their interactions with singlet oxygen together with their spectral characteristics in such a complex environment were investigated. PS phosphorescence in liposomes exhibits two components, the shorter one caused by PS in the middle of the lipid bilayer and the longer one caused by PS near the surface of the lipid bilayer, which is in contact with water. Differences of longer lifetime of the PS triplets near the surface of lipids bilayer between H_2O and D_2O environment suggest quenching of PS by the solvent. Lifetimes of singlet oxygen phosphorescence indicate that increasing of oxygen concentration in water medium is accompanied by only slight increase of oxygen concentration inside lipid bilayer. Based on this effect, the differences in behaviour of effective lifetimes of singlet oxygen phosphorescence under changes of oxygen concentration between H_2O and D_2O were explained.

7. References

[1] V. Prosser a kol., Experimentální metody biofyziky, Academia, Praha, 1989.

[2] M. J. Davies, Singlet oxygen-mediated damage to proteins and its consequences, Biochemical and Biophysical Research Communications, 305 (2003) 761-770.

[3] M. C. Derosa and R. J. Crutchley, Photosensitized singlet oxygen and its applications, Coordination Chemistry Reviews, 233 (2002) 351-371.

[4] F. Wilkinson, W. P. Helman, and A. B. Ross, Rate Constants for the Decay and Reactions of the Lowest Electronically Excited Singlet-State of Molecular-Oxygen in Solution - An Expanded and Revised Compilation, Journal of Physical and Chemical Reference Data, 24 (1995) 663-1021.

[5] C. Schweitzer and R. Schmidt, Physical mechanisms of generation and deactivation of singlet oxygen, Chemical Reviews, 103 (2003) 1685-1757.

[6] S. J. Arnold, M. Kubo, and E. A. Ogryzlo, Relaxation and Reactivity of Singlet Oxygen, Advances in Chemistry Series, (1968) 133-&.

[7] P. B. Merkel and D. R. Kearns, Remarkable Solvent Effects on Lifetime of Delta-1-G Oxygen, Journal of the American Chemical Society, 94 (1972) 1029-&.

[8] T. Takabatake, T. Miyazawa, M. Hasegawa, and C. S. Foote, Reaction of 4,7-dimethylbenzofurazan with singlet oxygen, Tetrahedron Letters, 42 (2001) 987-989.

[9] M. J. Steinbeck, A. U. Khan, and M. J. Karnovsky, Intracellular Singlet Oxygen Generation by Phagocytosing Neutrophils in Response to Particles Coated with A Chemical Trap, Journal of Biological Chemistry, 267 (1992) 13425-13433.

[10] T. W. Stief, The physiology and pharmacology of singlet oxygen, Medical Hypotheses, 60 (2003) 567-572.

[11] T. W. Stief, Singlet oxygen potentiates thrombolysis, Clinical and Applied Thrombosis-Hemostasis, 13 (2007) 259-278.

[12] K. Mullerbreitkreutz, H. Mohr, K. Briviba, and H. Sies, Inactivation of Viruses by Chemically and Photochemically Generated Singlet Molecular-Oxygen, Journal of Photochemistry and Photobiology B-Biology, 30 (1995) 63-70.

[13] M. Nepraš and M. Titz, Základy teorie elektronových spekter, SNTL, Praha 1983.

[14] J. Baier, T. Maisch, M. Maier, E. Engel, M. Landthaler, and W. Baumler, Singlet oxygen generation by UVA light exposure of endogenous photosensitizers, Biophysical Journal, 91 (2006) 1452-1459.

[15] A. Baier, M. Maier, R. Engl, M. Landthaler, and W. Baumler, Time-resolved investigations of singlet oxygen luminescence in water, in phosphatidylcholine, and in aqueous suspensions of phosphatidylcholine or HT29 cells, Journal of Physical Chemistry B, 109 (2005) 3041-3046.

[16] R. Dedic, A. Svoboda, J. Psencik, L. Lupinkova, J. Komenda, and J. Hala, Time and spectral resolved phosphorescence of singlet oxygen and pigments in photosystem II particles, Journal of Luminescence, 102 (2003) 313-317.

[17] A. A. Krasnovsky, P. Cheng, R. E. Blankenship, T. A. Moore, and D. Gust, The Photophysics of Monomeric Bacteriochlorophylls-C and Bacteriochlorophylls-D and Their Derivatives - Properties of the Triplet-State and Singlet Oxygen Photogeneration and Quenching, Photochemistry and Photobiology, 57 (1993) 324-330.

[18] M. Niedre, M. S. Patterson, and B. C. Wilson, Direct near-infrared luminescence detection of singlet oxygen generated by photodynamic therapy in cells in vitro and tissues in vivo, Photochemistry and Photobiology, 75 (2002) 382-391.

[19] C. A. Parker, Photoluminescence of Solutions, Elsevier, New York 1968.

[20] S. Yamaguchi and Y. Sasaki, Spectroscopic determination of very low quantum yield of singlet oxygen formation photosensitized by industrial dyes, Journal of Photochemistry and Photobiology A-Chemistry, 142 (2001) 47-50.

[21] J. Catalan, C. Diaz, and L. Barrio, Analysis of mixed solvent effects on the properties of singlet oxygen ^1D_g, Chemical Physics, 300 (2004) 33-39.

[22] S. Mashiko, N. Suzuki, S. Koga, M. Nakano, T. Goto, T. Ashino, I. Mizumoto, and H. Inaba, Measurement of Rate Constants for Quenching Singlet Oxygen with A Cypridina Luciferin Analog (2-Methyl-6-[Para-Methoxyphenyl]-3,7-Dihydroimidazo[1,2-A]Pyrazin-3-One) and Sodium-Azide, Journal of Bioluminescence and Chemiluminescence, 6 (1991) 69-72.

[23] M. Y. Li, C. S. Cline, E. B. Koker, H. H. Carmichael, C. F. Chignell, and P. Bilski, Quenching of singlet molecular oxygen (O-1(2)) by azide anion in solvent mixtures, Photochemistry and Photobiology, 74 (2001) 760-764.

[24] R. Le Panse, L. Dubertret, and B. Coulomb, p38 mitogen-activated protein kinase activation by ultraviolet A radiation in human dermal fibroblasts, Photochemistry and Photobiology, 78 (2003) 168-174.

[25] H. C. Wei, Q. Y. Cai, R. Rahn, and X. S. Zhang, Singlet oxygen involvement in ultraviolet (254 nm) radiation-induced formation of 8-hydroxy-deoxyguanosine in DNA, Free Radical Biology and Medicine, 23 (1997) 148-154.

[26] E. L. Clennan, New mechanistic and synthetic aspects of singlet oxygen chemistry, Tetrahedron, 56 (2000) 9151-9179.

[27] A. A. Frimer, Singlet O2, CRC Press, Boca Raton, Florida 1985.

[28] D. R. Kearns, Physical and Chemical Properties of Singlet Molecular Oxygen, Chemical Reviews, 71 (1971) 395-&.

[29] R. Bonnett and G. Martinez, Photobleaching of sensitisers used in photodynamic therapy, Tetrahedron, 57 (2001) 9513-9547.

[30] M. B. Ericson, S. Grapengiesser, F. Gudmundson, A. M. Wennberg, O. Larko, J. Moan, and A. Rosen, A spectroscopic study of the photobleaching of protoporphyrin IX in solution, Lasers in Medical Science, 18 (2003) 56-62.

[31] J. Ferreira, P. F. C. Menezes, C. Kurachi, C. H. Sibata, R. R. Allison, and V. S. Bagnato, Comparative study of photodegradation of three hematoporphyrin derivative: Photofrin (R), Photogem (R) and Photosan, Laser Physics Letters, 4 (2007) 743-748.

[32] J. Moan, G. Streckyte, S. Bagdonas, O. Bech, and K. Berg, Photobleaching of protoporphyrin IX in cells incubated with 5-aminolevulinic acid, International Journal of Cancer, 70 (1997) 90-97.

[33] R. Rotomskis, G. Streckyte, and S. Bagdonas, Phototransformations of sensitizers .1. Significance of the nature of the sensitizer in the photobleaching process and photoproduct formation in aqueous solution, Journal of Photochemistry and Photobiology B-Biology, 39 (1997) 167-171.

[34] R. Sorensen, V. Iani, and J. Moan, Kinetics of photobleaching of protoporphyrin IX in the skin of nude mice exposed to different fluence rates of red light, Photochemistry and Photobiology, 68 (1998) 835-840.

[35] R. Gerdes, D. Wohrle, W. Spiller, G. Schneider, G. Schnurpfeil, and G. Schulz-Ekloff, Photo-oxidation of phenol and monochlorophenols in oxygen-saturated aqueous solutions by different photosensitizers, Journal of Photochemistry and Photobiology A-Chemistry, 111 (1997) 65-74.

[36] M. Nowakowska and M. Kepczynski, Polymeric photosensitizers - 2. Photosensitized oxidation of phenol in aqueous solution, Journal of Photochemistry and Photobiology A-Chemistry, 116 (1998) 251-256.

[37] V. Iliev, V. Alexiev, and L. Bilyarska, Effect of metal phthalocyanine complex aggregation on the catalytic and photocatalytic oxidation of sulfur containing compounds, Journal of Molecular Catalysis A-Chemical, 137 (1999) 15-22.

[38] W. Spiller, D. Wohrle, G. SchulzEkloff, W. T. Ford, G. Schneider, and J. Stark, Photo-oxidation of sodium sulfide by sulfonated phthalocyanines in oxygen-saturated aqueous solutions containing detergents or latexes, Journal of Photochemistry and Photobiology A-Chemistry, 95 (1996) 161-173.

[39] V. Iliev, L. Prahov, L. Bilyarska, H. Fischer, G. Schulz-Ekloff, D. Wohrle, and L. Petrov, Oxidation and photooxidation of sulfide and thiosulfate ions catalyzed by transition metal chalcogenides and phthalocyanine complexes, Journal of Molecular Catalysis A-Chemical, 151 (2000) 161-169.

[40] V. Iliev, A. Ileva, and L. Bilyarska, Oxidation and photooxidation of sulfur-containing compounds in the presence of immobilized phthalocyanine complexes, Journal of Molecular Catalysis A-Chemical, 126 (1997) 99-108.

[41] W. Adam, Ch. R. Saha-Moeller, and O. Weichold, Synthesis of Optically Active á-Methyl â-Hydroperoxy Esters by Diastereoselective Singlet Oxygen Ene Reaction and Horseradish Peroxidase Catalyzed Kinetic Resolution, Monatshefte fur Chemie, 131 (2000) 697-705.

[42] H. Takeya, H. Ueki, S. Miyanari, T. Shimizu, and M. Kojima, A new synthesis of 5-aminolevulinic acid via dye-sensitized oxygenation of N-furfurylphthalimide, Journal of Photochemistry and Photobiology A-Chemistry, 94 (1996) 167-171.

[43] E. Choe and D. B. Min, Chemistry and reactions of reactive oxygen species in foods, Journal of Food Science, 70 (2005) R142-R159.

[44] E. Choe and D. B. Min, Chemistry and reactions of reactive oxygen species in foods, Critical Reviews in Food Science and Nutrition, 46 (2006) 1-22.

[45] J. E. Brown, B. B. Brown, and D. I. Vernon, Photosensitizing drug-their potential in oncology, Expert Opinion on Investigational Drugs, 8 (1999) 1967-1979.

[46] J. E. Brown, S. B. Brown, and D. I. Vernon, Photodynamic therapy - new light on cancer treatment, Journal of the Society of Dyers and Colourists, 115 (1999) 249-253.

[47] J. Fuchs and J. Thiele, The role of oxygen in cutaneous photodynamic therapy, Free Radical Biology and Medicine, 24 (1998) 835-847.

[48] M. Ochsner, Photophysical and photobiological processes in the photodynamic therapy of tumours, Journal of Photochemistry and Photobiology B-Biology, 39 (1997) 1-18.

[49] W. M. Sharman, C. M. Allen, and J. E. van Lier, Photodynamic therapeutics: basic principles and clinical applications, Drug Discovery Today, 4 (1999) 507-517.

[50] G. Jori, Molecular biology of photodynamic action, in: R. Pratesi and C. A. Sacchi (Eds.), Laser in Photomedicine and Photobiology, Proceedings of the European Physical Society. Quantum Electronics Division. Conference. Florence, Italy. September 3-6, 1979, Springer-Verlag, Berlin, 1980, pp. 58-66.

[51] M. J. Davies, The oxidative environment and protein damage, Biochimica et Biophysica Acta-Proteins and Proteomics, 1703 (2005) 93-109.

[52] R. A. Floyd, M. S. West, K. L. Eneff, and J. E. Schneider, Methylene-Blue Plus Light Mediates 8-Hydroxyguanine Formation in Dna, Archives of Biochemistry and Biophysics, 273 (1989) 106-111.

[53] R. A. Floyd, M. S. West, J. E. Schneider, J. J. Watson, and M. L. Maidt, Hematoporphyrin D plus light mediates 8-hydroxyguanine formation in DNA and RNA, Free Radical Biology and Medicine, 9 (1990) 76.

[54] J. E. Schneider, S. Price, L. Maidt, J. M. C. Gutteridge, and R. A. Floyd, Methylene-Blue Plus Light Mediates 8-Hydroxy 2'-Deoxyguanosine Formation in Dna Preferentially Over Strand Breakage, Nucleic Acids Research, 18 (1990) 631-635.

[55] B. Epe, Genotoxicity of Singlet Oxygen, Chemico-Biological Interactions, 80 (1991) 239-260.

[56] J. Piette, Biological Consequences Associated with Dna Oxidation Mediated by Singlet Oxygen, Journal of Photochemistry and Photobiology B-Biology, 11 (1991) 241-260.

[57] T. P. A. Devasagayam, S. Steenken, M. S. W. Obendorf, W. A. Schulz, and H. Sies, Formation of 8-Hydroxy(Deoxy)Guanosine and Generation of Strand Breaks at Guanine Residues in Dna by Singlet Oxygen, Biochemistry, 30 (1991) 6283-6289.

[58] J. Piette, C. M. Calbergbacq, and A. V. Devorst, Alteration of Guanine Residues During Proflavine Mediated Photosensitization of Dna, Photochemistry and Photobiology, 33 (1981) 325-333.

[59] Y. N. Konan, R. Gurny, and E. Allemann, State of the art in the delivery of photosensitizers for photodynamic therapy, Journal of Photochemistry and Photobiology B-Biology, 66 (2002) 89-106.

[60] V. R. Litle, J. D. Luketich, N. A. Christie, P. O. Buenaventura, M. velo-Rivera, J. S. McCaughan, N. T. Nguyen, and H. C. Fernando, Photodynamic therapy as palliation for esophageal cancer: Experience in 215 patients, Annals of Thoracic Surgery, 76 (2003) 1687-1692.

[61] S. J. Tang, P. Fellow, and N. E. Marcon, Photodynamic therapy in the esophagus, Photodiagnosis and Photodynamic Therapy, 1 (2004) 65-74.

[62] C. F. Lee, C. J. Lee, C. T. Chen, and C. T. Huang, delta-Aminolaevulinic acid mediated photodynamic antimicrobial chemotherapy on Pseudomonas aeruginosa planktonic and biofilm cultures, Journal of Photochemistry and Photobiology B-Biology, 75 (2004) 21-25.

[63] R. F. V. Lopez, N. Lange, R. Guy, and M. V. L. B. Bentley, Photodynamic therapy of skin cancer: controlled drug delivery of 5-ALA and its esters, Advanced Drug Delivery Reviews, 56 (2004) 77-94.

[64] P. Jezek, M. Nekvasil, E. Skobisova, E. Urbankova, M. Jirsa, M. Zadinova, P. Pouckova, and N. Klepacek, Experimental photodynamic therapy with meso-tetrakisphenylporphyrin (TPP) in liposomes leads to disintegration of human amelanotic melanoma implanted to nude mice, International Journal of Cancer, 103 (2003) 693-702.

[65] D. L. Akins, H. R. Zhu, and C. Guo, Aggregation of tetraaryl-substituted porphyrins in homogeneous solution, Journal of Physical Chemistry, 100 (1996) 5420-5425.

[66] L. Kelbauskas, S. Bagdonas, W. Dietel, and R. Rotomskis, Excitation relaxation and structure of TPPS4 J-aggregates, Journal of Luminescence, 101 (2003) 253-262.

[67] O. Ohno, Y. Kaizu, and H. Kobayashi, J-Aggregate Formation of A Water-Soluble Porphyrin in Acidic Aqueous-Media, Journal of Chemical Physics, 99 (1993) 4128-4139.

[68] R. F. Pasternack, C. Fleming, S. Herring, P. J. Collings, J. dePaula, G. DeCastro, and E. J. Gibbs, Aggregation kinetics of extended porphyrin and cyanine dye assemblies, Biophysical Journal, 79 (2000) 550-560.

[69] P. Kubat and J. Mosinger, Photophysical properties of metal complexes of meso-tetrakis(4-sulphonatophenyl)porphyrin, Journal of Photochemistry and Photobiology A-Chemistry, 96 (1996) 93-97.

[70] M. Lapes, J. Petera, and M. Jirsa, Photodynamic therapy of cutaneous metastases of breast cancer after local application of meso-tetra-(para-sulphophenyl)-porphin (TPPS4), Journal of Photochemistry and Photobiology B-Biology, 36 (1996) 205-207.

[71] R. Dedic, A. Svoboda, J. Psencik, and J. Hala, Phosphorescence of singlet oxygen and meso-tetra (4-sulfonatophenyl)porphin: time and spectral resolved study, Journal of Molecular Structure, 651 (2003) 301-304.

[72] M. Korinek, R. Dedic, A. Svoboda, and J. Hala, Luminescence study of singlet oxygen production by meso-tetraphenylporphine, Journal of Fluorescence, 14 (2004) 71-74.

[73] R. Kilger, M. Maier, R. M. Szeimies, and W. Baumler, Bidirectional energy transfer between the triplet T-1 state of photofrin and singlet oxygen in deuterium oxide, Chemical Physics Letters, 343 (2001) 543-548.

[74] E. Skovsen, J. W. Snyder, J. D. C. Lambert, and P. R. Ogilby, Lifetime and diffusion of singlet oxygen in a cell, Journal of Physical Chemistry B, 109 (2005) 8570-8573.

[75] W. F. Linke, Solubilities of Inorganic and Metal Organic Compounds, American Chemical Society, Washington DC, 1965.

[76] S. Sugio, A. Kashima, S. Mochizuki, M. Noda, and K. Kobayashi, Crystal structure of human serum albumin at 2.5 angstrom resolution, Protein Engineering, 12 (1999) 439-446.

[77] E. S. Lee, K. Na, and Y. H. Bae, Polymeric micelle for tumor pH and folate-mediated targeting, Journal of Controlled Release, 91 (2003) 103-113.

[78] S. Mordon, J. M. Devoisselle, and S. Soulie, Fluorescence Spectroscopy of Ph In-Vivo Using A Dual-Emission Fluorophore (C-Snafl-1), Journal of Photochemistry and Photobiology B-Biology, 28 (1995) 19-23.

[79] M. Stubbs, P. M. J. McSheehy, J. R. Griffiths, and C. L. Bashford, Causes and consequences of tumour acidity and implications for treatment, Molecular Medicine Today, 6 (2000) 15-19.

[80] K. Chikakane and H. Takahashi, Measurement of skin pH and its significance in cutaneous diseases, Clinics in Dermatology, 13 (1995) 299-306.

[81] H. C. Korting and O. BraunFalco, The effect of detergents on skin pH and its consequences, Clinics in Dermatology, 14 (1996) 23-27.

[82] B. Ehrenberg, J. L. Anderson, and C. S. Foote, Kinetics and yield of singlet oxygen photosensitized by hypericin in organic and biological media, Photochemistry and Photobiology, 68 (1998) 135-140.

[83] W. K. Subczynski and J. S. Hyde, Concentration of Oxygen in Lipid Bilayers Using A Spin-Label Method, Biophysical Journal, 41 (1983) 283-286.

8. List of enclosures

1) **A. Molnár**, R. Dědic, M. Kořínek, A. Svoboda, J. Hála, Protoporphyrin IX and hematoporphyrin derivatives interactions with oxygen studied by time and spectral resolved phosphorescence, Journal of Molecular Structure 744 (2005) 723-726.

2) R. Dědic, **A. Molnár**, M. Kořínek, A. Svoboda, J. Pšenčík and J. Hála, Spectroscopic study of singlet oxygen photogeneration in meso-tetra-sulphonatophenyl-porphin, Journal of Luminiscence 108 (2004) 117-119.

3) R. Dědic, M. Kořínek, **A. Molnár**, A. Svoboda and J. Hála, Singlet oxygen quenching by oxygen in tetraphenyl-porphyrin solutions, Journal of Luminiscence 119 (2006): 209-213.

4) M. Kořínek , R. Dědic, **A. Molnár**, and J. Hála, The influence of human serum albumin on the photogeneration of singlet oxygen by meso-tetra(4-sulphonatophenyl)porphyrin. Infrared emission study., Journal of Fluorescence 16 (2006) 355-359.

5) **A. Molnár**, R. Dědic, A. Svoboda and J. Hála, Singlet oxygen production by lipophilic photosensitizers in liposomes studies by time and spectral resolved phosphorescence, Journal of Molecular Structure 834 (2007) 488-491.

6) **A. Molnár**, R. Dědic, A. Svoboda, J. Hála, Spectroscopic study of singlet oxygen photogeneration by lipophilic photosensitizer in liposomes, Journal of Luminiscence, accepted for publication.

Enclosure 1

A. Molnár, R. Dedic, M. Korínek, A. Svoboda, J. Hála, Protoporphyrin IX and hematoporphyrin derivatives interactions with oxygen studied by time and spectral resolved phosphorescence, Journal of Molecular Structure 744 (2005) 723-726.

Available online at www.sciencedirect.com
SCIENCE DIRECT
Journal of Molecular Structure 744–747 (2005) 723–726
Journal of MOLECULAR STRUCTURE
www.elsevier.com/locate/molstruc

Protoporphyrin IX and hematoporphyrin derivatives interactions with oxygen studied by time and spectral resolved phosphorescence

A. Molnár*, R. Dědic, M. Kořínek, A. Svoboda, J. Hála

Department of Chemical Physics and Optics, Faculty of Mathematics and Physics, Charles University, Ke Karlovu 3, CZ 121 16 Praha 2, Czech Republic

Received 7 September 2004; accepted 18 October 2004
Available online 15 December 2004

Abstract

In this contribution energy transfer from chemically similar porphyrin-like molecules of hematoporphyrin derivatives and protoporphyrin IX, used in photodynamic therapy as photosensitizers was investigated. The photosensitizers phosphorescence (about 840 nm) kinetics together with singlet oxygen production were measured by means of IR time and spectral resolved phosphorescence (at 1275 nm) in wide range of the photosensitizer concentrations (5–200 μM). The submicrosecond photosensitizers triplet life-times were compared to submicrosecond singlet oxygen phosphorescence rise-times. Moreover, microsecond singlet oxygen phosphorescence life-times and rate constants of singlet oxygen quenching by the photosensitizers were determined. The differences in obtained life-times and concentration trends were discussed and explained in the frame of the photosensitizers aggregation. Hematoporphyrin derivatives behave as non-aggregating photosensitizer, while protoporphyrin IX exhibits an aggregation.
© 2004 Elsevier B.V. All rights reserved.

Keywords: Hematoporphyrin derivatives; Protoporphyrin IX; Singlet oxygen; Photodynamic therapy

1. Introduction

Photodynamic therapy (PDT) is a promising way of cancer treatment. The main advantage of this method is in high selectivity towards diseased tissue. That means that PDT destroys tumor only, with no effect to healthy tissue. The selectivity of PDT stems from both the localization of the photosensitizer (PS) in the tumor and the ability to confine activation of the PS by local illumination of the tumor region solely. Generally accepted reasons of PS localization in the tumor are higher acidity of tumor together with different intercellular space, the leaky vasculature and the poor lymphatic drainage of tumor cells compared to healthy tissue [1,2].

In PDT, a light, a light-sensitive drug (PS), and oxygen are combined to the produce highly reactive substances lethal to tumor cells. First, the PS is administered into patient's body. After a delay, when PS is accumulated predominantly in tumor tissue, the tumor is irradiated at appropriate wavelength. The light source can be as simple as a projector lamp, although lasers and fiber optics are often used. After the irradiation, PS undergoes transition into the excited singlet state, which easily converts to the triplet state. The ground state of molecular oxygen is a triplet. On the other hand, the first excited state of oxygen is a singlet. As the triplet state of PS exhibits higher energy than the singlet state of oxygen, energy transfer from PS to singlet oxygen occurs easily. This way highly reactive singlet oxygen is produced, which destroys biologically significant molecules, such as proteins or lipids [3]. While it is widely accepted that singlet oxygen is the cytotoxic agent responsible for direct destroying of tumor cells, other reactions, for example, radical formation, may also play a supporting role.

Derivatives of hematoporphyrin (HpD) were one of the first photosensitizers used for PDT [4]. Acetylation and reduction of hematoporphyrin produces a complex mixture of HpD with strong photosensitizing properties. Photofrin®,

* Corresponding author. Tel.: +420 221 911 307; fax: +420 221 911 249.
E-mail address: egi@matfyz.cz (A. Molnár).

0022-2860/$ - see front matter © 2004 Elsevier B.V. All rights reserved.
doi:10.1016/j.molstruc.2004.10.087

which is a partially purified form of HpD, has received approval for clinical use in the treatment of esophageal cancer [5,6].

Photoporphyrin IX is a metabolic product of δ-aminolevulinic acid (PDT drug Levulan® from DUSA) in human body [7]. Fluorescent and photosensitizing properties of PpIX accumulated after the exogenous administration of δ-aminolevulinic acid, can be used to visualize and destroy malignant cells in the so-called photodynamic diagnosis and PDT of cancer. Many clinical δ-aminolevulinic acid PDT applications to malignant and non-malignant pathologies are currently in use [8].

Besides chemical methods [9], photoproduction of singlet oxygen can be quantified also using spectroscopic methods [10]. The main advantages of spectroscopic methods over the chemical ones is their ability not only to determine singlet oxygen quantum yields but also describe and explain excitation energy transfer between PS and oxygen. Phosphorescence spectra and kinetics together with their concentration dependencies of phtalocyanine photosensitizers as well as that of singlet oxygen were measured [11]. In this article, similar direct spectroscopic study of porphyrin-like PS HpD and PpIX is presented.

2. Materials

Both photosensitizers used in this study (HpD and PpIX) were obtained from Frontier Scientific Porphyrin Products. The purity of the materials was checked by their absorption and fluorescence spectra. HpD and PpIX were dissolved in acetone. All samples were prepared in the set of concentrations: 5, 10, 20, 30, 50, 75, 100, 150 and 200 μmol l^{-1}.

3. Methods

Absorption spectrometer Perkin Elmer Lambda 12 UV/VIS was used to measure absorption spectra of PS between 300 and 800 nm with resolution of 1 nm. Standard spectroscopic cells (optical path 0.1, 1 and 2 mm) were used.

Home-built set-up was used to measure time and spectral resolved phosphorescence of singlet oxygen [12]. The samples were excited at 420 nm by laser pulses (20 ns, ≈40 μJ, 40 Hz repetition) provided by a dye laser Lambda Physik FL 3001 (Stilbene 3 in methanol), pumped by excimer laser Lambda Physik LPX 100. The laser beam was focused to a fluorescence cuvette through its bottom. The phosphorescence of singlet oxygen and PS was collected from 0.8 mm high sample spot by lens assembly through a long-pass filter (Schott RG 7) and high luminosity monochromator Jobin-Yvon H20 IR to the infrared sensitive photomultiplier Hamamatsu R5509 (cooled to −80 °C by liquid nitrogen). The photomultiplier output was fed through the Becker-Hickl HF AC-26 dB preamplifier to the Becker-Hickl MSA 200 photon counter/multiscaler triggered by a fast PIN photodiode. Time-resolved measurements of singlet oxygen with 5 ns resolution were performed in the spectral region from 1242 to 1306 nm, with steps of 4 nm. Phosphorescence of PS was measured from 750 to 990 nm, with steps of 16 nm. This way we obtained the set of time and spectral resolved phosphorescence data of both PS and singlet oxygen.

Fluorescence of PS was collected perpendicularly to the excitation beam to multichannel spectrometer Avantes S2000, using an optic fiber.

4. Results

Absorption spectra of PpIX and HpD in acetone were measured in wide range of concentration. Linear dependence of absorbance on concentration was found in HpD (Fig. 1). HpD exhibited no concentration-induced changes in the spectral positions and shapes of fluorescence bands (data not shown). On the other hand, absorbance of PpIX at 420 nm shows non-linear dependence for higher concentrations. Red shifts of the fluorescence maxima were found when concentration was increased.

Fig. 2 presents absorption, fluorescence, and phosphorescence of HpD accompanied by phosphorescence of singlet oxygen. HpD phosphorescence exhibits its maximum around 840 nm independent of concentration. The singlet oxygen phosphorescence peak lies at 1275 nm with FWHM of 27 nm.

Phosphorescence of HpD follows mono-exponential decay with life-time of (0.35 ± 0.01) μs independent of HpD concentration. Kinetics of singlet oxygen phosphorescence is described by equation:

$$I(t) = \frac{I_0}{k_2 - k_1}[e^{-k_1 t} - e^{-k_2 t}]$$

where $I(t)$ is the intensity of phosphorescence in the time t after excitation pulse, k_1 and k_2 are rate constants of

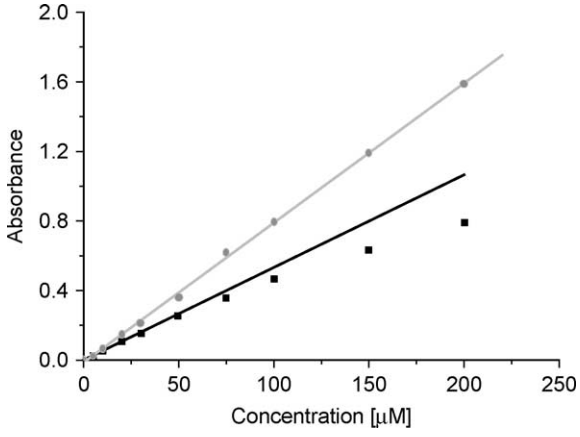

Fig. 1. Concentration dependence of HpD (circles) and PpIX (squares) absorbance at 420 nm.

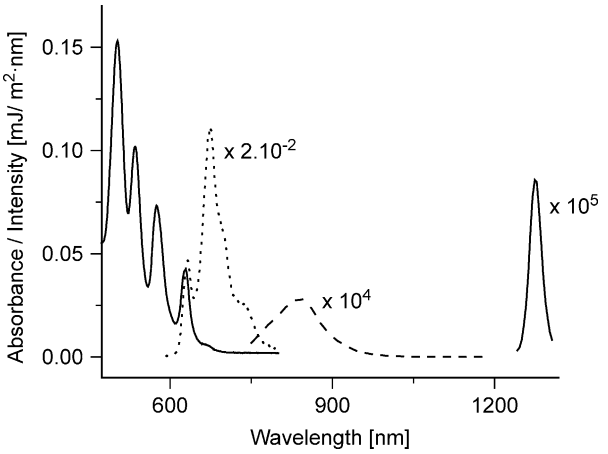

Fig. 2. Red part of absorption spectra (*solid*) together with fluorescence (*dotted*), and phosphorescence (*dashed*) of HpD in acetone and phosphorescence of singlet oxygen (*solid*).

population and depopulation of singlet oxygen: $k_1 = 1/\tau_1$, $k_2 = 1/\tau_2$. The fast rise-time of singlet oxygen phosphorescence τ_1 (0.28 ± 0.01) μs does not depend on HpD concentration. On the other hand, the life-time of singlet oxygen τ_2 decreases with increasing HpD concentration. This decrease corresponds to bimolecular quenching of singlet oxygen by HpD expressed in Stern-Volmer equation:

$$k_2(c_{\mathrm{HpD}}) = k_0 + k_q \cdot c_{\mathrm{HpD}}$$

(see Fig. 3). The value of the quenching constant k_q was determined as $(12.4 \pm 1.2) \times 10^6\ \mathrm{M}^{-1}\ \mathrm{s}^{-1}$. Life-time of singlet oxygen extrapolated to zero HpD concentration is (52.3 ± 1.1) μs.

PpIX triplet life-time increases with increasing PpIX concentration from (0.15 ± 0.02) μs to saturated value (0.22 ± 0.02) μs (Fig. 4). Rise-time of singlet oxygen of (0.24 ± 0.02) μs does not depend on PpIX concentration. It is somewhat bigger than the longest life-times of PpIX triplets. Life-time of singlet oxygen again decreases with increasing PpIX concentration, but in this case the decrease does not follow bimolecular quenching.

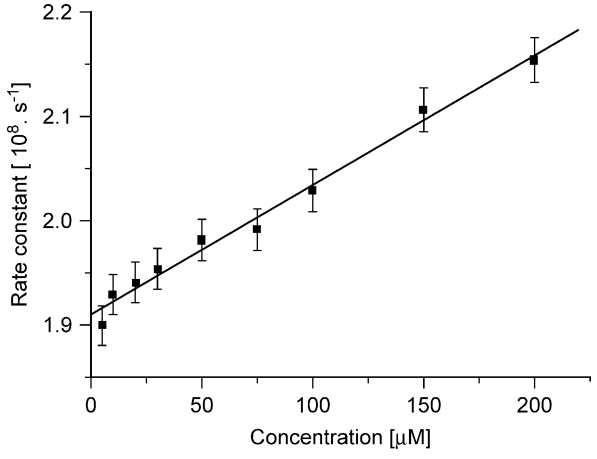

Fig. 3. Singlet oxygen rate constant dependence on HpD concentration.

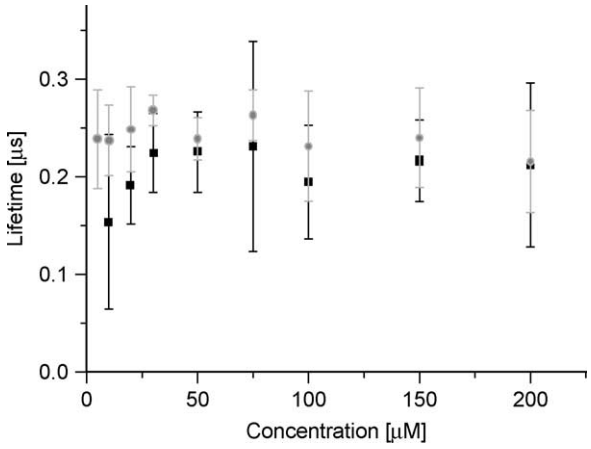

Fig. 4. ^{3}PpIX life-time (squares) and $^1O_2$ rise-time (circles) dependence on PpIX concentration.

5. Discussion

Linear dependence of HpD absorbance at 420 nm (see Fig. 1) confirms presence of just one spectroscopic form of HpD in acetone in whole studied concentration range. It is also proved by fluorescence spectra. Nevertheless, to explain the discrepancy between life-times of HpD triplets of (0.35 ± 0.01) μs and singlet oxygen phosphorescence rise-times of (0.28 ± 0.01) μs, an existence of two distinct forms of HpD has to be assumed. One of them, with life-times equal to rise-time of singlet oxygen, transfers its excitation energy to oxygen. The other one, spectrally indistinguishable from the first one, cannot be quenched by oxygen making the effective life-times of HpD longer. Similar behavior was reported earlier for meso-tetraphenylporphyrin in acetone [13].

Deviation from linear dependence (see Fig. 1) indicates the aggregation of PpIX in acetone. Factor analysis results suggest a presence of at least two spectral components. The aggregation is also supported by bathochromic shifts observed in fluorescence spectra. The increase of PpIX triplet life-times with concentration corresponds to increasing ratio of aggregates to monomeric forms. This behavior is in a very good agreement with that observed in aggregating meso-tetra(4-sulfonatophenyl)porphyrin in buffers [14]. However, the difference between the saturated life-times of PpIX of (0.22 ± 0.02) μs and the rise-times of $^1O_2$ of (0.24 ± 0.02) μs cannot be explained in the frame of only two components: monomers and aggregates. Suggested explanation is based on dividing of the aggregated molecules into two sets: envelope and core ones. Only those in the envelope can effectively transfer excited energy to oxygen and their phosphorescence life-times are equal to the singlet oxygen rise-times. The core molecules, inaccessible to oxygen quenching cause the shorter effective life-times of PpIX aggregates.

Deviations from Stern-Volmer equation can be due to quenching of singlet oxygen predominantly by

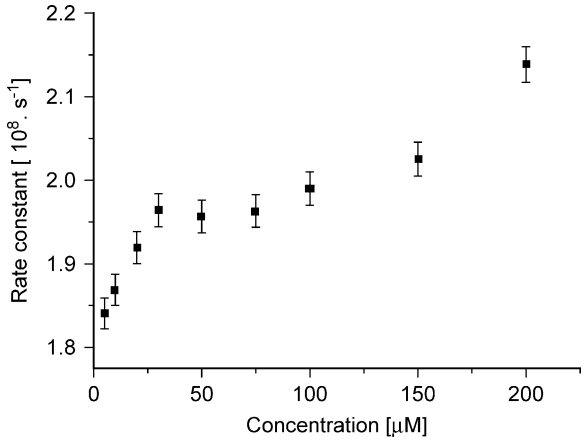

Fig. 5. Singlet oxygen rate constant dependence on PpIX concentration.

PpIX monomers. This results in faster quenching constants in the low concentration region of Fig. 5, where monomeric form prevails. As with increasing concentration of PpIX portion of the monomers decreases, decreases also the quenching constant.

6. Conclusion

Infrared time and spectral resolved phosphorescence of protoporphyrin IX and hematoporphyrin derivatives were measured together with by them photogenerated singlet oxygen in wide range of photosensitizer concentration. The obtained photosensitizer triplet life-times were compared to singlet oxygen phosphorescence rise-times. The differences and concentration trends were discussed and explained in the frame of aggregation. Hematoporphyrin derivatives, where are no spectral features of aggregation, behave qualitatively the same as non-aggregating meso-tetraphenylporphyrin. On the contrary, protoporphyrin IX exhibits an aggregation similar to aggregating meso-tetra(4-sulfonatophenyl)porphyrin. Chemically similar porphyrin-like molecules, hematoporphyrin derivatives and protoporphyrin IX, exhibit striking difference in photosensitizer properties due to their different aggregation.

Acknowledgements

This work was supported by grants GP202/01/D100 from Grant Agency of the Czech Republic and project MSM13200001 from the Ministry of Education of the Czech Republic. The authors would like to thank to Assoc. Prof. Peter Mojzeš from Institute of Physics of Charles University in Prague for his kind help with the factor analysis.

References

[1] Y.N. Konan, R. Gurny, E. Allemann, J. Photochem. Photobiol. B 66 (2002) 89.
[2] M. Ochsner, J. Photochem. Photobiol. B 39 (1997) 1.
[3] M.J. Davies, C. Hawkins, A. Wright, Free Radic. Biol. Med. 33 (2002) S420.
[4] R. Bonnett, G. Martinez, Tetrahedron 57 (2001) 9513.
[5] S.J. Tang, P. Fellow, N.E. Marcon, Photodiagn. Photodyn. Ther. 1 (2004) 65.
[6] V.R. Litle, J.D. Luketich, N.A. Christie, P.O. Buenaventura, M. Alvelo-Rivera, J.S. McCaughan, N.T. Nguyen, H.C. Fernando, Ann. Thorac. Surg. 76 (2003) 1687.
[7] C.F. Lee, C.J. Lee, C.T. Chen, C.T. Huang, J. Photochem. Photobiol. B 75 (2004) 21.
[8] R.F.V. Lopez, N. Lange, R. Guy, M.V.L.B. Bentley, Adv. Drug Deliver. Rev. 56 (2004) 77.
[9] C. Tanielian, C. Schweitzer, R. Mechin, C. Wolff, Free Radic. Biol. Med. 30 (2001) 208.
[10] A.A. Abdel-Shafi, D.R. Worrall, F. Wilkinson, J. Photochem. Photobiol. A 142 (2001) 133.
[11] M. Niedre, M.S. Patterson, B.C. Wilson, Photochem. Photobiol. 75 (2002) 382.
[12] R. Dedic, A. Svoboda, J. Psencik, J. Hala, J. Mol. Struct. 651 (2003) 301.
[13] M. Korinek, R. Dedic, A. Svoboda, J. Hala, J. Fluoresc. 14 (2004) 71.
[14] R. Dedic, A. Molnar, M. Korinek, A. Svoboda, J. Psencik, J. Hala, J. Lumin. 108 (2004) 117.

Enclosure 2

R. Dedic, **A. Molnár**, M. Korínek, A. Svoboda, J. Pšencík and J. Hála, Spectroscopic study of singlet oxygen photogeneration in meso-tetra-sulphonatophenyl-porphin, Journal of Luminiscence 108 (2004) 117-119.

Available online at www.sciencedirect.com
SCIENCE DIRECT®
Journal of Luminescence 108 (2004) 117–119
JOURNAL OF LUMINESCENCE
www.elsevier.com/locate/jlumin

Spectroscopic study of singlet oxygen photogeneration in meso-tetra-sulphonatophenyl-porphin

Roman Dědic*, Alexander Molnár, Miloslav Kořínek, Antonín Svoboda, Jakub Pšenčík, Jan Hála

Department of Chemical Physics and Optics, Faculty of Mathematics and Physics, Charles University, Ke Karlovu 3, 121 16 Prague 2, Czech Republic

Abstract

Meso-tetra(4-sulphonatophenyl)porphin ($TPPS_4$) is commonly used as a photosensitiser in photodynamic therapy. In this contribution, we have studied the dependence of singlet oxygen photogeneration by $TPPS_4$ in buffer on concentration and pH. From the obtained two-dimensional matrix of data (phosphorescence intensity as a function of time and wavelength) we determined lifetimes of the photosensitiser triplet state together with those belonging to both the rise and decay of the singlet oxygen emission. Excitation quenching was studied and discussed within a wide range of concentrations.
© 2004 Elsevier B.V. All rights reserved.

PACS: 32.50.+d; 33.50.Dq; 33.50.Hv

Keywords: $TPPS_4$; Singlet oxygen; Phosphorescence; PDT

1. Introduction

Photodynamic therapy (PDT) is an emerging method of treatment of cancer as well as of some chronic diseases, such as atherosclerosis, rheumatoid and inflammatory arthritis, or psoriasis. It exploits the unique ability of photosensitisers to accumulate selectively in the affected tissue due to their selective up-take and delayed elimination relative to the normal tissue. The photosensitiser is excited by absorption of light and subsequently may undergo inter-system crossing to its triplet state. As the lifetime of the photosensitiser triplet state is rather long, it can be quenched by oxygen via triplet–triplet (T–T) reaction, producing oxygen in its singlet excited state. This highly reactive moiety oxidizes neighboring molecules causing necrosis of the diseased tissue.

Meso-tetra(4-sulphonatophenyl)porphine ($TPPS_4$) is a water-soluble porphyrin derivative, used in the Czech Republic for treatment of some types of tumors [1].

This contribution presents new $TPPS_4$ and singlet-oxygen phosphorescence spectral and kinetic data, especially pH and concentration effects.

*Corresponding author. Tel.: +420-221-911-307; fax: +420-221-911-249.
E-mail address: roman@kchf-43.karlov.mff.cuni.cz (R. Dědic).

0022-2313/$ - see front matter © 2004 Elsevier B.V. All rights reserved.
doi:10.1016/j.jlumin.2004.01.027

2. Experimental

$TPPS_4$ was purchased from Frontier Scientific Porphyrin Products. Three stock solutions of 200 μmol l^{-1} $TPPS_4$ in 10 mmol l^{-1} phosphate buffers of pH 7.4, 6.5, and 5.5, corresponding to pH of blood, cancer tissue, and skin, respectively, were prepared. Further dilution of the stock solutions in respective buffers provided a set of photosensitiser concentrations ranging from 5 to 200 μmol l^{-1} for each pH.

Both time- and spectral-resolved phosphorescence of the photosensitiser and singlet oxygen were measured simultaneously. Detailed description of the experimental setup was given in our previous publication [2]. Briefly, the samples were excited through the optically polished bottom of a standard 1×1 cm fluorescence cuvette by laser pulses at 420 nm with energy of ≈ 30 μJ. The infrared emission was detected by an IR sensitive photomultiplier together with a photoncounter/multiscaler with 5 ns per channel. Phosphorescence of $TPPS_4$ and singlet oxygen in each sample was measured under three different oxygen concentrations: without oxygen (purged for 1 h by N_2 gas), air saturated, and oxygen saturated (purged for 1 h by O_2 gas).

3. Results

$TPPS_4$ phosphorescence exhibits its maximum around 820 nm independent of concentration or pH. Its shape is the same in solution saturated by air or oxygen. In the case of N_2-purged solutions, the position of the main band remains the same and, in addition, a shoulder with maximum around 1060 nm appears. The quantum efficiency of photosensitiser phosphorescence increases with a decrease of oxygen concentration.

The lifetime of $TPPS_4$ phosphorescence strongly depends on oxygen concentration. Moreover, it depends also on concentration of the photosensitiser. In air saturated samples, the lifetime slowly increases from 1.8 ± 0.2 μs at 5 μmol l^{-1} to a saturated value of 3.0 ± 0.2 μs at the highest concentrations (Fig. 1). The lifetimes obtained at each concentration are, within an experimental error, the same for all three values of pH. The situation is qualitatively the same for oxygen saturated samples, but values range from 0.37 ± 0.07 μs to 0.65 ± 0.08 μs (Fig. 1). In N_2 saturated samples, the phosphorescence decays exhibit two components. The lifetime of the shorter one cannot be determined in our setup. The lifetime of the longer one, which corresponds to the decay of the 1060 nm phosphorescence band, depends strongly on the efficiency of oxygen removal by gaseous N_2 causing a big dispersion of the obtained values. Nevertheless, the values exhibit a slight decrease with increasing photosensitiser concentration from approximately 250 μs at 5 μmol l^{-1} to 100 μs at 200 μmol l^{-1}, independent of pH.

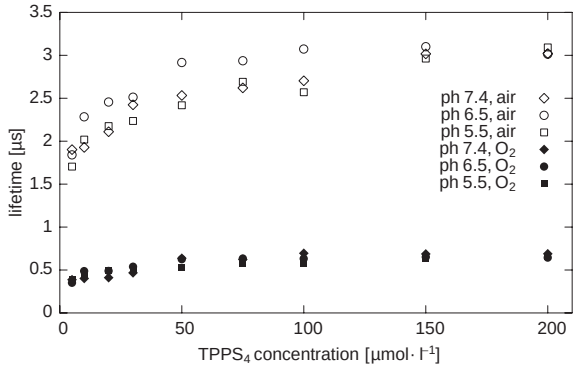

Fig. 1. Lifetimes of $TPPS_4$ phosphorescence in air—open symbols and O_2-saturated samples for pH 5.5 (squares), 6.5 (circles), and 7.4 (diamonds).

The maximum of singlet-oxygen phosphorescence lies around 1280 nm. Its position and shape depends neither on $TPPS_4$ and oxygen concentration nor on sample pH.

Both the rise and decay times of the singlet oxygen phosphorescence were resolved in air- and O_2-saturated samples (Fig. 2), while in N_2-saturated ones the low phosphorescence signal made it impossible. Both lifetimes were independent of $TPPS_4$ concentration and sample pH. The rise and decay times in air-saturated samples were 1.75 ± 0.05 and 3.7 ± 0.1 μs, respectively, while in O_2-saturated ones they were 0.41 ± 0.02 and 3.5 ± 0.1 μs. Using oxygen concentrations of 0.28 mmol l^{-1} in air and 1.4 mmol l^{-1} in

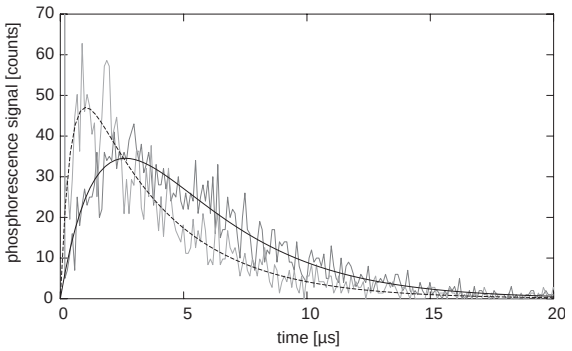

Fig. 2. Singlet-oxygen phosphorescence kinetics together with corresponding fits. Detection at 1282 nm, $TPPS_4$ concentration 20 μmol l^{-1}, samples saturated with air (solid line) and oxygen (dashed line).

O_2-saturated solutions [3], a rate-constant of quenching $TPPS_4$ phosphorescence by oxygen was found to be $16.9 \pm 0.8 \times 10^8$ l mol^{-1} s^{-1}.

4. Discussion

The lifetime of $TPPS_4$ phosphorescence for the lowest concentration of the photosensitiser corresponds well to the rise-time of singlet oxygen. For higher photosensitiser concentrations, the $TPPS_4$ phosphorescence lifetime grows while the singlet-oxygen rise time remains constant. This may be caused by the appearance of another form of $TPPS_4$, probably aggregates, that are unable to transfer energy to oxygen and thus exhibit a longer phosphorescence lifetime. This behavior is common to all pH values and both air- and O_2-saturated samples.

The value of the bimolecular constant of quenching $TPPS_4$ phosphorescence by oxygen of $16.9 \pm 0.8 \times 10^8$ l mol^{-1} s^{-1} is in good agreement with values obtained from T–T absorption $(20 \pm 1) \times 10^8$ l mol^{-1} s^{-1} by Kubát et al. [4] and 18×10^8 l mol^{-1} s^{-1} by Mosinger et al. [5].

The lifetime of the long component of $TPPS_4$ phosphorescence in N_2-saturated samples of 250 μs for low photosensitiser concentrations fits well with 290 μs obtained by Mosinger et al. [5]. Decrease of this value with increasing photosensitiser concentration is probably caused by shorter excited-state lifetime of $TPPS_4$ aggregates.

The lifetime of singlet-oxygen phosphorescence exhibits a slight decrease with increasing oxygen concentration (from 3.7 ± 0.1 μs in air-saturated samples to 3.5 ± 0.1 μs in O_2-saturated ones). This is probably caused by quenching of singlet oxygen by collisions with other oxygen molecules.

5. Conclusions

A systematic study of $TPPS_4$ and singlet-oxygen phosphorescence did not reveal any influence of buffer pH on the corresponding lifetimes within the studied range (pH of blood, cancer tissue, and skin). No concentration dependence was observed in rise and decay times of singlet-oxygen emission. On the other hand, the lifetimes of $TPPS_4$ phosphorescence exhibit increase with increasing concentration. These lifetimes are in a good agreement with the rise times of singlet-oxygen luminescence for the lowest concentrations. Increased oxygen concentration leads to faster quenching of $TPPS_4$ triplets. A corresponding quenching constant of $16.9 \pm 0.8 \times 10^8$ l mol^{-1} s^{-1} was determined.

Acknowledgements

This work was supported by grants GP202/01/D100 from Grant Agency of the Czech Republic and GA UK 184/2002 from the Charles University and project MSM13200001 from the Ministry of Education of the Czech Republic.

References

[1] M. Lapeš, J. Petera, M. Jirsa, J. Photochem. Photobiol. B: Biol. 36 (1996) 205.
[2] R. Dědic, A. Svoboda, J. Pšenčík, J. Hála, J. Mol. Struct. 651–653 C (2003) 301.
[3] W.F. Linke, Solubilities of Inorganic and Metal–organic Compounds, American Chemical Society, Washington, DC, 1965.
[4] P. Kubát, J. Mosinger, J. Photochem. Photobiol. A: Chem. 96 (1–3) (1996) 93.
[5] J. Mosinger, M. Deumié, K. Lang, P. Kubát, D.M. Wagnerová, J. Photochem. Photobiol. A: Chem. 130 (2000) 13.

Enclosure 3

R. Dedic, M. Korínek, **A. Molnár**, A. Svoboda and J. Hála, Singlet oxygen quenching by oxygen in tetraphenyl-porphyrin solutions, Journal of Luminiscence 119 (2006) 209-213.

Available online at www.sciencedirect.com
SCIENCE DIRECT®
Journal of Luminescence 119–120 (2006) 209–213
JOURNAL OF LUMINESCENCE
www.elsevier.com/locate/jlumin

Singlet oxygen quenching by oxygen in tetraphenyl-porphyrin solutions

Roman Dědic, Miloslav Kořínek, Alexander Molnár, Antonín Svoboda, Jan Hála*

Charles University, Faculty of Mathematics and Physics, Ke Karlovu 3, CZ121 16 Praha 2, Czech Republic

Available online 10 March 2006

Abstract

Time-resolved measurement of singlet oxygen infrared phosphorescence is a powerful tool for determination of quantum yields and kinetics of its photosensitization. This technique was employed to investigate in detail the previously observed effect of singlet oxygen quenching by oxygen. The question whether the singlet oxygen is quenched by oxygen in ground or in excited state was addressed by study of two complementary dependencies of singlet oxygen lifetimes: on dissolved oxygen concentration and on excitation intensity.

Oxygen concentration dependence study of meso-tetra(4-sulphonato)phenylporphyrin ($TPPS_4$) phosphorescence kinetics showed linearity of the dependence of $TPPS_4$ triplet state rate-constant. Corresponding bimolecular quenching constant of $(1.5\pm0.1)\times10^9$ l/mol s was obtained. On the other hand, rate constants of singlet oxygen depopulation exhibit nonlinear dependence on oxygen concentration. Comparison of zero oxygen concentration-extrapolated value of singlet oxygen lifetime of (6.5 ± 0.4) μs to (3.7 ± 0.1) μs observed under air-saturated conditions indicates importance of the effect of quenching of singlet oxygen by oxygen. Upward-sloping dependencies of singlet oxygen depopulation rate-constant on excitation intensity evidence that singlet oxygen is predominantly quenched by oxygen in excited singlet state.
© 2006 Elsevier B.V. All rights reserved.

Keywords: Singlet oxygen; Quenching by oxygen; Phosphorescence; $TPPS_4$; TPP

1. Introduction

The photodynamic therapy (PDT) is a modern way of treatment of various diseases (e.g. cancer, psoriasis, age-related macular degeneration, or arthritis). It is based on selective uptake of a photosensitizing drug in the affected tissue, while its concentration in the healthy tissue remains very low. Upon localized illumination, the emergent triplet states of the photosensitizers transfer their excitation energy to molecular oxygen, bringing it to its excited singlet state. Several orders higher

*Corresponding author. Tel.: +420 221 911 421; fax: +420 221 911 249.
E-mail address: hala@karlov.mff.cuni.cz (J. Hála).

0022-2313/$ - see front matter © 2006 Elsevier B.V. All rights reserved.
doi:10.1016/j.jlumin.2005.12.032

reactivity of the singlet oxygen (compared to its ground triplet state) leads to a rapid oxidative damage of the treated cells, causing either rapid necrosis or delayed apoptosis of the diseased tissue. To develop highly efficient treatment methods, deep understanding of the processes of singlet oxygen photosensitization and quenching is crucial. In the last years, the development of near infrared-sensitive photomultipliers and time-resolved photon counters has enabled direct observations of singlet oxygen population kinetics by detecting its weak infrared phosphorescence around 1280 nm.

In our previous experiments, the decrease of singlet oxygen lifetime from $(3.7\pm0.1)\,\mu s$ to $(3.5\pm0.1)\,\mu s$ was observed in buffer solutions of *meso*-tetra(4-sulphonato)phenyl-porphyrin ($TPPS_4$), when the concentration of dissolved oxygen in the sample was changed from air-saturated value of $280\,\mu mol\,l^{-1}$ to the oxygen-saturated one ($1400\,\mu mol\,l^{-1}$) [1]. The very same effect has been observed in solutions of *meso*-tetraphenyl-porphyrin (TPP, lipophillic analogue of $TPPS_4$) in dimethyl-sulfoxide, where the singlet oxygen lifetime changed from $(1.8\pm0.5)\,\mu s$ in air-saturated material ($460\,\mu mol\,l^{-1}$ oxygen) to $(1.2\pm0.1)\,\mu s$ in oxygen-saturated one ($2200\,\mu mol\,l^{-1}$ oxygen) [2]. These observations led to conclusion that singlet oxygen is quenched not only by molecules of the solvent or the photosensitizer [1–6] but also by another oxygen molecule.

Question arises, whether it is quenched predominantly by oxygen in the ground state or by another singlet oxygen. We have addressed this problem by two different methods. In the first one, the overall concentration of oxygen in the sample was altered by purging of the solutions by either gaseous nitrogen or oxygen. In the other one, the excitation intensity was varied (e.g. increased), which is reflected in initial concentration of the photosensitizer triplet states and subsequent increase of singlet oxygen concentration accompanied by decrease of triplet oxygen.

2. Materials and methods

The oxygen concentration dependencies were measured on $20\,\mu mol\,l^{-1}$ solutions of $TPPS_4$ in potassium phosphate buffer of $pH = 7.4$. The excitation intensity dependencies were measured on the same material as well as $100\,\mu mol\,l^{-1}$ solution of TPP in acetone. Both photosensitizers were obtained from Frontier Scientific Porphyrin Products, USA. Oxygen concentrations in buffer solutions were measured using Clark-type electrode Jenway 9010. Their values ranged from 100 to $1400\,\mu mol\,l^{-1}$.

The excitation pulses provided by excimer-pumped dye laser of approx. 15 ns at wavelengths corresponding to the Soret and the redmost absorption band of the photosensitizers were used. Absorbed energies were determined using simple two-channel method with two fast PIN photodiodes [2]. Their values ranged from 25 to 0.05 μJ; for oxygen concentration dependencies, absorbed energy of approx. 10 μJ was used.

Time- and spectral-resolved data of weak infrared phosphorescence of photosensitizers and singlet oxygen were measured using our home-built set-up based on Hamamatsu R5509 photomultiplier [1].

3. Results and discussion

As expected, the lifetimes of $TPPS_4$ triplets decrease with increasing total oxygen concentration. Corresponding rate-constants exhibit perfect linear dependence on oxygen concentration (see Fig. 1). This proves that the process of excitation energy transfer from photosensitizers to oxygen follows bimolecular mechanism even in the range of much lower oxygen concentrations than that was published in Ref. [7]. The value of the respective bimolecular quenching constant was determined as $(1.5\pm0.1)\times10^9\,l/mol\,s$, which is in a perfect agreement with our previously published value of $(1.7\pm0.8)\times10^9\,l/mol\,s$ [1] and $1.8\times10^9\,l/mol\,s$ obtained by Mosinger et al. [8], this time with significantly higher precision. Rise-times of singlet oxygen follow qualitatively the same dependence with slightly lower values (and thus bigger rate-constants, see Fig. 1), providing the bimolecular quenching constant of $(1.4\pm0.1)\times10^9\,l/mol\,s$.

Fig. 2 displays dependence of singlet oxygen depopulation rate-constants on overall oxygen concentration. In contrast to the linear dependence of rate-constants from Fig. 1, the obtained behavior is

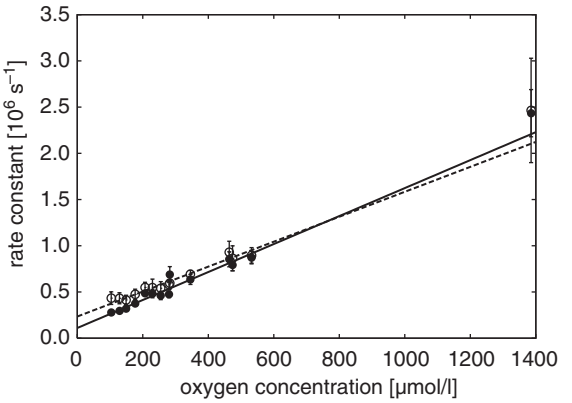

Fig. 1. Linear dependencies of both photosensitizer depopulation (full circles, solid line) and singlet oxygen photogeneration rate-constants (open circles, dashed line) on dissolved oxygen concentration, $TPPS_4$ in buffer (pH = 7.4).

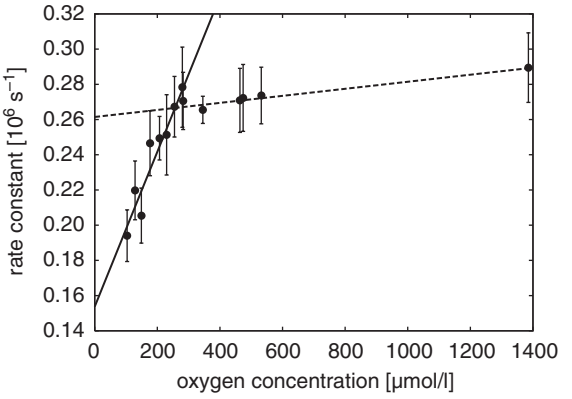

Fig. 2. Nonlinear dependence of singlet oxygen depopulation rate-constant on dissolved oxygen concentration in $TPPS_4$ in buffer. Solid and dashed lines represent fits of quasilinear regions of the dependence for low and high oxygen concentrations, respectively.

more complex. The most surprising fact is the pronounced increase of the singlet oxygen lifetimes with decreasing dissolved oxygen concentration in the region below 280 μmol l^{-1} of oxygen. Extrapolation of this quasi-linear dependence to the zero oxygen concentration yields rather high lifetime of singlet oxygen in water of (6.5 ± 0.4) μs, which differs significantly from the generally accepted value of (3.90 ± 0.04) μs, which would be obtained if the much less steep quasi-linear dependence between air- and oxygen-saturated concentrations were extrapolated. This dependence also shows that the process of quenching of singlet oxygen by oxygen may play much more important role than that was previously expected. Owing to complicated behavior of the rate-constants, it is not possible to distinguish whether singlet or triplet oxygen dominates the quenching.

The dependence of singlet oxygen depopulation rate-constants on absorbed energy in $TPPS_4$ in air-saturated buffer is presented in Fig. 3. The rate-constants remain constant, within our experimental accuracy, in the region of absorbed energies higher than approximately 3 μJ. On the other hand, the rate constants decrease for lower absorbed energies. Unfortunately, the very low signal of singlet oxygen phosphorescence in water makes more detailed investigation of this interesting phenomenon impossible. Therefore, we have studied similar dependence in TPP in air-saturated acetone (2400 μmol l^{-1} oxygen), where the singlet oxygen luminescence signal as well as its concentration is substantially higher, using the same blue excitation wavelength. Fig. 4 documents that for the absorbed intensities less than 3 μJ, the dependence is quasi-linear. The deviation from quasi-linearity leading to a saturated rate-constant value of approximately $21.5 \times 10^3\ s^{-1}$ is observed for higher absorbed energies. This effect can be explained by an assumption that the triplet concentration is not proportional to the measured absorbed energy due to fraction of energy absorbed via triplet–triplet transitions (around 440 nm [9]), which grows with increasing excitation intensity and becomes significant when majority of photosensitizer molecules is excited. Since there is no triplet–triplet

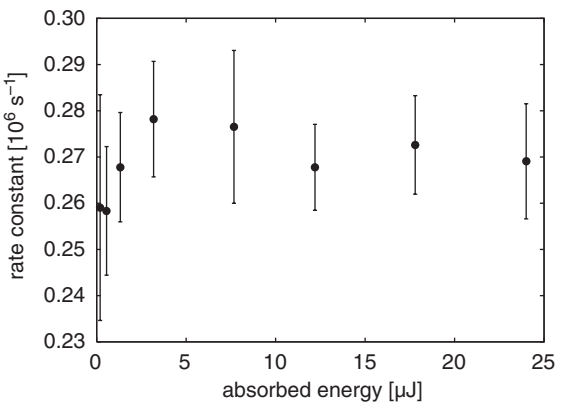

Fig. 3. Absorbed energy dependence of singlet oxygen depopulation rate-constant in $TPPS_4$ in buffer.

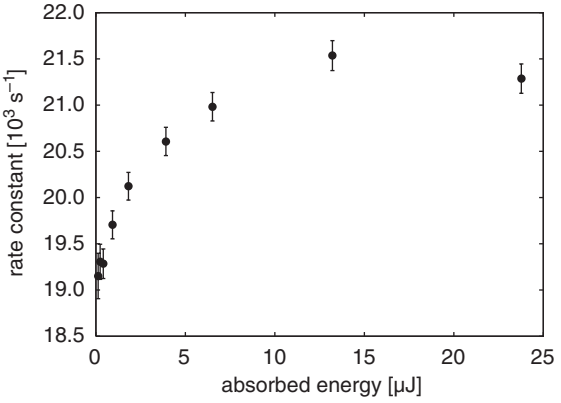

Fig. 4. Absorbed energy dependence of singlet oxygen depopulation rate-constant in TPP in acetone under blue excitation.

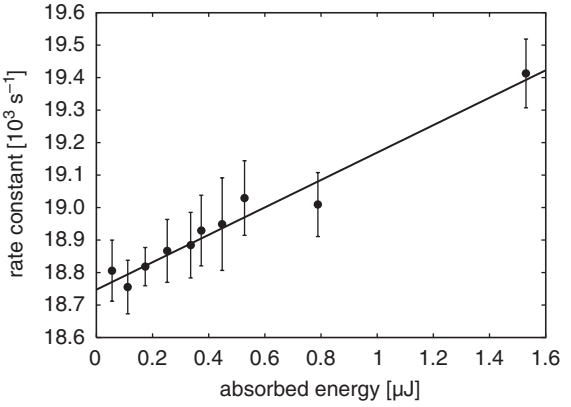

Fig. 5. Absorbed energy dependence of singlet oxygen depopulation rate-constant in TPP in acetone under red excitation together with its linear fit.

absorption in the red spectral region, no such effect would be observed in the case of the red excitation. Therefore, we have employed also excitation to the weak redmost absorption band of TPP where significantly lower absorbed energies with reasonable excitation intensities can be obtained. The results are shown in Fig. 5 where the linear increase of the rate constants with increasing absorbed energy is clearly visible.

As the overall concentration of dissolved oxygen in the sample remains constant, the increase of concentration of photogenerated singlet oxygen with increasing absorbed energy has to be accompanied by decrease of the concentration of the triplet oxygen. In this case, the upward slope of the rate-constants dependence means that the contribution of faster quenching due to higher singlet oxygen concentration must be higher than the contribution of slowing-down of the quenching due to lower triplet oxygen concentration. Therefore, the singlet oxygen must be predominantly quenched by singlet oxygen. This fact is further supported by the observed linearity of the rate-constants dependence for low absorbed energies, while the observed lifetimes of photosensitizer-excited triplets were found to be constant (≈ 300 ns, data not shown) within the whole range of the excitation intensities. These results seem to be in contrast with the latest accepted hypothesis of predominant quenching of singlet oxygen by the triplet one [6,10].

4. Conclusions

Systematic oxygen concentration dependence study of $TPPS_4$ phosphorescence kinetics showed that the dependence of $TPPS_4$ triplet state rate-constant on oxygen concentration is linear. It proves bimolecular quenching mechanism with the quenching constant of $(1.5 \pm 0.1) \times 10^9$ l/mol s. Lifetimes of singlet oxygen exhibit descending dependence on oxygen concentration. Zero oxygen concentration extrapolated value of singlet oxygen lifetime was found to be (6.5 ± 0.4) μs, showing that quenching of singlet oxygen by oxygen plays important role in singlet oxygen population dynamics. The increasing dependence of singlet oxygen depopulation rate-constant on excitation intensity proves that singlet oxygen is predominantly quenched by oxygen in excited singlet state.

Acknowledgments

This work was supported by project MSM0021620835 from the Ministry of Education of the Czech Republic.

References

[1] R. Dědic, A. Molnár, M. Kořínek, A. Svoboda, J. Pšenčík, J. Hála, J. Lumin. 108 (2004) 117.

[2] M. Kořínek, R. Dědic, A. Molnár, A. Svoboda, J. Hála, J. Mol. Struct. 744–747 (2005) 727.
[3] A.A. Krasnovsky, P. Cheng, R.E. Blankenship, T.A. Moore, D. Gust, Photochem. Photobiol. 57 (1993) 324.
[4] H. Küpper, R. Dědic, A. Svoboda, J. Hála, P.M.H. Kroneck, Biochim. Biophys. Acta: General Subjects 1572 (2002) 107.
[5] M. Kořínek, R. Dědic, A. Svoboda, J. Hála, J. Fluor. 14 (2004) 71.
[6] C. Schweitzer, R. Schmidt, Chem. Rev. 103 (2003) 1685.
[7] S.Y. Egorov, V.F. Kamalov, N.I. Koroteev, A.A. Krasnovsky Jr., B.N. Toleutaev, S.V. Zinukov, Chem. Phys. Lett. 163 (1989) 421.
[8] J. Mosinger, M. Deumie, K. Lang, P. Kubat, D.M. Wagnerova, J. Photochem. Photobiol. A: Chem. 130 (2000) 13.
[9] M. Lovcinsky, J. Borecky, P. Kubat, P. Jezek, Gen. Physiol. Biophys. 18 (1999) 107.
[10] E. Afshari, R. Schmidt, Chem. Phys. Lett. 182 (1991) 128.

Enclosure 4

M. Korínek , R. Dedic, **A. Molnár**, and J. Hála, The influence of human serum albumin on the photogeneration of singlet oxygen by meso-tetra(4-sulphonatophenyl)porphyrin. Infrared emission study., Journal of Fluorescence 16 (2006) 355-359.

Journal of Fluorescence, Vol. 16, No. 3, May 2006 (© 2006)
DOI: 10.1007/s10895-005-0057-5

The Influence of Human Serum Albumin on The Photogeneration of Singlet Oxygen by *meso*-Tetra(4-Sulfonatophenyl)Porphyrin. An Infrared Phosphorescence Study

M. Kořínek,[1,2] R. Dědic,[1] A. Molnár,[1] and J. Hála[1]

Received October 3, 2005; accepted December 26, 2005
Published online: February 9, 2006

meso-Tetra(4-sulfonatophenyl)porphyrin ($TPPS_4$) is a water soluble photosensitizer, which is currently clinically tested as a PDT drug. In our contribution, we present IR spectral- and time-resolved phosphorescence data reflecting the influence of human serum albumin (HSA) on singlet oxygen photogeneration by $TPPS_4$. IR emission of $TPPS_4$ was studied in samples containing various concentrations of HSA in phosphate buffer. The observed changes in spectral and temporal behaviour of $TPPS_4$ and singlet oxygen phosphorescence caused by the addition of HSA are equivalent to the effect of nitrogen purging of HSA-free solutions of $TPPS_4$. The main feature induced by addition of HSA appears to be the occurrence of a long-lived (tens of microseconds) photosensitizer phosphorescence at 900 nm besides ordinary short-lived ($\approx 2\ \mu$s) one at 820 nm. It is accompanied by presence of a long-lived component of singlet oxygen emission with lifetime roughly corresponding to that of the long photosensitizer phosphorescence component. Moreover, the quantum yield of singlet oxygen phosphorescence decreases with increasing HSA concentration, while total quantum yield of $TPPS_4$ phosphorescence rises. These facts are explained by a shielding effect of HSA on bound molecules of $TPPS_4$ against quenching by oxygen which is analogous to oxygen removal by nitrogen purging.

KEY WORDS: $TPPS_4$; Singlet oxygen; Human serum albumin; Infrared phosphorescence; Photodynamic therapy.

INTRODUCTION

Porphyrin dyes are used in medicine for tumour detection and also for photodynamic therapy of cancer (PDT). Deep understanding of mechanisms of interaction between photosensitizers, proteins and oxygen is crucial for further progress in PDT of tumours. *meso*-Tetra(4-sulphonatophenyl)porphyrin ($TPPS_4$) is one of the drugs currently being tested for PDT. It is a water-soluble porphyrin exhibiting high quantum yield of singlet oxygen ($^1O_2$), equal to 0.62 in water [1]. Its photosensitizing properties were thoroughly explored in solutions [2–4]. Up to date, the investigation of $TPPS_4$ interaction with albumins has been based mainly on photosensitizer time-resolved triplet–triplet absorption [5–7].

Human serum albumin (HSA) is the most abundant serum protein consisting of 585 amino acid residues with molecular weight of approximately 66 kDa. HSA exhibits high affinity towards wide diversity of ligands that can be reversibly bound and thus distributed around human body [8]. According to Bartosova [9], HSA possesses one major binding site for $TPPS_4$ with binding constant of $3 \times 10^6\ M^{-1}$ and two to three sites of substantially lower affinity. Relatively little is known about the

[1] Charles University, Faculty of Mathematics and Physics, Department of Chemical Physics and Optics, Ke Karlovu 3, 121 16, Praha 2, Czech Republic.
[2] To whom correspondence should be addressed. E-mail: miloslav.korinek@seznam.cz

1053-0509/06/0500-0355/1 © 2006 Springer Science+Business Media, Inc.

production of $^1O_2$ by $TPPS_4$ in the presence of HSA as well as about the chemical (photosensitized oxidation) and physical quenching of $^1O_2$ by HSA. The reaction constant of $(5 \pm 3) \times 10^8$ M^{-1} s^{-1} for oxidation of HSA by $^1O_2$ was determined by Davila [5].

The aim of this contribution is to investigate the production of $^1O_2$ by $TPPS_4$ at various HSA concentrations under aerobic and anaerobic conditions together with effects of $^1O_2$ interaction with HSA using direct time- and spectral-resolved measurements of both the photosensitizer and $^1O_2$ phosphorescence.

EXPERIMENTAL

Phosphate buffer (pH = 7.4, the pH value of human blood) solutions of $TPPS_4$ (Frontier Scientific Porphyrin Products) of concentration of 10 μM were used for all measurements. This concentration ensures that $TPPS_4$ is present in its monomeric form predominantly [10]. The samples differed in HSA (Sigma Aldrich) concentration (0, 1, 5, 50 μM). The sample preparation was carried out under dim light to avoid any photodegradation.

Absorption spectra were measured by Avantes Avaspec-1024 spectrometer. Infrared sensitive emission spectrometer equipped with Hamamatsu R5509 photomultiplier was used for measurements of $TPPS_4$ and singlet oxygen emission between 750 and 1350 nm with 5 ns time resolution. For detailed description of experimental set-up see Ref. [3]. One millilitre of fresh material was used for each phosphorescence measurement. Two thousand of excitation laser pulses of approximately 10 ns and 17 μJ at 420 nm were applied to obtain each kinetics. In HSA-photosensitized oxidation studies, 38 successive kinetics were measured at fixed wavelengths of 862, 1022 and 1278 nm and further processed.

RESULTS AND DISCUSSION

Typical absorption spectra of $TPPS_4$ in buffer exhibit Soret band maximum at 413 nm accompanied by Q_X and Q_Y maxima at 516, 553, 580 and 633 nm. As the concentration of HSA increases, the fraction of $TPPS_4$ bound to HSA increases as well. This is accompanied by bathochromic shifts of the respective absorption maxima to 421, 517, 553, 591 and 647 nm for 50 μM HSA. These observed absorption band shifts are exactly the same as those of $TPPS_4$–HSA complexes published by Andrade [10]. It is worth noting that even a very weak measurement light in absorption spectrometer was sufficient to induce photosensitized oxidation of HSA and thus only N_2 purged samples can provide reliable absorption spectra.

Table 1. Lifetimes (t_1, t_2) of Decays of Nitrogen-Purged $TPPS_4$ at Various HSA Concentrations

HSA concentration (μM)	t_1 (μs)	t_2 (μs)
0	1.7 ± 0.1	405 ± 20
1	1.8 ± 0.3	430 ± 20
5	1.9 ± 0.4	640 ± 50
50	1.9 ± 0.5	990 ± 120

Photosensitizer Phosphorescence

Phosphorescence of $TPPS_4$ in the absence of HSA was described in [3,4]. Under anaerobic conditions, the $TPPS_4$ phosphorescence comprises of two distinct components, each of them exhibiting monoexponential kinetics. The short component with emission maximum at 820 nm decays with lifetime of (1.7 ± 0.1) μs. The maximum of the long one is located at 900 nm and its lifetime is (405 ± 20) μs for 10 μM $TPPS_4$.

In the case of N_2 purged samples containing HSA, the $TPPS_4$ phosphorescence spectra and kinetics consist again of two components. The lifetime of the shorter one remains constant for all HSA concentrations (Table 1). Maximum of this component remains at the same wavelength as in HSA-free sample. While the spectral position of the long component maximum is constant in the whole HSA concentration range, its lifetime rises with increasing concentration of HSA from (405 ± 20) μs in HSA-free sample to (990 ± 120) μs in 50 μM HSA (see Table 1). This phenomenon can be explained by HSA preventing depopulation of the bound triplet $TPPS_4$ molecules by water, analogically to what has been published by Foley on phthalocyanine–HSA solutions [6]. The exchange between free and bound forms is substantially faster than their respective triplet lifetimes and therefore only single lifetime t_2 increasing with HSA concentration is observed.

$TPPS_4$ phosphorescence in the absence of HSA under aerobic conditions exhibits strictly monoexponential decay with lifetime of (1.9 ± 0.1) μs, which is in a very good agreement with earlier published (1.8 ± 0.1) μs [3] and (1.9 ± 0.2) μs [4]. Second exponential phosphorescence component of much longer lifetime arises after the addition of HSA. It is documented in Fig. 1, which shows typical time- and spectral-resolved emission of air saturated sample containing 5 μM HSA. These two components can be distinguished within entire spectral region of 750–1240 nm. Figure 2 presents typical $TPPS_4$

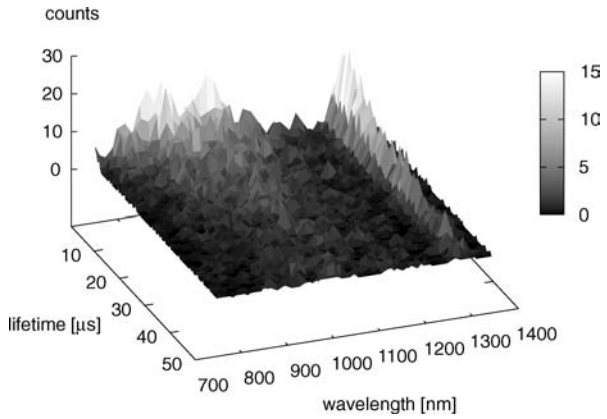

Fig. 1. Three-dimensional plot of time- and spectral-resolved phosphorescence of $TPPS_4$ (around 900 nm) and singlet oxygen (at 1280 nm) under aerobic conditions with 5 μM HSA. Raw data are shown for the sake of clarity.

phosphorescence decay at 1022 nm of 1 μM HSA sample together with its biexponential fit.

Lifetimes of the fast component were found around 2 μs independent of HSA concentration. On the other hand, lifetimes of the slow component increase from (15.0 $\pm$ 1.4) to (100 $\pm$ 90) μs with increasing HSA concentration (see Table 2).

This lifetime increase is accompanied by the increase of relative integral intensity of the slow component at the expense of the fast one. Since the fraction of $TPPS_4$ bound to the protein increases with increasing HSA concentration, the 2 μs component can be attributed to the phosphorescence of the free $TPPS_4$, while the other one corresponds to phosphorescence of $TPPS_4$ bound to HSA. The longer lifetime of bound $TPPS_4$ can be explained by

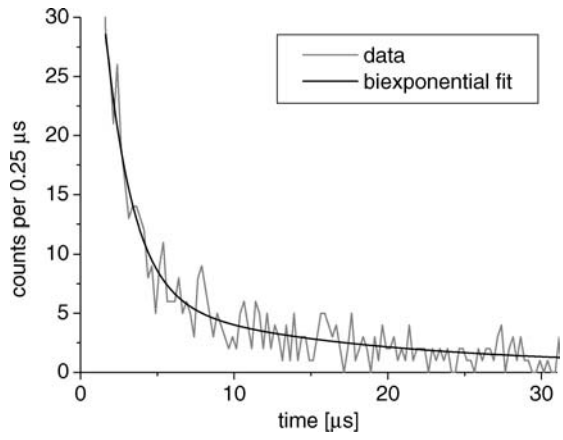

Fig. 2. Typical $TPPS_4$ phosphorescence decay of 1 μM HSA sample at 1022 nm together with its biexponential fit.

Table 2. The Lifetimes (t_1, t_2) of Biexponential Decays and Integral Intensities of the Short and Long Components (I_1, I_2) of Air-Saturated Samples at 1022 nm

HSA concentration (μM)	t_1 (μs)	t_2 (μs)	I_1 (a.u.)	I_2 (a.u.)
0	1.9 $\pm$ 0.1	—	0.21 $\pm$ 0.08	0
1	1.7 $\pm$ 0.3	15.0 $\pm$ 1.4	0.56 $\pm$ 0.05	0.50 $\pm$ 0.05
5	2.1 $\pm$ 0.5	25.1 $\pm$ 3.4	0.35 $\pm$ 0.06	1.29 $\pm$ 0.07
50	2.4 $\pm$ 2	100 $\pm$ 90	0.3 $\pm$ 0.1	3.7 $\pm$ 3.3

Note. The zero exposition-extrapolated values are presented to diminish the effect of photoinduced oxidation.

shielding of $TPPS_4$ by HSA against quenching by oxygen in accordance with [7,11].

Moreover, the spectral behaviour of the long component is exactly the same as that of N_2 purged samples, which proves that shielding of $TPPS_4$ molecules by HSA has very similar effect on $TPPS_4$ triplet properties as removal of oxygen by N_2 purging.

Singlet Oxygen Phosphorescence

Immediately after the excitation pulse the phosphorescence of singlet oxygen rises and past reaching its maximum it decays. The rise is attributed to gradual population of singlet oxygen via excitation energy transfer from the photosensitizer triplets. The decline occurs due to deactivation of singlet oxygen together with weakening of its photogeneration.

In the absence of HSA, it is reflected in the formula for singlet oxygen emission intensity:

$$I_{SO}(t) = b\{\exp(-t/t_{SO}) - \exp(-t/t_1)\} \qquad (1)$$

where t_{SO} represents the lifetime of singlet oxygen in the sample and t_1 corresponds to the lifetime of $^3TPPS_4$ [3]. In the presence of HSA, the situation becomes more complicated. As is shown earlier, $TPPS_4$ phosphorescence revealed existence of at least two distinct groups of photosensitizer triplets, which were ascribed to free and bound $TPPS_4$. Therefore, the singlet oxygen phosphorescence intensity has to follow time evolution in the form of linear combination of at least two expressions of Eq. (1) type with two different photosensitizer triplet lifetimes t_1 and t_2. Taking into account oxygen diffusion constant in water of 2 $\times$ 10^{-5} cm^2 s^{-1} [12], singlet oxygen travels 200 nm during its 4 μs lifetime. Its path is therefore substantially longer than the size of HSA molecules as well as the distance between them. Hence, it is reasonable to assume that each $^1O_2$ molecule interacts with both water

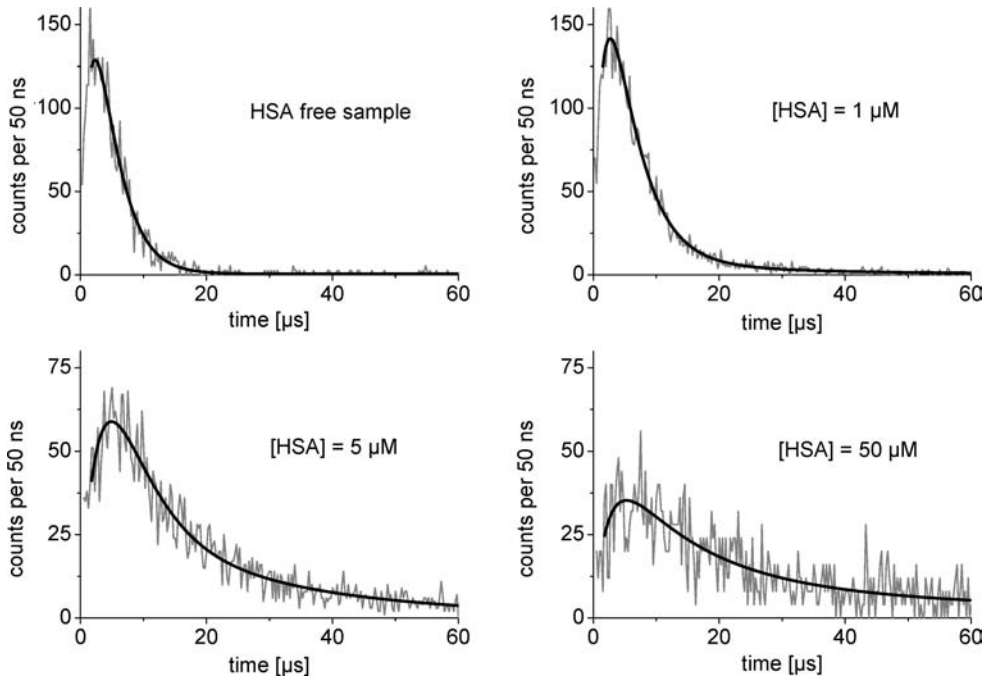

Fig. 3. Singlet oxygen phosphorescence kinetics at 1278 nm at various HSA concentrations and their fits by Eq. (2).

and HSA environment during its lifetime. This makes the question whether singlet oxygen was produced by free or bound $TPPS_4$ irrelevant and that is why the same effective value of t_{SO} for both components in Eq. (2) was used.

$$I_{SO}(t) = d\{\exp(-t/t_{SO}) - \exp(-t/t_1)\} + f\{\exp(-t/t_2) - \exp(-t/t_{SO})\} = I_f(t) + I_b(t) \quad (2)$$

Phosphorescence kinetics of singlet oxygen photogenerated by $TPPS_4$ in samples of different HSA concentrations are shown in Fig. 3. Equation (2) provides reliable fits of all singlet oxygen kinetics in the presence of HSA. The obtained lifetimes t_1 remain constant within our experimental accuracy in the whole HSA concentration range and fit well with the lifetime of $TPPS_4$ triplet in HSA-free samples under aerobic conditions determined from the photosensitizer phosphorescence. This further justifies the identification of the first component in Eq. (2) with singlet oxygen photogenerated by free $TPPS_4$ molecules. In the case of t_2 lifetimes, the correspondence with bound $TPPS_4$ triplet lifetimes is not so striking. Nevertheless, they both exhibit identical increase with HSA concentration.

The prolonging of effective lifetime of singlet oxygen with HSA concentration can be interpreted in this way: Water is well known for rapid quenching of singlet oxygen [13]. On the other hand, singlet oxygen lives much longer in majority of organic environments. Increasing HSA concentration changes effective singlet oxygen environment from water-like towards the more organic one. The observed $^1O_2$ lifetime increase indicates that the above-mentioned prolonging of $^1O_2$ lifetime prevails any shortening of $^1O_2$ lifetime due to chemical quenching by HSA.

Table 3. Lifetimes and Integral Intensities Obtained by Fitting $^1O_2$ Kinetics by Eq. (2)

HSA concentration (μM)	t_1 (μs)	t_2 (μs)	t_{SO} (μs)	$\int_0^\infty I_f(t)dt$	$\int_0^\infty I_b(t)dt$
0	1.8 ± 0.5	—	3.6 ± 0.5	4.2 ± 1.8	0
1	1.8 ± 0.2	24 ± 4	4.2 ± 0.3	5.2 ± 0.3	1.0 ± 0.2
5	2.1 ± 0.5	31 ± 3	8.8 ± 2.0	3.2 ± 0.4	2.6 ± 0.5
50	2.5 ± 0.8	47 ± 19	12.4 ± 4.9	3.4 ± 0.4	2.9 ± 0.5

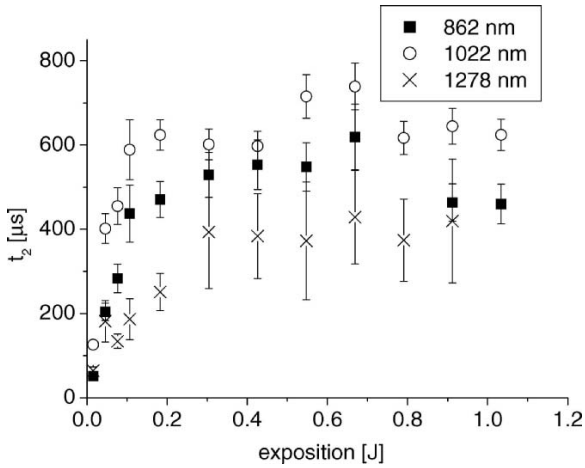

Fig. 4. The dependence of t_2 determined from phosphorescence at 862, 1022 and 1278 nm on the exposition of 50 μM HSA air-saturated sample.

Overall integral intensity of singlet oxygen phosphorescence (equal to the sum of respective integral intensities displayed in Table 3) remains constant for all studied HSA concentrations. Since the effective lifetime of singlet oxygen rises with HSA concentration, it means that the quantum yield of $^1O_2$ production decreases.

Interaction of HSA with Singlet Oxygen

HSA is oxidized by singlet oxygen photogenerated during phosphorescence measurements. Although the reaction rate of this oxidation is rather small $(5 \pm 3) \times 10^8$ M^{-1} s^{-1} [5], resulting changes are reflected in the growth of $TPPS_4$ phosphorescence lifetimes t_2. To investigate this phenomenon, we have analysed 38 successively measured kinetics at 862, 1022 and 1278 nm. No detectable changes were observed for 1 and 5 μM HSA samples. On the other hand, significant increase of t_2 appeared in 50 μM HSA (see Fig. 4). As the oxygen is consumed during HSA oxidation by singlet oxygen, total oxygen concentration in the sample decreases. It is reflected in the quintuple increase of t_2. The dependences presented in Fig. 4 represent quantification of HSA oxidation by singlet oxygen.

CONCLUSIONS

$TPPS_4$ phosphorescence lifetime under anaerobic conditions rises with increasing concentration of HSA due to HSA preventing water-induced depopulation of triplets of the $TPPS_4$ molecules bound to the protein.

Under aerobic conditions, spectral and temporal analysis of phosphorescence of triplet $TPPS_4$ as well as that of singlet oxygen revealed an additional HSA shielding of the protein-bound photosensitizer triplets from quenching by oxygen. The presented data reflect also photosensitized oxidation of HSA.

ACKNOWLEDGMENTS

This work was supported by project MSM00-21620835 from the Ministry of Education of the Czech Republic.

REFERENCES

1. J. Mosinger, M. Deumié, K. Lang, P. Kubát, and D. M. Wagnerová (2000). Supramolecular sensitizer: Complexation of meso-tetrakis(4-sulfonatophenyl)porphyrin with 2-hydroxypropyl-cyclodextrins. *J. Photochem. Photobiol. A.* **130**, 13–20.
2. M. Lovčinský, J. Borecký, P. Kubát, and P. Ježek (1999). Meso-tetraphenylporphyrin in liposomes as a suitable photosensitizer for photodynamic therapy of tumors. *Gen. Physiol. Biophys.* **18**, 107–118.
3. R. Dědic, A. Svoboda, J. Pšenčík, and J. Hála (2003). Phosphorescence of singlet oxygen and meso-tetra(4-sulfonatophenyl)porphin: Time and spectral resolved study. *J. Mol. Struct.* **651–653**, 301–304.
4. R. Dědic, A. Molnár, M. Kořínek, A. Svoboda, J. Pšenčík, and J. Hála (2004). Spectroscopic study of singlet oxygen photogeneration in meso-tetra-sulphonatophenyl-porphin. *J. Luminiscence* **108**, 117–119.
5. J. Davila and A. Harriman (1990). Photoreactions of macrocyclic dyes bound to human serum albumin. *Photochem. Photobiol.* **51**(1), 1.
6. M. S. C. Foley, A. Beeby, A. W. Parker, S. M. Bishop, and D. Phillips (1997). Excited triplet state photophysics of the sulphonated aluminium phthalocyanines bound to human serum albumin. *J. Photochem. Photobiol. B.* **38**, 10–17.
7. I. E. Borissevitch, T. T. Tominaga, and C. C. Schmitt (1998). Photophysical studies on the interaction of two water-soluble porphyrins with bovine serum albumin. Effects upon the porphyrin triplet state characteristics. *J. Photochem. Photobiol. A.* **114**, 201–207.
8. W. M., Sharman, J. E. van Lier, C. M., Allen (2004). Targeted photodynamic therapy via receptor mediated delivery systems. *Adv. Drug Deliv. Rev.* **56**, 53–76.
9. J. Bartošová, I. Kalousek, and Z. Hrkal (1994). Binding of meso-tetra(4-sulfonatophenyl) porphine to haemopexin and albumin studied by spectroscopy methods. *Int. J. Biochem.* **26**(5), 5.
10. S. M. Andrade and S. M. B. Costa (2002). Spectroscopic studies on the interaction of a water soluble porphyrin and two drug carrier proteins. *Biophys. J.* **82**, 1607–1619.
11. K. Lang, J. Mossinger, and D. M. Wagnerová (2004). Photophysical properties of porphyrinoid sensitizers non-covalently bound to host molecules; models for photodynamic therapy. *Coord. Chem. Rev.* **248**, 321–350.
12. D. R. Linde (1999). *Handbook of Chemistry and Physics*, 80th ed. CRC Press LLC, Boca Raton.
13. C. Schweitzer and R. Schmidt (2003). Physical mechanisms of generation and deactivation of singlet oxygen. *Chem. Rev.* **103**, 1685–1757.

Enclosure 5

A. Molnár, R. Dedic, A. Svoboda and J. Hála, Singlet oxygen production by lipophilic photosensitizers in liposomes studies by time and spectral resolved phosphorescence, Journal of Molecular Structure 834 (2007) 488-491.

Available online at www.sciencedirect.com
ScienceDirect
Journal of Molecular Structure 834–836 (2007) 488–491
Journal of MOLECULAR STRUCTURE
www.elsevier.com/locate/molstruc

Singlet oxygen production by lipophilic photosensitizers in liposomes studied by time and spectral resolved phosphorescence

A. Molnár *, R. Dědic, A. Svoboda, J. Hála

Charles University, Faculty of Mathematics and Physics, Department of Chemical Physics and Optics, Ke Karlovu 3, 121 16 Praha 2, Czech Republic

Received 7 October 2006; received in revised form 15 December 2006; accepted 19 December 2006
Available online 3 January 2007

Abstract

In this contribution, excitation energy transfer from lipophilic photosensitizers incorporated into the liposomes to singlet oxygen was investigated. Measurements were carried out on photosensitizers used in photodynamic therapy: haematoporphyrin derivatives and protoporphyrin IX. Solutions of L-α-phosphatidylcholine large unilamellar vesicles of 100 nm diameter prepared by extrusion were used. Kinetics of photosensitizer triplet states and singlet oxygen in the liposomes together with processes of excitation energy transfer were examined by direct detection of their weak near-infrared phosphorescence (894 and 1278 nm, respectively) with time and spectral resolution. The life-times of photosensitizer triplets and singlet oxygen in H_2O and D_2O solutions of liposomes were compared to those in acetone and in lipids droplets. The higher complexity of the liposomal systems is reflected in the fact that the phosphorescence kinetics of the photosensitizers do not follow monoexponential decay.
© 2007 Elsevier B.V. All rights reserved.

Keywords: Haematoporphyrin derivatives; Protoporphyrin IX; Singlet oxygen; Photodynamic therapy; Liposomes

1. Introduction

Photodynamic therapy (PDT) is a promising way of cancer treatment [1,2]. A light, a light-sensitive drug, photosensitizer (PS), and oxygen are combined to produce highly reactive substances lethal to tumor cells. First, the PS is administered into patient's body. After a delay, when PS is accumulated predominantly in tumor tissue, the tumor is irradiated at appropriate wavelength. In consequence, PS undergoes transition into the excited singlet state, which easily converts to the triplet state. The ground state of molecular oxygen is a triplet. On the other hand, the first excited state of oxygen is a singlet. As the triplet state of PS exhibits higher energy than the singlet state of oxygen, energy transfer from PS to singlet oxygen occurs easily. This way highly reactive singlet oxygen is produced, which destroys biologically significant molecules, such as proteins or lipids.

Derivatives of haematoporphyrin (HpD) were one of the first photosensitisers used for PDT [3]. Acetylation and reduction of hematoporphyrin produces a complex mixture of HpD with strong photosensitizing properties. Photofrin®, which is a partially purified form of HpD, has received approval for clinical use in the treatment of esophageal cancer [4,5].

Photoporphyrin IX is a metabolic product of δ-aminolevulinic acid (PDT drug Levulan® from DUSA) in human body [6]. Fluorescent and photosensitizing properties of PpIX accumulated after the exogenous administration of δ-aminolevulinic acid, can be used to visualize and destroy malignant cells in the so-called photodynamic diagnosis and photodynamic therapy of cancer. Many clinical δ-aminolevulinic acid-PDT applications to malignant and non-malignant pathologies are currently in use [7].

Besides chemical methods [8], photoproduction of singlet oxygen can be quantified also using spectroscopic methods [9]. The main advantage of spectroscopic methods

* Corresponding author. Tel.: +420 221 911 307; fax: +420 221 911 249.
E-mail address: egi@matfyz.cz (A. Molnár).

0022-2860/$ - see front matter © 2007 Elsevier B.V. All rights reserved.
doi:10.1016/j.molstruc.2006.12.019

over the chemical ones is their ability to determine not only singlet oxygen quantum yields but also describe and explain excitation energy transfer between PS and oxygen.

Phosphorescence spectra and kinetics together with their concentration dependencies of porphyrin-like PS HpD and PpIX in acetone as well as that of singlet oxygen were measured [10]. Both HpD and PpIX cannot be dissolved in water, which represent an environment suitable for PDT applications. Therefore, systematic spectroscopic study of PS HpD and PpIX in phosphatidylcholine liposomes in H_2O and D_2O is presented.

Liposomes are known to enhance the clinical effects of photosensitizers, to reduce their toxicity and to protect them from metabolism and immune responses. In addition, liposomes with specific characteristics can be used in order to achieve a better target-directed drug delivery.

The aim of the present investigations was the time-resolved PS and $^1O_2$ phosphorescence detection and interpretation of the energy transfer from PS to singlet oxygen inside complex environments such as lipid membranes using a very sensitive device with time and spectral resolution.

2. Materials

Photosensitizers (HpD and PpIX) were obtained from Frontier Scientific Porphyrin Products. Completely saturated lipid L-α-phosphatidylcholine (Avanti Polar Lipids) was used to eliminate possible chemical reaction of singlet oxygen with double bonds of the lipid. Lipid together with PS (approx. 10/1 w/w) were dissolved and thoroughly mixed in chloroform to assure a homogeneous mixture. Chloroform was then removed by evaporating with dry nitrogen to yield a lipid film. Hydration of the dry lipid film was accomplished simply by adding H_2O (or D_2O) to the container and agitating. The products of hydration were large, multilamellar vesicles, with each lipid bilayer separated by a water layer. After the stable, hydrated multilamellar vesicle suspension was produced, the particles were downsized by extrusion using Mini-extruder (Avanti Polar Lipids). The extrusion through filters with 100 nm pores improved the homogeneity of the size distribution of the final suspension (in comparison to sonication). It was done at a temperature ≈75 °C, above the transition temperature of the lipids (≈50 °C). This way, samples of HpD and PpIX incorporated in 100 nm liposomes in H_2O and D_2O were prepared.

3. Methods

Very sensitive home-built set-up was used to measure time and spectral resolved phosphorescence of singlet oxygen [11]. The samples were excited at 420 nm by laser pulses (20 ns, ≈40 μJ, 40 Hz repetition) provided by a dye laser Lambda Physik FL 3001 (Stilbene 3 in methanol), pumped by excimer laser Lambda Physik LPX 100. The laser beam was focused to a fluorescence cuvette through its bottom. The phosphorescence of singlet oxygen and PS was collected from 0.8 mm high sample spot by lens assembly through a long-pass filter (Schott RG 7) and high luminosity monochromator Jobin-Yvon H20 IR to the infrared sensitive photomultiplier Hamamatsu R5509 (cooled to −80 °C by liquid nitrogen). The photomultiplier output was fed through the Becker–Hickl HF AC-26 dB preamplifier to the Becker–Hickl MSA 200 photon counter/multiscaler triggered by a fast PIN photodiode. Time-resolved measurements of singlet oxygen at 1278 nm (together with 1242 and 1306 nm) were performed. Phosphorescence of PS was measured at 894 nm. In addition, measurements of phosphorescence from 750 to 1350 nm, with steps of 16 nm were carried out. All experiments were carried out at room temperature (≈20 °C), well under the transition temperature of the used lipids.

4. Results

Fig. 1 presents phosphorescence spectra of HpD in liposomes dissolved in H_2O and D_2O together with singlet oxygen phosphorescence. For better comparison phosphorescence spectrum of HpD in acetone scaled to appropriate range is also shown (data from [10]). There are no differences between shape of phosphorescence spectra of HpD and PpIX in acetone and in liposomes. Phosphorescence of PS exhibits its maxima around 830 nm while singlet oxygen phosphorescence maximum is found around 1278 nm. Fig. 1 makes it evident, that infrared $^1O_2$ phosphorescence is very weak. Maximal intensity of $^1O_2$ phosphorescence was approximately 100 times weaker than that of PS in acetone. It is even more pronounced in liposomes, where this ratio is around 1000.

Non-linear shape of the semi-logarithmic plots of phosphorescence decays of HpD in liposomes at 894 nm shown in Fig. 2 indicates that the decays cannot be described by

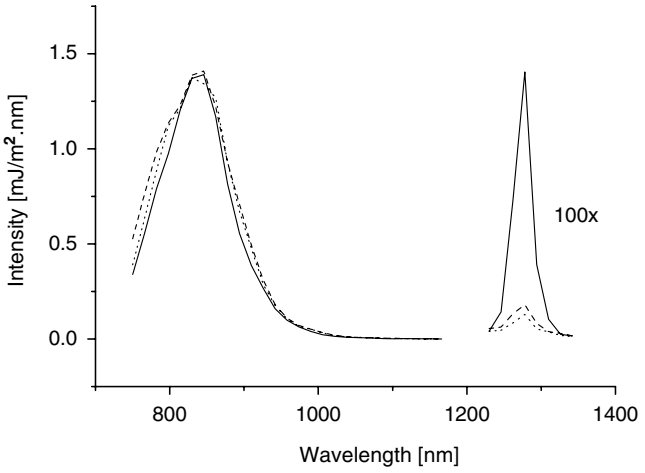

Fig. 1. Phosphorescence spectra of HpD in liposomes in H_2O (dotted), D_2O (dashed) and acetone (solid) together with singlet oxygen phosphorescence spectra. For sake of clarity, spectra of HpD in acetone were normalised to phosphorescence intensities observed in H_2O and D_2O.

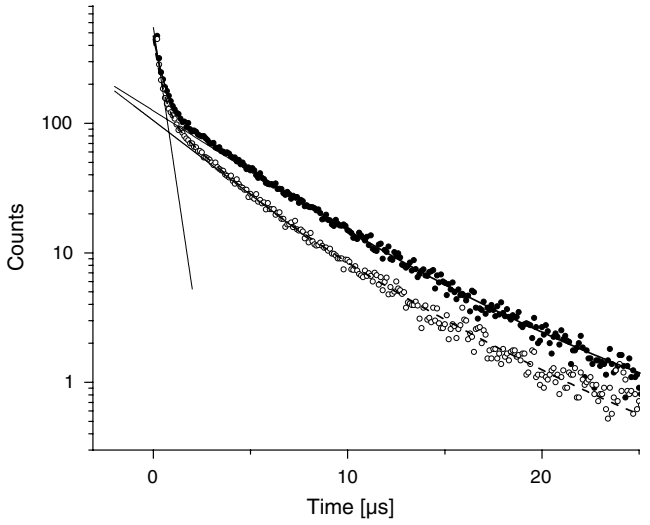

Fig. 2. Phosphorescence kinetics of HpD in liposomes in H_2O (open circles) and D_2O (full circles) at 894 nm, together with biexponential fits and lines corresponding to the slopes of the components of both decays.

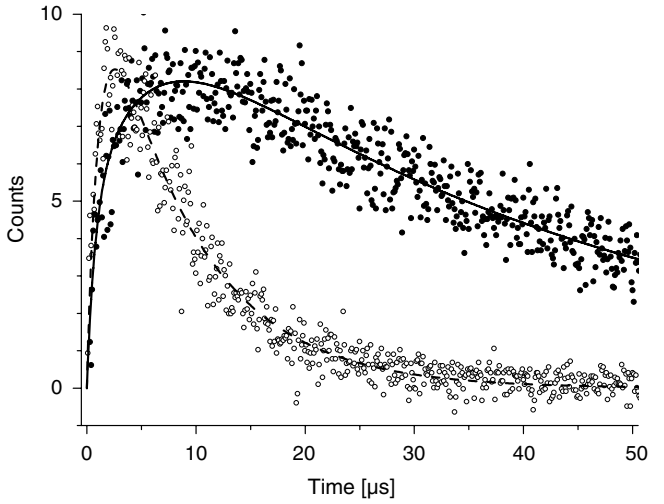

Fig. 3. Phosphorescence kinetics of singlet oxygen at 1278 nm generated by HpD in H_2O (open circles) and D_2O (full circles), together with corresponding fits.

single exponentials in H_2O nor in D_2O. However, Fig. 2 documents that two-exponential decay with lifetime t_1 of (0.42 ± 0.05) μs and t_2 of (3.8 ± 0.1) μs provides reliable fits in H_2O. In the case of D_2O the shorter component remained the same, while the longer one increased to the value of (4.6 ± 0.1) μs. The lines corresponding to the slopes of both decays are also added in Fig. 2 for the sake of clarity. The ratio of phosphorescence intensity of the shorter component to that of the longer one is approximately 1:4 for both solvents.

Similar trends were observed also in PpIX. The corresponding data are summarised in Table 1.

As mentioned above, the singlet oxygen phosphorescence maximum is located around 1278 nm. Phosphorescence kinetics recorded at 1242 and 1306 nm (outside the spectral band of singlet oxygen transition) showed non-negligible tail of PS phosphorescence lying under phosphorescence of singlet oxygen. Therefore, interpolated luminescence kinetics at 1242 and 1306 nm was taken as background of singlet oxygen phosphorescence. The data corrected to this background were fitted by

$$I(t) = \frac{I_1}{k_1 - k_3}\left[e^{-k_3 t} - e^{-k_1 t}\right] + \frac{I_2}{k_2 - k_3}\left[e^{-k_3 t} - e^{-k_2 t}\right]$$

Table 1
Summarised phosphorescence life-times of PS in liposomes in different environments together with the percentages of phosphorescence intensity of shorter (longer) component to the total phosphorescence intensity

PS	Liposome solvent	t_1		t_2	
		(μs)	(%)	(μs)	(%)
HpD	H_2O	0.42 ± 0.05	22	3.8 ± 0.1	78
	D_2O	0.43 ± 0.03	18	4.6 ± 0.1	82
PpIX	H_2O	0.28 ± 0.04	22	3.3 ± 0.1	78
	D_2O	0.26 ± 0.03	18	4.1 ± 0.1	82

Table 2
Table of life- and decay-times of singlet oxygen generated by HpD and PpIX in differ environments

PS	Liposome solvent	t_1 (μs)	t_2 (μs)	t_3 (μs)
HpD	H_2O	0.78 ± 0.31	1.6 ± 0.8	8.0 ± 0.7
	D_2O	0.63 ± 0.32	5.2 ± 0.9	41 ± 2
PpIX	H_2O	0.46 ± 0.31	2.2 ± 0.8	7.3 ± 0.6
	D_2O	0.75 ± 0.21	3.8 ± 1.0	37 ± 1

where $I(t)$ is the intensity of phosphorescence in the time t after excitation pulse, $k_1 = \frac{1}{t_1}$ and $k_2 = \frac{1}{t_2}$ are rate constants of population of singlet oxygen, and $k_3 = \frac{1}{t_3}$ is rate constant of depopulation of singlet oxygen.

The t_3 decay time of singlet oxygen generated by HpD in H_2O is (8.0 ± 0.7) μs. Singlet oxygen generated by PpIX in H_2O shows similar value of (7.3 ± 0.6) μs.

It is generally known, that lifetime of singlet oxygen in D_2O is many times longer compared to water. It is documented in Fig. 3 which shows phosphorescence kinetics of singlet oxygen at 1278 nm generated by HpD in H_2O and D_2O together with their fits. Decay time t_3 was (41 ± 2) μs for HpD and (37 ± 1) μs for PpIX in D_2O. All the lifetimes of singlet oxygen phosphorescence generated by both PS in liposomes in H_2O and D_2O are summarised in Table 2.

5. Discussion

It was published previously, that phosphorescence of both HpD and PpIX in acetone solutions follows mono-exponential decays [10]. On the contrary, bi-exponential decays are required to successfully fit phosphorescence of this pigments incorporated into liposomes. That suggests a presence of two distinct groups of the PS. As both studied PS are hydrophobic, their molecules are locked in

the lipid bilayer. The shorter component was the very same in both H_2O and D_2O. It suggests that this lifetime can be ascribed to the group of pigments buried deep into the lipid bilayer, where they are effectively shielded from outer environment influence. On the other hand, the longer component depends on whether the liposomes are surrounded by normal or heavy water. Therefore, the corresponding pigments are probably situated near the polar heads of the liposome. The shorter components of both HpD and PpIX phosphorescence lifetimes in liposomes in water are very close to the lifetimes of these PS in acetone: (0.35 ± 0.03) μs and (0.22 ± 0.01) μs, respectively [10].

Compared to the above-mentioned measurements of singlet oxygen luminescence in acetonic solution of the PS [10], the signal of singlet oxygen in the case of the liposomes was very weak, causing low signal-to-noise ratio. Moreover, it was superimposed on weak, but still not negligible tail of phosphorescence of both PS, which is in contrast to the results of Baier obtained on Photofrin [13].

Due to the presence of the two components of PS phosphorescence decay, the singlet oxygen should be photogenerated via two distinct pathways. On the other hand, due to rather long diffusion length of singlet oxygen (≈0.4 μm), it can easily escape the liposomes of 100 nm diameter and diffusion between different compartments is possible. Therefore, the decay of the singlet oxygen is mono-exponential with effective lifetime with no relation to whether it was photogenerated deep inside the bilayer or near the surface, making two different singlet oxygen decay times unnecessary.

Our data fit well with previously published results:

The slower rise time $t_2 = (1.6 \pm 0.8)$ μs for HpD is in a very good agreement with (1.6 ± 0.5) μs for Photofrin in aqueous suspensions of phosphatidylcholine published in [13].

The decay times $t_3 = (8.0 \pm 0.7)$ μs for HpD and $t_3 = (7.3 \pm 0.6)$ μs for PpIX are effective values between decay time (3.7 ± 0.1) μs of $^1O_2$ in water [12] and 12,2 μs in pure phosphatidylcholine [14]. Moreover, it is in a good agreement with $t_3 = (9 \pm 2)$ μs for $^1O_2$ generated by Photofrin in lipid droplets in water [13].

6. Conclusion

The influence of incorporation of two porphyrin-like PS into ≈100 nm unilamellar phosphatidylcholine liposomes on their photosensitising properties was investigated by means of direct detection of time and spectral resolved phosphorescence of the PS and singlet oxygen. PS phosphorescence in liposomes exhibits two components, the shorter one caused by PS in the middle of lipid bilayer and the longer one caused by PS near the surface of lipid bilayer, which is in contact with water. Differences of longer lifetime of the PS triplets near the surface of lipids bilayer between H_2O and D_2O environment suggest quenching of PS by the solvent.

Acknowledgement

This work was supported by project MSM 0021620835 from the Ministry of Education of the Czech Republic.

References

[1] Y.N. Konan, R. Gurny, E. Allemann, J. Photochem. Photobiol. B 66 (2002) 89.
[2] M. Ochsner, J. Photochem. Photobiol. B 39 (1997) 1.
[3] R. Bonnett, G. Martinez, Tetrahedron 57 (2001) 9513.
[4] S.J. Tang, P. Fellow, N.E. Marcon, Photodiagn. Photodyn. Ther. 1 (2004) 65.
[5] V.R. Litle, J.D. Luketich, N.A. Christie, P.O. Buenaventura, M. Alvelo-Rivera, J.S. McCaughan, N.T. Nguyen, H.C. Fernando, Ann. Thorac. Surg. 76 (2003) 1687.
[6] C.F. Lee, C.J. Lee, C.T. Chen, C.T. Huang, J. Photochem. Photobiol. B 75 (2004) 21.
[7] R.F.V. Lopez, N. Lange, R. Guy, M.V.L.B. Bentley, Adv. Drug Deliv. Rev. 56 (2004) 77.
[8] C. Tanielian, C. Schweitzer, R. Mechin, C. Wolff, Free Radic. Biol. Med. 30 (2001) 208.
[9] A.A. Abdel-Shafi, D.R. Worrall, F. Wilkinson, J. Photochem. Photobiol. A 142 (2001) 133.
[10] A. Molnar, R. Dedic, M. Korinek, A. Svoboda, J. Hala, J. Mol. Struct. 744 (2005) 723.
[11] R. Dedic, A. Svoboda, J. Psencik, J. Hala, J. Mol. Struct. 651 (2003) 301.
[12] R. Dedic, A. Molnar, M. Korinek, A. Svoboda, J. Psencik, J. Hala, J. Lumin. 108 (2004) 117.
[13] J. Baier, M. Maier, R. Engl, M. Landthaler, W. Bäumler, J. Phys. Chem. B 109 (2005) 3041.
[14] B. Ehrenberg, J.L. Anderson, C.S. Foote, Photochem. Photobiol. 68 (2) (1998) 135.

Enclosure 6

A. Molnár, R. Dedic, A. Svoboda, J. Hála, Spectroscopic study of singlet oxygen photogeneration by lipophilic photosensitizer in liposomes, Journal of Luminiscence, accepted for publication.

ARTICLE IN PRESS

Available online at www.sciencedirect.com

ScienceDirect

Journal of Luminescence ▮ (▮▮▮▮) ▮▮▮–▮▮▮

JOURNAL OF LUMINESCENCE

www.elsevier.com/locate/jlumin

Spectroscopic study of singlet oxygen photogeneration by lipophilic photosensitiser in liposomes

A. Molnár*, R. Dědic, A. Svoboda, J. Hála

Department of Chemical Physics and Optics, Faculty of Mathematics and Physics, Charles University, Ke Karlovu 3, 121 16 Praha 2, Czech Republic

Abstract

The time- and spectrally-resolved phosphorescence measurements of protoporphyrin IX (PpIX), haematoporphyrin (HpD) and singlet oxygen in liposomal samples under different oxygen concentrations were performed. We observed two different phosphorescence lifetimes of two distinct groups of photosensitisers (PSs). The group with shorter lifetime is located deep inside the nonpolar lipid bilayer, whereas the group with longer lifetime is exposed to H_2O due to its localisation near the bilayer surface. When the oxygen concentration in H_2O is increased about five times, a significant change in the slower decay component of the group of PS near the surface was observed from 3.8 to 1.3 μs (HpD) and from 3.3 to 1.2 μs (PpIX). On the other hand, the shorter phosphorescence components exhibit less-pronounced changes in lifetimes from 0.42 to 0.39 μs (HpD) and from 0.28 to 0.25 μs (PpIX). The singlet oxygen decay time decreases from 7.3 to 3.5 μs (PpIX) and from 8.0 to 3.5 μs (HpD) in H_2O. The results are discussed in the frame of a model, where an increase of the oxygen concentration in the aqueous medium is accompanied by only a slight increase of the oxygen concentration inside the lipid bilayer.

© 2007 Elsevier B.V. All rights reserved.

Keywords: Energy transfer; Phosphorescence; Singlet oxygen; Protoporphyrin IX; Haematoporphyrin; Liposomes

1. Introduction

In photodynamic therapy (PDT), light, light-sensitive drug—photosensitiser (PS) and oxygen, are combined to produce highly reactive substances lethal to tumour cells. Derivatives of haematoporphyrin (HpD) were one of the first PSs used for PDT [1]. Protoporphyrin IX (PpIX) is a metabolic product of δ-aminolevulinic acid in the human body [2]. Fluorescent and photosensitising properties of PpIX, accumulated after the exogenous administration of δ-aminolevulinic acid, can be used to visualise and destroy malignant cells [3].

HpD and PpIX are hydrophobic PS. There are several methods to transfer water-insoluble PS via the bloodstream to a tumour. Among others, usage of liposomes as drug-delivery systems seems to be very promising; they are easily decomposable in the organism, nontoxic, and usable as a controlled transport system [4].

The aim of this contribution is to investigate oxygen penetration into liposomes and to examine how the PSs incorporated inside the lipid bilayer are exposed to the environment of liposomes.

2. Materials and methods

HpD and PpIX were obtained from the Frontier Scientific Porphyrin Products, completely saturated L-α-phosphatidylcholine from the Avanti Polar Lipids.

Lipids together with PS were dissolved in chloroform. The chloroform was subsequently evaporated to prepare a dry PS-lipid film. Hydration of the film was accomplished by adding H_2O and agitating, providing multilamellar vesicles. The vesicles were downsized by extrusion through filters with 100 nm pores at a temperature of 75 °C (well above the transition temperature of the lipids). To achieve oxygen-saturated conditions, the samples were purged with oxygen for 1 h.

The measurement of time- and spectrally-resolved phosphorescence was performed on a very sensitive

*Corresponding author. Tel.: +420 22191307; fax: +420 221911249.
E-mail address: a.molnar@seznam.cz (A. Molnár).

0022-2313/$ - see front matter © 2007 Elsevier B.V. All rights reserved.
doi:10.1016/j.jlumin.2007.12.009

home-built set-up [5]. The samples were excited at 420 nm by laser pulses (20 ns, ≈40 μJ, 40 Hz repetition) provided by a dye laser Lambda Physik FL 3001 pumped by an excimer laser Lambda Physik LPX 100. The phosphorescence of singlet oxygen and PS was collected from the excitation spot through a lens assembly, a long-pass filter (Schott RG 7) and a high-luminosity monochromator Jobin–Yvon H20IR by an infrared-sensitive photomultiplier Hamamatsu R5509 (cooled to −80 °C). The photomultiplier output was fed through a Becker–Hickl HF AC-26 dB preamplifier to a Becker–Hickl MSA 200 photon counter/multiscaler. Time-resolved measurements of singlet oxygen were performed at 1278 nm, and phosphorescence of the PS was measured at 894 nm. All experiments were performed at 20 °C, under the transition temperature of the lipids used.

3. Results and discussion

We have previously shown that the kinetics of the phosphorescence of both investigated PSs exhibits bi-exponential character in liposomes [6]. Increasing the oxygen concentration does not change the bi-exponential character of the decays. However, the lifetimes of both components change. The kinetics of the HpD phosphorescence decays at 894 nm under both oxygen concentrations are shown in Fig. 1. All the PS lifetimes in liposomal samples saturated with oxygen are presented in Table 1. For the sake of comparison, decay times of PS from samples saturated with air were added (data from Ref. [6]).

As both HpD and PpIX are water-insoluble, it is reasonable to assume that all the PSs are locked inside the lipid bilayer, and singlet oxygen is generated in the liposomes solely. In our previous publication [6], we have ascribed the two observed lifetimes to two distinct groups of PS: the group exhibiting the shorter lifetime is located deep inside the nonpolar lipid bilayer, whereas the group

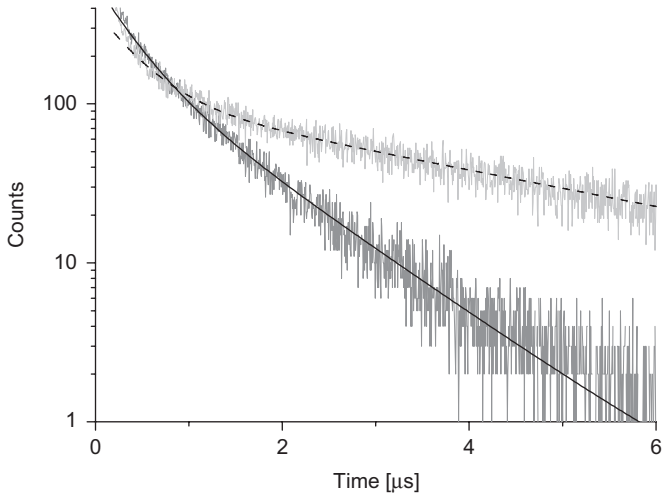

Fig. 1. Typical kinetics of the phosphorescence of HpD at 894 nm together with the respective fits in air- (dashed) and oxygen-saturated (solid) liposomal samples.

Table 1
Phosphorescence lifetimes of PS in liposomes under different oxygen concentrations

PS	Oxygen concentration ($\mu mol\,l^{-1}$)	t_1 (μs)	t_2 (μs)
PpIX	280	0.28 ± 0.04	3.3 ± 0.1
	1400	0.25 ± 0.08	1.2 ± 0.5
HpD	280	0.42 ± 0.05	3.8 ± 0.1
	1400	0.39 ± 0.20	1.3 ± 0.4

with longer lifetime is more exposed to the outer environment due to its localisation near the bilayer surface. The identification of the PS groups is further supported by our new data. The influence of increase of oxygen concentration on the group with longer lifetime is more pronounced.

While the longer component exhibits a dramatic decrease of the lifetime after purging with oxygen, the change of the shorter one is only slight. This behaviour is based on the fact that the change of oxygen concentration inside the lipid bilayer is probably not proportional to the change of concentration of oxygen in the outer medium. Significant increase of oxygen concentration in water leads only to a minor increase of oxygen concentration inside the lipid membrane. Oxygen concentration in water increases after purging the samples with oxygen about five times, causing a significant change in the slower decay component of the PS phosphorescence from 3.8 to 1.3 μs (HpD) and from 3.3 to 1.2 μs (PpIX).

The kinetics of the singlet oxygen phosphorescence was fitted by a model using double-exponential increase and single-exponential decay:

$$I(t) = \frac{I_2}{k_2 - k_3}\left[e^{-k_3 t} - e^{-k_2 t}\right] + \frac{I_1}{k_1 - k_3}\left[e^{-k_3 t} - e^{-k_1 t}\right],$$

where $I(t)$ is the intensity of the phosphorescence at time t after the excitation pulse, k_1 and k_2 are rate constants of population of singlet oxygen: $k_1 = 1/t_1$, $k_2 = 1/t_2$ and k_3 is the rate constant of singlet oxygen depopulation: $k_3 = 1/t_3$. A double-exponential increase was used to describe the photogeneration of singlet oxygen by the two different groups of PS. Taking into account the diffusion length of singlet oxygen of 0.2 μm in water [7] and 0.4 μm in pure lipids [8] compared to the 0.1 μm liposome diameter, singlet oxygen can diffuse back and forth several times between both phases during its lifetime. This justifies the approach of only one effective singlet oxygen lifetime for the decay part of the kinetics.

All the singlet oxygen rise- and decay-times in liposomal samples saturated with oxygen are presented in Table 2. For the sake of comparison, corresponding times from samples saturated with air were added (data from Ref. [6]).

A very low signal-to-noise ratio and a strong scattered excitation light make fitting of the data obtained for HpD by the presented model with two rise-times unsuitable, as the

Please cite this article as: A. Molnár, et al., J. Lumin. (2008), doi:10.1016/j.jlumin.2007.12.009

Table 2
Rise- and decay-times of singlet oxygen generated by HpD and PpIX under different oxygen concentrations

PS	Oxygen concentration ($\mu mol\,l^{-1}$)	t_1 (μs)	t_2 (μs)	t_3 (μs)
PpIX	280	0.46 ± 0.31	2.2 ± 0.8	7.3 ± 0.6
	1400	0.25 ± 0.26	1.1 ± 0.6	3.5 ± 0.3
HpD	280	0.78 ± 0.31	1.6 ± 0.8	8.0 ± 0.7
	1400	0.04 ± 0.21	0.5 ± 0.3	3.5 ± 0.3

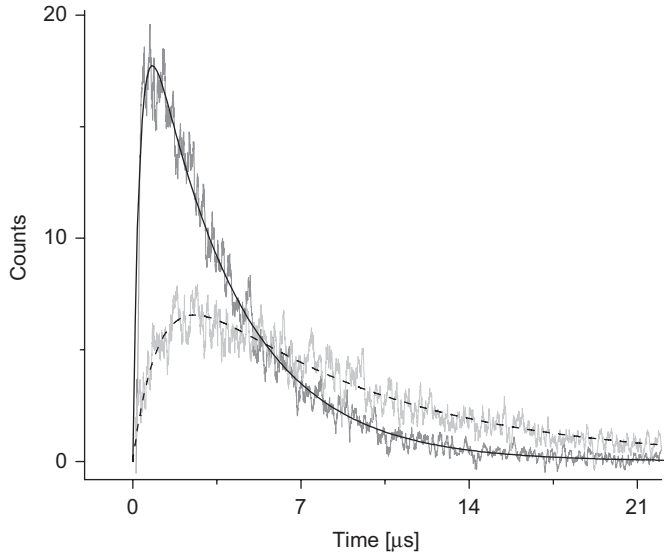

Fig. 2. Singlet oxygen phosphorescence kinetics at 1278 nm generated by HpD in air- (dashed) and oxygen-saturated (solid) liposomal samples together with their respective fits.

shorter component provides an unreasonably short value with an enormous error ($t_1 = 0.04\pm0.21\,\mu s$, see Table 2). The obtained value of $t_2 = 0.5\pm0.3\,\mu s$ (see Table 2) therefore represents an effective value of both the PS groups. Anyway, this value lies between the lifetimes of the HpD phosphorescence under oxygen-saturated conditions (Table 1). On the other hand, it is possible to obtain two values of $t_1 = 0.25\pm0.26\,\mu s$ and $t_2 = 1.1\pm0.6\,\mu s$ (see Table 2) in the case where singlet oxygen is generated by PpIX in oxygen-saturated H_2O. These values correspond well to the lifetimes of the PpIX phosphorescence (compare Table 1).

Comparison of singlet oxygen phosphorescence kinetics under air- and oxygen-saturated conditions is presented in Fig. 2. The obtained effective singlet oxygen lifetimes of 8.0 μs for HpD and 7.3 μs for PpIX (Table 2) in 100 nm liposomes [6] lie between decay times in pure lipids 12.2 μs [9] and in water 3.7 μs [10]. Under oxygen-saturated conditions the singlet oxygen decay time of $3.5\pm0.3\,\mu s$ for both HpD and PpIX (Table 2) fits well with the singlet oxygen lifetime of $3.5\pm0.1\,\mu s$ in oxygen-saturated sulphonato-tetraphenyl-porphyrin aqueous solutions [10]. Explanation lies in the fact that under oxygen saturation of the liposomal solution, the concentration of oxygen inside the lipid bilayer increases only slightly, while in water rises five times and thus the contribution of the singlet oxygen phosphorescence from the lipid bilayer to the overall phosphorescence drops to almost insignificant portion making the observed effective lifetime similar to that in oxygen-saturated water without liposomes.

4. Summary

The time- and spectrally resolved phosphorescence measurements of PpIX and HpD in liposomal samples under different oxygen concentrations confirmed our previously published model, based on two different PS groups with two different lifetimes (localised in the middle of the lipid bilayer and near to the liposome surface).

Lifetimes of singlet oxygen phosphorescence indicate that increasing the oxygen concentration in a water medium is accompanied by only a slight increase of its concentration inside the lipid bilayer. Based on this effect, the differences in behaviour of the effective lifetimes of singlet oxygen phosphorescence under different oxygen concentrations in H_2O were explained.

Acknowledgement

This work was supported by Project MSM 0021620835 from the Ministry of Education of the Czech Republic.

References

[1] R. Bonnett, G. Martinez, Tetrahedron 57 (2001) 9513.
[2] C.F. Lee, C.J. Lee, C.T. Chen, C.T. Huang, J. Photochem. Photobiol.—Biol. B 75 (2004) 21.
[3] R.F.V. Lopez, N. Lange, R. Guy, M.V.L.B. Bentley, Adv. Drug Deliv. Rev. 56 (2004) 77.
[4] Y.N. Konan, R. Gurny, E. Allemann, J. Photochem. Photobiol.—Biol. B 66 (2002) 89.
[5] R. Dedic, A. Svoboda, J. Psencik, J. Hala, J. Mol. Struct. 651 (2003) 301.
[6] A. Molnar, R. Dedic, A. Svoboda, J. Hala, J. Mol. Struct. 834–836 (2007) 488.
[7] D.R. Linde, Handbook of Chemistry and Physics, 80th ed., CRC Press, LLC, Boca Raton, FL, 1999.
[8] J. Baier, M. Maier, R. Engl, M. Landthaler, W. Bäumler, J. Phys. Chem. B 109 (2005) 3041.
[9] B. Ehrenberg, J.L. Anderson, C.S. Foote, Photochem. Photobiol. 68 (2) (1998) 135.
[10] R. Dedic, A. Molnar, M. Korinek, A. Svoboda, J. Psencik, J. Hala, J. Lumin. 108 (2004) 117.